Evaluation of the Pallet Deflection that Occurs under Forklift Handling Conditions

Yu Yang Huang Qiu

Thesis submitted to the faculty of the Virginia Polytechnic Institute and State University in partial fulfillment of the requirements for the degree of

Master of Science

In

Forest Products

Laszlo Horvath, Committee Chair

John Bouldin

Marshall S. White

August 11th, 2021

Blacksburg, VA

Keywords: Vibration, Forklift, Dynamic Load Capacity, Pallet Deflection, ISO 8611 Deflection Limit

Evaluation of the Pallet Deflection that Occurs under Forklift Handling Conditions

Yu Yang Huang Qiu

ABSTRACT

Industrial forklifts consist of one of the most common handling methods for pallets in warehouses and distribution centers. Pallets deflect while they are being transported by forklifts due to the weight of the unit load. Thus, most of the deflection is observed to occur on the outside edges and corners of the pallet. Several international standards are used in order to define the maximum deflection for pallet bending, including ISO 8611 and ASTM D1185. However, there is still a lack of understanding on the accuracy of these deflection limits and the exact performance of a pallet during a forklift support condition. Understanding pallet bending during forklift support condition and how it affects the stability of a unit load helps create an industry accepted deflection limit that will help to design safer and more cost-effective pallets.

For this research, two studies were proposed in order to assess pallet deflection and unit load stability. The first study consisted of measuring and analyzing the vibration levels for three different industrial forklifts affect by factors such as the speed, the payload of the unit load carried, sensor location, forklift type, and road conditions. The results obtained showed that the highest vibration intensity occurred at 3-4 Hz, while the highest overall G_{rms} value observed was 0.145 G^2/Hz (between 1-200 Hz). An increase in the forklift speed caused an increase in vibration intensity. In contrast, an increase in the unit load weight carried by the forklift caused a decrease in vibration intensity. Among the three forklifts studied, the gas-powered forklift had the highest vibration intensity, and all forklifts, when driven on asphalt, experienced more vibration.

The second study of the research project consisted of evaluating pallet deflection under forklift handling conditions. These conditions included fork tines configuration (leveled and 4° angle), unit load condition (bound and unbound), pallet orientation (across width and across length), and type of handling condition (static and dynamic). The results showed that when unit loads were handled in a static condition, they survived the throughout the entire testing. However, when they were tested under a dynamic condition, and specifically, with the unbound unit loads, they did not survive the entire testing. Moreover, unit loads that were tested with the 4° angle fork

tines configuration tended to survive longer during the dynamic testing. For this particular case, the unit load capacity obtained based on the ISO 8611 standard was too conservative.

Evaluation of the Pallet Deflection that Occurs under Forklift Handling Conditions

Yu Yang Huang Qiu

PUBLIC ABSTRACT

Forklifts play an important role in the transportation of materials goods in the supply chain. Pallets experience vibration when they are handled by industrial forklifts. This vibration plus the combined effects mainly due to the unit load weight affects the amount that pallets bend. Thus, depending on the amount of pallet bending, they can produce unit load instability. Currently, there is a lack of understanding of how much pallet bending is acceptable. Therefore, the goal of this research was to understand the behavior of pallet bending when they are handled under forklift conditions.

Two experiments were conducted in order to study pallet deflection under forklift handling conditions. The first experiment, which consisted in analyzing forklift vibration, showed that an increase in the forklift speed caused an increase in vibration intensity. In contrast, an increase in the payload of the unit load resulted in a decrease in vibration intensity. Among the three forklifts studied, the gas-powered forklift showed the highest vibration intensity. Forklifts driven on asphalt experienced more vibration in comparison to the ones driven on concrete.

The second experiment, which consisted in assessing pallet deflection under a simulated forklift handling condition, showed that unit loads under a dynamic environment (vibration) increased the probability of unit load instability. Furthermore, it was observed that applying stretch wrap to a unit load decreased its instability and at the same time increases its survivability. Also, the results showed that the proposed ISO 8611 deflection limit is too conservative for this particular handling condition.

ACKNOWLEDGEMENTS

I would like to express my sincere gratitude to everyone that have helped me towards the culmination of my academic degree at Virginia Tech as well as to my personal and professional growth. In particular, I would like to thank my advisor professor Dr. Laszlo Horvath for the continuous support of my master's study and research, for his patience, motivation, enthusiasm, and immense knowledge. His guidance, help and support contributed to the culmination of my master's degree program.

Besides my advisor, I would like to thank the rest of my thesis committee: Dr. John Bouldin, and Dr. Marshall White for their insightful contributions, encouragement, and always looking towards producing a high-quality work. Thank you to Angela Riegel, Kate Bridgeman, Matt Hixon, and David Jones for helping me whenever I needed.

My sincere thanks also go to the Structural Engineering and Materials lab at Virginia Tech, in special to Dr. Matthew Eatherton, Dr. David Mokarem, and Raul Avellaneda for their help in constructing the jig that was required to conduct the experiments of my research project. Also, I would like to thank Dr. Péter Böröcz from Széchenyi István University for his immense contribution in my research project.

I would also like to express my gratitude towards the grad students. In special to Nico, Mary, and Juan for all the help they provided me during my stay in the United States and for accompanying me on this journey to do a master's degree. Their help, support, and advice was invaluable towards the culmination of my studies.

Last but not least, I would like to thank my family and friends for all the help and support they have given me during these years of study. Their support and advice have been important to achieve all the goals that I have set.

Table of Contents

1. GENERAL INTRODUCTION

Industrial forklifts consist of one of the most common handling methods for pallets in warehouses and distribution centers. Pallets deflect while they are being transported by forklifts due to the weight of the unit load. Most of the deflection is observed to occur on the outside edges and corners of the pallet. Several international standards are used in order to define the maximum deflection for the pallet bending, including ISO 8611 and ASTM D1185. However, there is still a lack of understanding on the accuracy of these deflection limits and the exact performance of a pallet during a forklift support condition. Understanding pallet bending during forklift support condition and how it affects the stability of a unit load helps create an industry accepted deflection limit that will help to design safer and more cost-effective pallets.

For this research, two studies were conducted in order to measure and analyze pallet deflection and unit load stability. The first study consisted of evaluating vibration intensities for three different industrial forklifts and how they are affected by factors such as the speed, the payload of the unit load, sensor location, forklift type, and road conditions. The most conservative vibration profile was obtained and used as the input for study 2 of the research project.

The second study of the research project consisted of evaluating pallet deflection under forklift handling conditions. The bending of the pallet was measured for several handling conditions. These conditions included the static and dynamic handling of the pallet with a bound and unbound unit load in the across the width and across the length orientation. The forklift jig allowed the simulation of two handling conditions: when the fork tines are leveled and when they are titled with a 4° angle.

2. RESEARCH OBJECTIVES

Goals

- Determine the correlation between unit load stability and static pallet deflection using the fork tine support condition.

Objectives

- Examine the effects of road conditions, unit load weight, speed, forklift type, and sensor location on vibration levels.
- Analyze the vibration levels produced by three different industrial forklifts in order to determine the most conservative conditions experienced by the forklifts.
- Evaluate the effect of dynamic vibration on pallet creep and bending using bound and unbound unit load.
- Determine the correlation between the ISO nominal load deflection limit with a forklift support condition and unit load stability.

3. LITERATURE REVIEW

3.1.Pallet Market

Pallets are ubiquitous in the supply chain with 2.6 billion pallets in circulation within the U.S. in 2019 (Freedonia, 2015). Wood pallets are the dominant pallet material in the U.S. As shown in Figure 1, it is estimated that 93% of companies are using wooden pallets and that 849 million wooden pallets (508 million new and 341 million recycled) were produced annually (Gerber, Horvath, Araman, & Gething, 2020). In comparison to 2011 (the last year of recorded data), these estimations represent a 14% growth in overall production, with a 22% and 5% growth in new and recycled production, respectively (Gerber, Horvath, Araman, & Gething, 2020). These numbers reflect the continued growth that has occurred over the years as the economy continues to pick up after the 2008 downturn (Gerber, Horvath, Araman, & Gething, 2020).

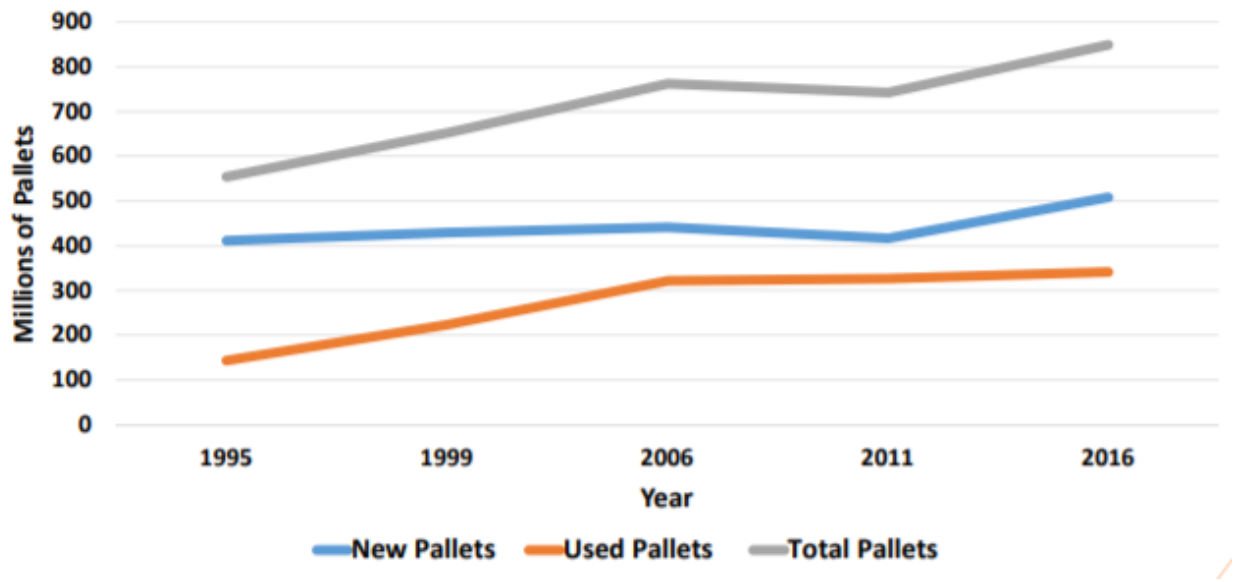

Figure 1. Estimation of the Number of Pallets Produced *(Gerber, Horvath, Araman, & Gething, 2020)*

3.2. Pallet Concept

Pallet is defined as a portable, horizontal, rigid, composite platform used as base for assembling, storing, stacking, handling, and transporting goods as unit load; often equipped with superstructure (MH1, 2016). Pallets are often characterized by their class, use, type, style, bottom deck, size, and design (MH1, 2016).

3.3. Pallet Classification

Depending on the components of the pallet, they can be classified as block or stringer pallets.

3.3.1. Stringer Pallet

Stringer pallet consists of a double-deck pallet with stringer spacers between deck (MH1, 2016). Stringer pallets are the most commonly used pallets in the United States with 76% of the new pallets, and the majority of recycled wooden pallets are stringer class (Gerber, Horvath, Araman, & Gething, 2020). Stringer pallets are composed of stringers that are boards typically made out of 2 x 4's or 3 x 4's (Conner Industries, 2019). As shown in Figure 2, these stringers are connected to deckboards with fasteners. Pallets with solid stringers typically allow two-way entry (at each end of the pallet), while notched stringers allow partial four-way entry (by forklifts through the notches, as well as full access from the ends) (Leblanc, 2019).

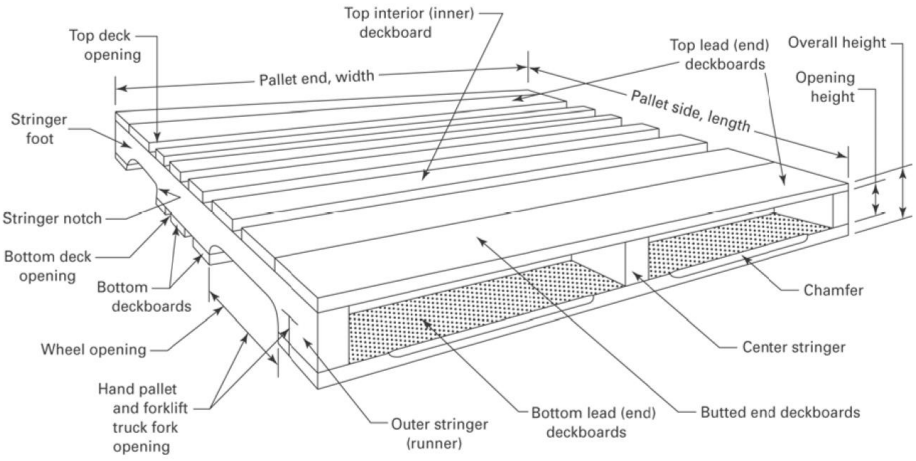

Figure 2. Principal Parts of Wood Stringer Pallets *(MH1, 2016)*

3.3.2. Block Pallet

Block pallets are pallets with blocks between decks or beneath top deck (MH1, 2016). As shown in Figure 3, there are typically nine blocks in a block pallet, with a solid wood block placed in each of the four corners, in the center of each side of the pallet, and in the center of the pallet itself to support the unit load (Conner Industries, 2019). The blocks are connected to a stringer board, which is nailed to the deckboards. These bottom decks are connected directly to the blocks. A block pallet is also known as a "four-way" pallet because the tines of a pallet jack or forklift can access and lift it from all four sides of the pallet (Conner Industries, 2019). Therefore, block pallets provide more options for pallet entry by material handling equipment (Leblanc, 2019).

According to a study conducted by Gerber, Horvath, Araman & Gething (2020), it reported that 21% of new wooden pallets accounted to be block pallets.

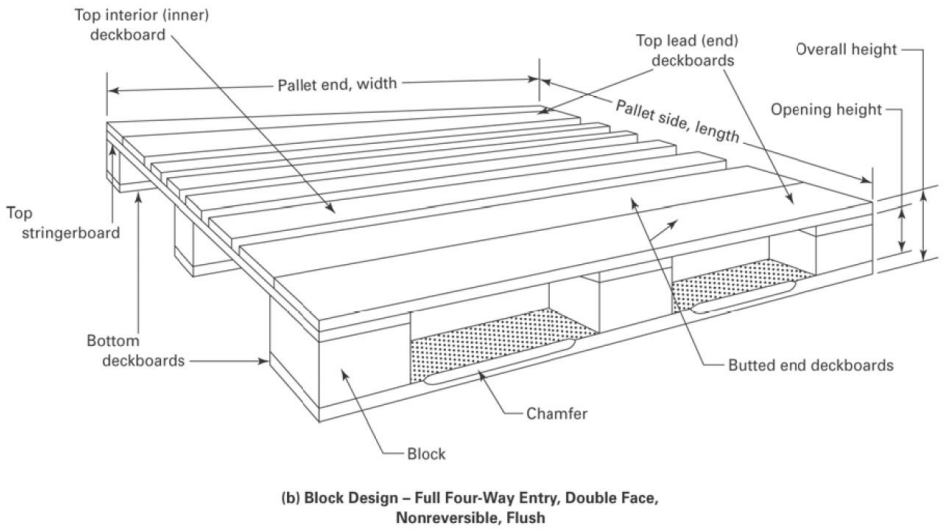

Figure 3. Principal Parts of Wood Block Pallets *(MH1, 2016)*

3.3.3. Use Categories

Based on their reusability, pallets are classified into reusable or single-use pallets. Reusable pallet is intended for more than one-unit load, while single-use pallet is intended to be loaded once for one-unit trip (MH1, 2016). Pallets that can be reused provide a lower cost per trip and less environmental impact than pallets, which can be used only once, subject to the cost of reverse logistics (Leblanc, 2019). In reusable pallet applications, an investment in a better-quality pallet

usually lasts longer, providing a lower cost per use than cheaper alternatives (Leblanc, 2019). The comparison between reusable and single-use pallets is shown in Table 1.

Table 1. Differences between reusable pallet and single-use pallet *Adapted from Leblanc (2019), The Solid Waste Management Coordinating Board, and the Reusable Pallet & Coalition (n.d.)*

Reusable pallet	Single-use pallet
• Intended for more than one-unit load • Lower cost per trip • Less environmental impact • Higher cost of fabrication • Eliminate the purchase and disposal costs	• Intended to be loaded once for one-unit trip • More expensive per trip • Depends on the cost of reverse logistics

3.3.4. Entry Type

A pallet is classified as either two-way entry pallet, a partial four-way entry pallet, or a full four-way entry pallet, as presented in Figure 4. Stringer pallets can either be two-way pallets or partial four-way pallets. A two-way entry pallet has solid stringer boards that can be accessed from the two ends using either a pallet jack or a forklift. On the other hand, a partial four-way pallet has notched stringers. These notched stringers provide additional access from the sides of the pallet using a forklift. However, the notches are not designed large enough to be operated with a pallet jack. Finally, full four-way pallet has openings at both ends and sides with the accessibility of all openings using both a pallet jack and a forklift.

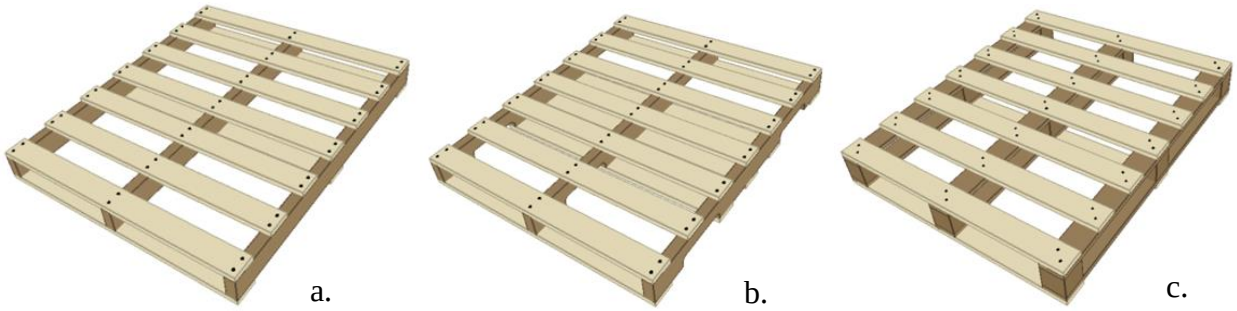

Figure 4. Example of a) two-way, b) partial four-way, and c) four-way wooden pallets

3.3.5. Styles

There are several design characteristics that can be used to classify pallets. One design characteristic is defined by the face construction of the pallet. It can be either single-face or double-face. A single face pallet has no bottom deckboards and are often called skids. Most pallets used in the industries are double-faced pallets that have both top and bottom deckboards. Double-faced pallets can be subdivided into reversible and nonreversible. Reversible pallets have the same top and bottom deck designs allowing the pallet to be flipped over; however, this type of pallet is not commonly used. Nonreversible pallets differ in top and bottom deck construction and therefore have designated top and bottom. Examples of single face, double face nonreversible, and double face fully reversible pallets are shown in Figure 5.

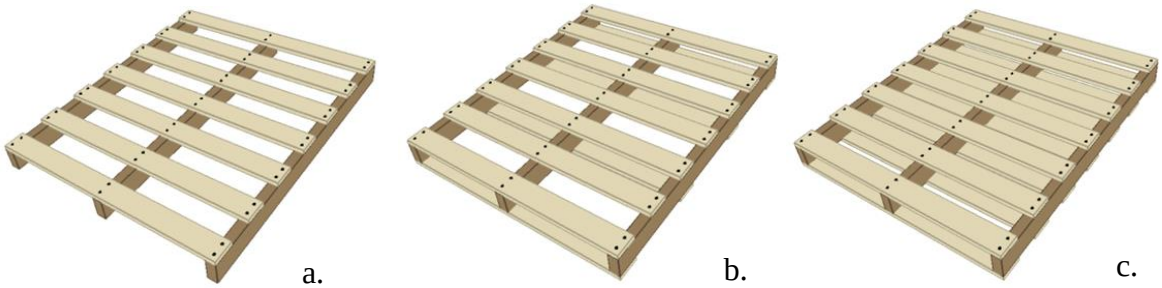

Figure 5. Examples of a) single face, b) double face non-reversible, and c) double face fully reversible pallets

Another design characteristic is the alignment of the top and bottom deckboards with the stringers or stringer boards, as shown in Figure 6. If the deckboards are evenly aligned with the stringers or stringer boards, then the pallet is called a flush pallet (MH1, 2016). If the top deckboards overhang the stringers or stringer boards, then the pallet is considered a single winged pallet (MH1, 2016). If both the top and bottom deckboards overhang, then the pallet is considered a double winged pallet (MH1, 2016).

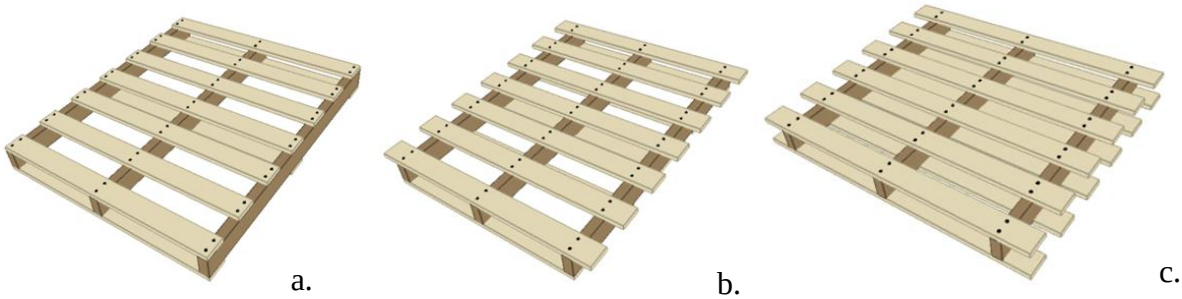

a. b. c.

Figure 6. Examples of a) flush, b) single-winged, and c) double-winged stringer pallets

3.3.6. Top Deck Constructions

Top deck construction can change depending on the pallet designs. For stringer pallets, they can use either deckboards or a panel connected directly to the stringers to create the top deck surface. However, for block pallets, they need an extra component when using deckboards and employ the use of stringer boards to connect the top deckboards to the blocks below. When using a panel as the top deck surface, the panel can either be connected directly to the blocks, or it can be connected using the same stringer board.

3.3.7. Bottom Deck Constructions

The bottom deck construction can vary between pallet designs. For the unidirectional base design, all bottom deck boards are oriented in the same direction of the pallet length or width (MH1, 2016). Block pallets used in Europe often have unidirectional base design, and almost all stringer pallets are considered unidirectional.

Block pallets can have an overlapping, a perimeter, or a cruciform base design. An overlapping base design is when the bottom boards are oriented in both directions of the length and width of the pallet containing both bottom deckboards and bottom stringer boards. Due to handling difficulties with a pallet jack, this design is not commonly used in the industry. Perimeter base design is when the bottom deckboards are butted up against each other instead of overlapping. Most wooden pool pallets in the U.S. have a perimeter base. A cruciform base also uses a butted bottom deckboard design, but it includes an extra bottom deckboard across the center width of the pallet. In the case of wooden pallets with a cruciform bottom deck design, they are commonly created using an overlapping configuration. Plastic pallets can have a single-layer cruciform

bottom deck design due to their manufacturing method. Examples of a overlapping pallet, cruciform pallet, and perimeter base pallet are shown in Figure 7.

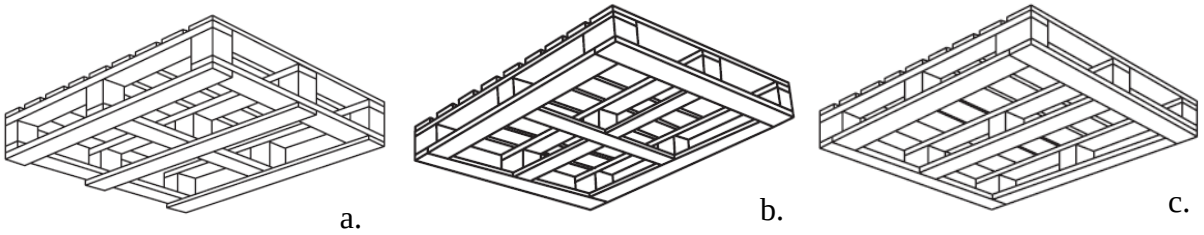

Figure 7. Examples of bottom deck construction pallets: a) overlap, b) cruciform, and c) perimeter base pallet *(ISO 445:2008)*

3.4. Sizes

The pallet dimension is specified by length, width and overall pallet height (NWPCA, 2014). The pallet length is the dimension between the extreme pallet ends, parallel to the stringers or top stringerboards (MH1, 2016). For panel-deck block pallets without stringerboards, it is the top deck pallet dimension parallel to the face grain for plywood (strong panel axis) (MH1, 2016). The pallet width is the dimension between the extreme pallet sides, parallel to and corresponding to the length of the top deckboards (MH1, 2016). For panel deck block pallets without stringerboards, it is the top deck panel dimension perpendicular to the face grain for plywood (strong panel axis) (MH1, 2016). The most common pallet sizes by region are shown in Table 2.

Table 2. Most common pallet sizes by region *(ISO 6780, 2003)*

Metric size (mm)	US size (in.)	Region
1200 x 1000	47.24 x 39.37	Europe, Asia
1200 x 800	47.24 x 31.50	Europe
1219 x 1016	48.00 x 40.00	North America
1140 x 1140	44.88 x 44.88	Australia
1100 x 1100	43.30 x 43.30	Asia

1067 x 1067	42.00 x 42.00	North America, Europe, Asia

The wood pallet sizes which are most commonly used in the United States are presented in Table 3 by industry and percentage of new wood pallet production. The 48 in. x 40 in pallet accounted for 35% of all wood pallets produced in the U.S. in 2016 (Gerber, Horvath, Araman, & Gething, 2020). The percentage of new wooden pallets manufactured according to the pallet size is presented in Figure 8.

Table 3. Most popular wood pallet sizes by industry and percentage of new wood pallet production in the United States in various years *(Gerber, Horvath, Araman, & Gething, 2020)*

Industry	Dimensions (in)	Share of Annual Production (%)
Grocery	48 x 40	35
Military	40 x 48	4
Drums	48 x 48	7
Automotive	48 x 45	5
Chemical, Beverage	48 x 42	3
Beverage, Shingles, Packaged Paper	48 x 36	1
Chemical	42 x 42	5
Beverage	37 x 37	<1
European	800 mm x 1200 mm	1
Various	Other	39

3.5. Materials

There are several different materials used in the pallet construction. Wood pallets dominate the marketplace, followed by other materials, including plastic, paper, wood composite, and metal pallets (Leblanc, 2019). The breakdown of pallet composition remains familiar, as 93% of respondents use wood, more than a third use plastic, while wood composite (14%), metal (6%), and cardboard (4%) bring up the rear (Modern Materials Handling, 2018). The materials used to make pallets will depend on the cost, functionality, and availability of the raw material.

3.5.1. Solid Wood

Wood pallets dominate the marketplace due to their excellent value regarding price and performance (Leblanc, 2019). Wood is a stiff material, inexpensive, and easily fabricated into various sizes as required (Leblanc, 2019).

Solid wood pallets can be made of hardwoods or softwoods and the species varies between different regions. The selected species is usually limited depending on the species that are native to the given manufacturing region. A database of the major resources of U.S. woods according to region can be obtained in the U.S forest service (United States Department of Agriculture Forest Service, 2010).

For pallet production in 2016, the lumber usage between hardwood and softwood was estimated to be 4.1 billion board feet and 5.0 billion board feet, respectively, as presented in Figure 8 (Gerber, Horvath, Araman, & Gething, 2020). This represents a ratio of 45% of hardwood and 55% of softwood. The hardwood market continues to recover from the 2008 downturn, but softwood appears to remain the more popular material for pallet manufacture at this point (Gerber, Horvath, Araman, & Gething, 2020).

Some of the advantages of using wood pallets are that they offer a great combination of weight, stiffness, durability, and cost (Leblanc, 2019).

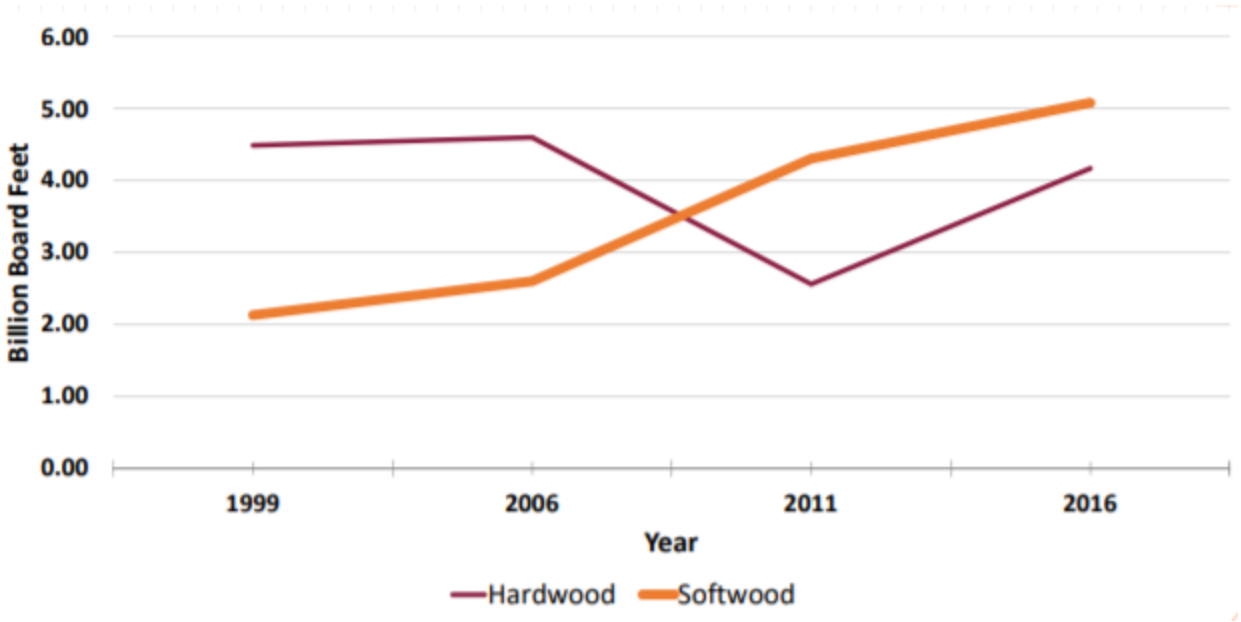

Figure 8. Estimation of Lumber Usage *(Gerber, Horvath, Araman, & Gething, 2020)*

Hardwood used for pallets comes from angiosperm trees that are not monocots. These types of trees are usually broad-leaved and have vessel elements that transport water throughout the wood. Hardwoods are more likely to be found in high-quality furniture, decks, flooring, and construction that needs to last. Some examples of hardwood trees include alder, beech, hickory, maple and oak. They can be found with mixed low density, medium density and high density. Usually, hardwoods have a higher density and slower growth rate compared to most softwoods. Besides, they are typically more expensive than softwood.

Softwood comes from gymnosperm tress which usually have needles and cones. Medullary rays and tracheids transport water and produce sap. About 80% of all timber comes from softwood. Softwoods have a wide range of applications and are found in building components (e.g. windows, doors), furniture, medium-density fiberboard (MDF) and paper, among others. Examples of softwood trees used in pallets are Douglas fir, southern pine and spruce-pine-fir. Most softwoods have a lower density and faster rate of growth than most hardwoods. Also, they are less expensive compared to hardwood.

The main physical characteristics that can be observed between these two types of woods are represented in the Figure 9

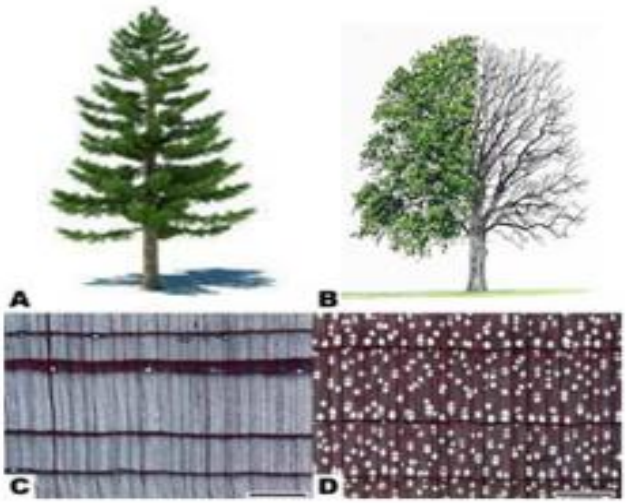

Figure 9. Structure of Hardwood and Softwood. A) general form of a generic softwood tree, B) general form of a generic hardwood tree, C) transverse section of Pseudotsuga mensiezii, a typical softwood, and D) transverse section of Betula allegheniensis, a typical hardwood; the many large, round white structures are vessels or pores, the characteristic feature of a hardwood *(United States Department of Agriculture Forest Service, 2010)*

3.5.2. Plastic

Plastic pallets typically are more expensive than wood pallets for comparable applications but are valued for attributes such as extreme durability, the precision of manufacture, and ease of sanitation (Leblanc, 2019). Plastic is currently the second most common material for pallet manufacturing, with 37% of the United States companies using plastic pallets (McCrea, 2016). Plastic pallets can be composed of durable, high-performance design, or lightweight and inexpensive, suitable for export (Leblanc, 2019). High-density polyethylene (HDPE) and polypropylene (PP) are the two most common types of plastics used for pallet manufacturing (Freedonia, 2015). The main reason for using plastic pallets is their resistance to moisture. Thus, this helps eliminate problems with insects, mold, and product damage due to desorption of the water in the wood.

3.5.3. Wood Composite

Wood composites are another alternative for pallet materials. In the United States, 15% of the companies use composite pallets (McCrea, 2016). The biggest problem addressed by wood composite pallets is the high variability in material properties associated with solid wood (Li,

Wang, & Zhou, 2018). They randomize wood growth variations increasing the overall homogeneity of the pallet (Li, Wang, & Zhou, 2018). Moreover, they have fewer issues relating to moisture than solid wood pallets (Li, Wang, & Zhou, 2018). Due to these material properties, wood composite pallets cost more than solid wood pallets; however, they are usually cheaper than plastic or metal pallets. The disadvantages of wood composite pallets include costly repairs, problems associated with fastener withdrawal, and moisture problems in wet environments when compared to plastic (Li, Wang, & Zhou, 2018). These pallets are mainly used in situations where pest regulations are a concern or where increased durability or strength is needed (Li, Wang, & Zhou, 2018). Examples of wood composites are plywood, LVL, PSL, and OSB.

3.5.4. Metal

Metal is another type of material used in pallet construction. However, due to their high initial cost, only 5% of companies in the United States currently use metal pallets (McCrea, 2016). The primary use of metal pallets is to transport and store heavy loads. Metal pallets are extremely durable, have high strength and stiffness values, and are easy to recycle (Clarke, 2004). These pallets are also free of issues relating to moisture, fasteners, and sanitation (Clarke, 2004). The disadvantages of this kind of materials include a high cost, heavy pallet weight, and low surface friction (Clarke, 2004). Examples of metal used in pallets include carbon steel, stainless steel, and aluminum.

3.5.5. Paper-based

Paper-based pallets are another alternative for pallet materials. While paper-based pallets are lightweight, easy to recycle, and have high adaptability, the price is similar to that of wood pallets (Leblanc, 2019). These pallets tend to have low stiffness, low durability, and a high level of moisture related issues; as such, paper-based pallets are expected to be single-use pallets (Leblanc, 2019).

A comparison between the different types of materials used to construct pallets is shown in Table 4.

Table 4. Characteristics of the Different Types of Pallets *(OSHA, 2018)*

Wood Pallets	Metal Pallets	Plastic Pallets	Corrugated
• Strength and durability • Cost less than other pallet materials • Quick to build and easy to repair • Can be repaired • Breaks down in landfills	• Weather-resistant • Support high weights • Do not rot or decay • Exempt from phytosanitary treatments • Do not splinter • Can be recycled • Good sanitation	• Long lifespan of more than 10 years • Resist humidity and corrosion • Easy to clean • Safe handling due to lack of screws, nails, and splinters. • 100% recyclable • Exempt from phytosanitary treatments	• Exempt from phytosanitary treatments

3.6.Load capacity

When pallets are selected for a determined application, many factors need to be taken into consideration, including size, weight, cost, load capacity, accessibility, stiffness, sanitation, etc. The load capacity of a pallet is a term used to describe the maximum payload that the pallet is capable to handle safely. The load capacity of a pallet is one of its most important characteristics. If the pallet cannot safely handle the payload, then it cannot fulfil one of its fundamental purpose which is the transportation of products.

The load capacity of the pallet can be determined using laboratory testing or computer modeling. The most common standards used to measure the load capacity of the pallet in the United States are ISO 8611 and ASTM D1185.

3.6.1. ASTM D1185

The ASTM D1185 is a standard that establishes the test methods for pallets and related structures employed in materials handling and shipping. The standard differentiates general purpose and special purpose pallets. General-purpose pallets are designed and constructed to support a wide range of loads using a variety of applicable handling devices, while special-purpose pallets are designed and constructed to support a specified load using certain handling devices (ASTM D1185, 2009). Two types of testing are described in the ASTM D1185 standard: static

test and dynamic test. Static tests are performed to determine the strength and stiffness of the pallet under specified load and support conditions (ASTM D1185, 2009). To perform the static tests, uniformly distributed case goods or bag loads are simulated using an inflatable bag or a tube restrained in a testing rig or by using a vacuum chamber (ASTM D1185, 2009). On the other hand, dynamic tests are performed to determine the durability of the pallet when exposed to elements of the handling and shipping environment (ASTM D1185, 2009).

3.6.2. ISO 8611

Another standard used in the industry in materials handling for pallets is the ISO 8611. The ISO 8611 differentiate nominal load and maximum working load tests. Nominal load is the lowest safe load value for the specified support conditions, independent of the type of load, while maximum working load is the greatest payload that a pallet is permitted to carry in a specific loading and support condition (ISO 8611, 2011).

Contrary to ASTM D1185, ISO 8611 uses rigid bars to apply the load instead of an airbag. The standard differentiates several conditions based on the intended use such as handling goods with racking and stacking, stacking without racking, without stacking and racking, and special applications such as conveyor and sling handling. The tests described in the standard are bending test, forklifting test, compression test for blocks or stringers, stacking test, bottom deck bending test and wing pallet bending test.

To determine the load capacity of a pallet, support and loading condition needs to be specified. The most common support conditions include rack support, floor support, fork tine support, conveyor support and sling support. The most common loading conditions include uniformly distributed flexible load, uniformly distributed rigid load, rigid line load, point load, and discrete load by the actual product.

The load capacity of the pallet is determined considering the results of a strength test and stiffness test. During the strength test, a pallet is loaded until ultimate failure is reached. As a result, the load is called Ultimate or Failure Load. The Ultimate Load is then divided by a factor (2 (ISO 8611) to 2.85 (ASTM D1185)) to determine the Test or Creep Load. During the stiffness test, a Test Load is placed on the pallet for a defined period of time (creep time) during which the

deflection of the pallet is monitored. Following the creep time, the test load is removed, and the relaxation of the pallet is determined after a defined period of time (relaxation time). The creep time and relaxation time depend on the testing standard and the material of the pallets. The deflection of the pallet after the creep test is compared to a defined performance criteria published by the standards. If the defection of the pallet after the creep test did not exceed the performance limit, then the Test Load becomes the Safe Load. However, if the deflection of the pallet exceeds the performance limit, then the creep test is conducted again with a lower Test Load. For the purpose of the research project, the ISO 8611 standard is used as a baseline to determine the load capacity of the pallets used in the experiments.

3.7. Industrial Packaging on Pallets

The goods or products, which pallets support, are often transported in industrial packaging. The primary purpose of packaging is to protect the product from different risks. Products should be packaged in a way that the quality, quantity, and property do not decline or damaged from the exposure to the environment, or during the transportation or handling process. Some of the packaging materials used in the industry are corrugated boxes, pails, drums, FIBC, bottles, and plastic containers. The use of the different types of packaging depends on the product to be transported, the cost, the amount, among others.

3.7.1. Corrugated Box

One of the factors that define the properties of the corrugated material is the types of paper used in its fabrication. The two main types of paper that are used for the liners are known as Kraft and Test liners. Kraft paper is manufactured from softwood trees (Daggar, 2019). Due to the "virgin" fibres, it is both the strongest type of paper and also the easiest to print on (Daggar, 2019). As a result, it is the most commonly used outside liner when selecting material to produce corrugated boxes and packaging (Daggar, 2019). On the other hand, Test paper is a double layered (or duplex) paper (Daggar, 2019). Since this type is recycled, Test paper is not as strong as Kraft or easy to print on, so it is commonly used for the inside liner; however, it is less costly than Kraft paper.

Despite Kraft and Test liners are widely used, there are other more options in the industry. The available paper grades for outer and inner liners when manufacturing cardboard are (Daggar, 2019):

- KRAFT (K): Virgin Kraft paper
- TEST 2 (T2): Partly recycled liner paper
- TEST 3 (T): Fully recycled liner
- CHOP (C): Waste based liners
- FULLY BLEACHED WHITE (BW): Fully bleached Kraft liner
- WHITE TOP (WT): White coated recycled liner
- MOTTLED KRAFT (MK): Mottled white Kraft
- OYSTER (OY): Mottled test liner
- SEMI CHEM (SC): Virgin fibres using neutral sulphite semi-chemical process
- WASTE BASED (WB): 100% recycled fibres

The basis weights of paper are also an important property of the corrugated boxes. They are common measured in pounds per square inch. The most common paperweights used for corrugated materials are 115/125GSM, 140/150 GSM, 185/200 GSM and 300 GSM.

Corrugated is a complete, high-performance material design, manufacturing, and delivery system (Fibre Box Association, 2019). Corrugated is the preferred packaging material since it is durable, versatile, lightweight with a high strength-to-weight ratio, sustainable, environmentally responsible, customizable, protective, and cost-effective (Fibre Box Association, 2019). Two main components of corrugated fiberboard or "combined board" are the liner and the medium. Linerboard is the flat material, typically on the outer surfaces of the board but also on the inside for some structure, that adheres to the medium (Fibre Box Association, 2019). Medium is the paper that is formed into arches or flutes on the single facer and glued between the linerboard facings (Fibre Box Association, 2019).

The four types of combined board are single face, single wall (double face), double wall and triple wall. A single face is composed of a corrugated medium and a single sheet of linerboard glued together. A single wall or double face is made of a corrugated medium and two sheets of

liner board (one on each side) that are glued together. A double wall is made of three sheets of linerboard that are glued to two mediums. A triple wall is composed of four sheets of linerboard that are glued to three mediums.

The medium of corrugated boxes has five basic flute classifications also called flute profiles. The classification consists of A flute, B flute, C flute, E flute and F flute. There are also combinations between these flutes. The A flute is the original flute size with approximately 33 flutes per foot (Packsize, 2013). The B flute has smaller flutes than A flute and has approximately 47 flutes per foot (Packsize, 2013). The C flute was created to serve as an all-purpose size and has 38 flutes per foot (Packsize, 2013). The E flute is thinner with 90 flutes per foot (Packsize, 2013). The F flute was created to be used as a folding carton (to hold light to medium weight) and consists of approximately 128 flutes per foot (Packsize, 2013). An example of these flute profiles is illustrated in Figure 10.

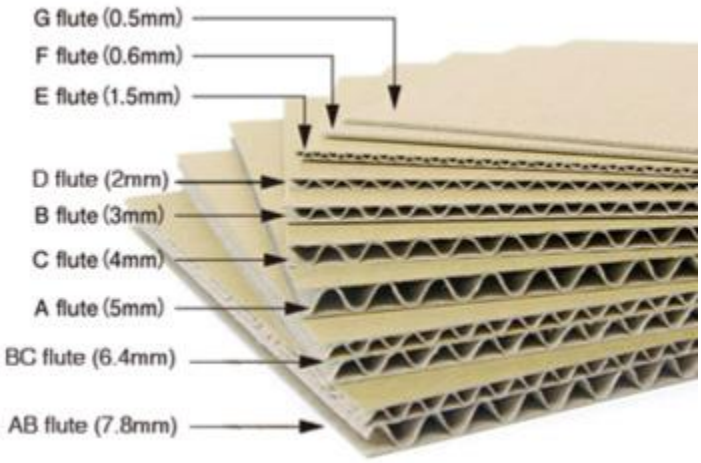

Figure 10. Classification of corrugated box according to the medium fluting *(Deprintedbox, n.d.)*

The performance of the corrugated board is also rated according to ECT and burst test. A basis weight test is performed in the corrugated board. This testing consists of a measurement of mass per unit area that is expressed in pounds per thousand square feet. Basis weight is used to describe linerboard, corrugating medium, and boxes. The Mullen Burst Test measures bursting strength of the corrugated board (iPS Packaging, 2016). The Mullen test presses a rubber diaphragm bubble against the board in a defined area to measure the pounds of pressure per square inch (psi) it takes to burst the board (iPS Packaging, 2016). ECT (Edge Crush Test) measures the

box board's top-to-bottom compression strength (also known as stacking strength) (iPS Packaging, 2016). This test measures the box compression strength and the stacking strength.

The FEFCO (International fibreboard case code) code is an international guideline used for corrugated and solid board packaging design. It contains the design of the most common box types with a code number assigned to each design. Several types of packaging designs are used in the industry. The most common types of corrugated boxes are regular slotted container (RSC), half slotted container (HSC), overlap slotted container (OSC), full overlap slotted container (FOL) and center special slotted container (CSSC) (FEFCO, 2007).

Regular slotted container (RSC) is the most common box style (PCA, n.d.). For this type of box, all the flaps are of the same length, and the two outer flaps are one-half container's width so that they meet at the center of the box when it is closed. Half slotted container (HSC) is similar to the regular slotted container but without one set of flaps.

In the overlap slotted container (OSC), all the flaps have the same length, and the outer flaps overlap around one inch. This type of design is commonly used when the length of the box is considerably greater than the width, resulting in a long gap between the inner flaps. The sealed overlap helps to keep the outer flaps from pulling apart.

In the case of the full overlap slotted container (FOL), all flaps are of the same length. When closed, the outer flaps come within one inch of complete overlap. This style is usually used when the container requires rough handling.

In the case of the center special slotted container (CSSC), the inner and outer flaps are cut to different lengths. Both pairs of flaps meet at the center of the box. This kind of box is especially strong because both the top and bottom have double the thickness of the corrugated board. Each of these packaging designs are shown in Figure 11.

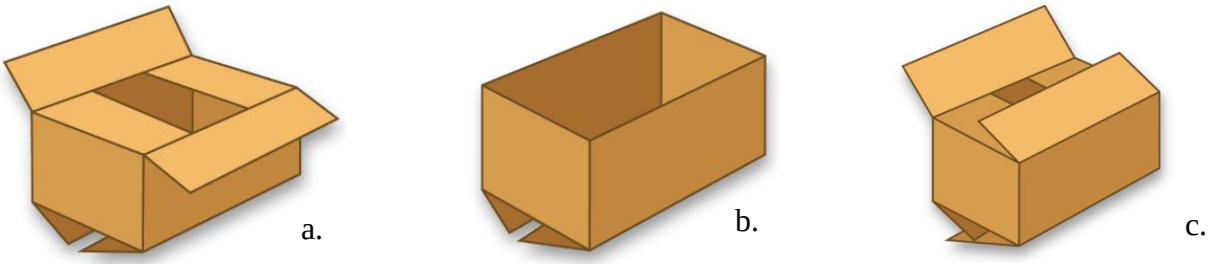

a. b. c.

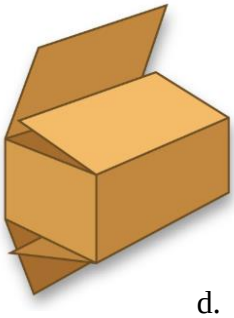

d.

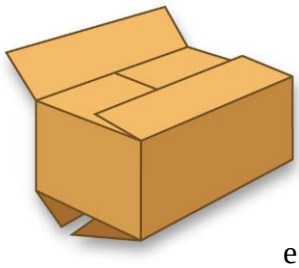

e.

Figure 11. Representative pictures of basic box flat design: a) Regular slotted contained (RSC), b) Half slotted contained (HSC), c) Overlap slotted container (OSC), d) Full overlap slotted container (FOL), and e) Center special slotted container (CSSC) *(PCA, n.d.)*

3.7.2. Reusable Plastic Containers, Small Handheld Containers, or Totes

The use of returnable plastic crates (RPCs) for harvest, packing, transport, and storage have been increasing in recent years since they reduce damage and allow the product to withstand transport over rough roads. Returnable, reusable plastic containers are designed to be durable containers and have become common in the agri-food industry (Vigneault, Thompson, & Wu, 2009).

An important factor to consider when selecting RPCs is the shapes and sizes of plastic crates and the intended use. The use of RPCs is intended to serve two purposes: to ease bulk handling by providing a convenient sized load for handlers, and to provide protection for the product during handling (Kitinoja, 2013). RPCs can be found as a shallow style, medium size, or large crates (Kitinoja, 2013).

Most plastic crates are manufactured from high density polyethylene (HDPE). Polyethylene offers good strength against impact (preventing breakage) and provides a high level of protection against degradation by ultraviolet radiation from sunlight (Rapusas & Rolle, 2009).

There are three typical designs for RPCs, and all three provide for ease of handling and protection of the produce (Kitinoja, 2013). The first type is stackable, but not “nestable”. The crates can be stacked one on top of other; however, they do not fit inside each other (are not nestable). The empty crates take up the same amount of space as full crates. The second type of RPC is made to be nestable when empty. Nestable crates are available in a variety of sizes and shapes and are slightly sloped with a narrower bottom so they can fit “nested” down inside one

another when empty and stacked. The third type of RPC is designed to be collapsible when empty. Collapsible crates take up much less space when empty and folded up (typically $1/5^{th}$ of the space required for a full crate), but can be more difficult to find, more expensive to purchase, and have hinges that can break with repeated use (Kitinoja, 2013). Both designs, the nestable and the collapsible RPC, help reduce the transport costs associated with empty RPC returns. Harvest totes, lugs, and RPCs typically have lengths of less than 28 inches, enabling them to be manually handled with ease (TranPack, n.d.).

3.7.3. Pails

Pails are a steel shipping container, with or without bail or handle, having a capacity of 1 to 12 gallons, inclusive, constructed of steel sheet, 29-gage or heavier, and designed for storage or shipment as an outer package requiring neither boxing nor crating (ANSI MH2, 1991). They are commonly used for packaging and transporting materials. These materials may be solids, liquids, or pastes, aqueous or organic, acidic or alkaline, e.g., detergent solutions, lattices, foods or condiments, fine chemicals, among others (United States Patent No. US4014452A, 1977).

The most common sizes are the three and a half, five- and six-gallon (United States Patent No. US4014452A, 1977). Because of inertness and toughness, plastics such as high-density polyethylene or other inert moldable thermoplastic resins are preferred materials (United States Patent No. US4014452A, 1977). Pails are filled with the contents, capped, perhaps stored, and shipped. They can be stored after they are transported. In storage, these containers are stacked one upon the other. There are two common types of container constructions: the wide mouth or open-head pail and the closed mouth or tight-head pail (United States Patent No. US4014452A, 1977). Pails can be made of steel, tinplate, aluminum, fiber, paperboard, or plastics.

3.7.4. Drums

Drums are defined as a straight-sided cylindrical shipping container having a capacity of 13 to 110 gallons, with or without hoops, having appropriate ends designed for storage and shipment as an unsupported outer package without boxing or crating. There are two types of container constructions: the full-removable-head container and the tight-head container.

Fiber drums provide high strength and low tare weight for the packaging of industrial commodities (Gordon, 2009). Fiber drums are manufactured in a wide range of diameters and capacities: in diameter from about 8 in. (200mm) to 23 in. (584mm) in 1 ½ in. (38 mm) increments, and in capacity from 0.75 gal (2.8L) to 75 gal (285L), with almost infinite variability, since capacity is controlled by the slit width of the tube, which can be adjusted in 1/8 in. (3mm) increments (Gordon, 2009).

3.7.5. Bottles

A bottle is a container, typically made of glass or plastic and with a narrow neck, used for storing drinks or liquids (Vocabulary, n.d.). Plastic bottles can be classified according to the color, shape and material (Bottle & Packaging, Inc., n.d.). The color can be found in natural, white, clear, blue, amber, green, black or purple (Bottle & Packaging, Inc., n.d.). The shape of the bottle includes round, wide mouth, narrow mouth, cosmo, cylinder, oval, oblong and plastic jugs (Bottle & Packaging, Inc., n.d.). The material for the plastic bottle includes PET, LDPE, HDPE, and PVC (Bottle & Packaging, Inc., n.d.).

3.7.6. FIBC

FIBC Bulk Bags, or Flexible Intermediate Bulk Containers, are made of woven polypropylene with lifting straps that allow the container to be filled from top and discharged from the bottom (Material Motion, n.d.). FIBC Bags are suitable for the transport of chemicals, pharmaceuticals, fertilizers, food products, grains and seeds, construction materials such as sand or gravel and plastics.

The standard size bag is 35 inches wide by 35 inches deep by 40 inches tall (commonly known as 35 by 35 by 40) (United States Department of Agriculture Forest Service, 2005).

The types of bags used are 4 panel bags, u panel bags, circular, seamless, or tube bags and baffled bags (Material Motion, n.d.). A 4-panel bulk bag is constructed from 4 separate fabric panels which are stitched together at the edges to form a box (Material Motion, n.d.). A separate sheet of fabric is used to make the square bottom of the bag. U-panel bulk bags consist of a large “U” piece of fabric with 2 side panels sewn to each of the opposite sides. The U-panel bags will maintain a square shape when filled, especially a U-panel bag with baffles (Material Motion, n.d.).

U-panel bags offer high safe working loads and solid durability. The seamless bulk bags are a good alternative to 4 panel bags (Material Motion, n.d.). They are made from fabric woven on a circular loom and cut to a specified bag height. Baffled bulk bags are typically 4-Panel or U-Panel bags that employ internal fabric baffles to improve the bag's squareness and stability (Material Motion, n.d.). These bags are designed to maximize storage and shipping space.

Some of the stitching patterns used to create FIBC Bulk Bags are over lock, single chain, double chain, dust proof and felt stitching (ISO 21898, 2004). All categories of FIBC shall be manufactured from flexible materials (ISO 21898, 2004). The properties of the materials may be modified by additives to improve the resistance of the materials against, for example, degradation by heat and sunlight, and to reduce the effect of static electricity (ISO 21898, 2004).

Depending on the electrostatic properties, FIBC can be classified as Type A, Type B, Type C or Type D. Type A bulk bags does not present electrostatic safety features (Material Motion, n.d.). Type B bulk bags are not capable of generating propagating brush discharges (Material Motion, n.d.). The wall of this FIBC exhibits a breakdown voltage of 4 kilovolts or less (Material Motion, n.d.). Type C bulk bags are conductive FIBC (Material Motion, n.d.). They are constructed from electrically conductive fabric, designed to control electrostatic charges by grounding (Material Motion, n.d.). Type D bulk bags are anti-static FIBCs, essentially refers to those bags which have anti-static or static dissipative properties without the requirement of grounding (Material Motion, n.d.).

3.7.7. Sacks / Multi Wall Bags

Multiwall paper sacks are concentric tubes of one to six layers (or plies) of paper with a choice in the type of end closure (Kirwan, 2012). The designs of multiwall paper sacks differ mainly in respect of whether the sack is to be filled through an open mouth or a valve, which in turn depends on the product and the volume to be handled (Kirwan, 2012). Valve sacks are closed manually or automatically and can be equipped with valve sealing; while open mouth sacks can equally be sealed manually or automatically with various methods, including sealing through hotmelt, sewing, etc (Kirwan, 2012).

The materials used in multiwall paper sacks are divided into those of the sack body and the ancillary materials. The construction of a multiwall paper sack is based on the use of sack kraft, which is a strong and durable and versatile paper that can be coated, laminated with other materials, modified to give it additional strength properties, printed, glued and sewn in the converting operations to produce a product of high strength and quality (Kirwan, 2012).

3.8.Load Containment Force

Load containment force is defined as the amount of force that is applied by a stretch wrap to secure packages stacked on the pallet. Elastic recovery, the tendency of stretch wrap to return to its initial state after being stretched, is directly related to load containment forces; hence, films with a higher elastic recovery will exhibit a greater containment force (Bisha, 2012). Stretch film will elongate when a pulling force is applied although how it elongates depends on its temperature, speed of elongation and the volume of material tested (Bisha, 2012).

Stretch wrap films have various applications in the industry. Tensioned stretch film may be used to secure a handling base (skids, platforms, pallets, slip sheets, etc.) to a unit load to expedite handling (tertiary package); to secure cushioning, edge protection, or other package components to an individual item (office furniture, windows, etc.) (primary/secondary package); as a primary protective wrap for individual products (rolled products, metal coils, etc.) (primary package; to bundle multiple products and provide surface protection (metal extrusions, wood molding) (primary package); and/or be applied to rolled forage crops to facilitate the decomposition into silage (primary package) (ASTM D4649, 2009).

Stretch wrap is applied to unit loads using one of three methods based on the level of automation required: manual, semi-automatic, or fully automatic (Bisha, 2012). The manual stretch wrapping method requires no automation, and instead, the unit load is wrapped by hand. Although this method does not require equipment, it is a labor-intensive process subject to inaccuracy and uneven containment. Semi-automated application is when the unit loads are manually loaded onto stretch wrappers, and once in place, the machine applies the stretch wrap (Bisha, 2012). Fully automated stretch wrappers are able to load and stretch wrap the unit loads without physical labor, usually through the use of conveyors and electronic sensors (Bisha, 2012).

3.9. Vibration

In distribution and packaging, vibration is a mechanical phenomenon very common in transport vehicles, forklifts, conveyors, etc, that affect every packaged product during the handling and transportation process. The vibration produced is not smooth oscillatory motion, it is a shaped mix of various frequencies and amplitudes, constantly changing (ISTA, 2013). Vibration spectra (graphs of amplitude plotted against frequency) are average of these changing conditions over time (ISTA, 2013). A representation of vibration data in an acceleration versus time plot is shown in Figure 12.

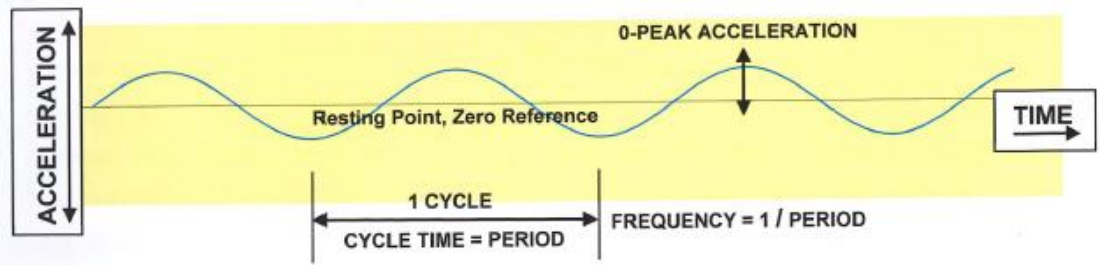

Figure 12. Representation of vibration data in an acceleration vs time plot *(ISTA, 2013)*.

Vibration data is often collected in a time-domain; however, it is difficult to describe the characteristics of the motion or use it as a control target for the random vibration test system. Therefore, the Power Spectral Density (PSD) plot is an alternative way to present vibration data. PSD plot charts the average intensity of the vibration against the frequency of the vibration (ISTA, 2013). This new form is a frequency-domain representation, where the horizonal axis is frequency. A representation of a PSD plot is shown in Figure 13.

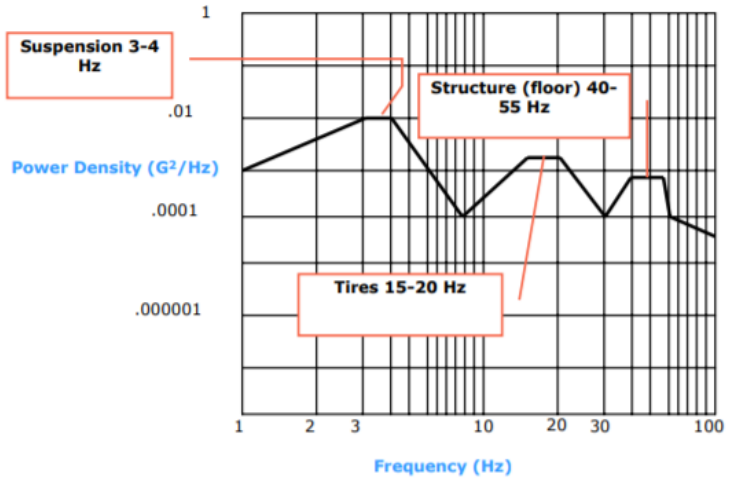

Figure 13. Example of a PSD plot *(Singh, Singh, & Joneson, 2006)*

Random vibration PSDs are also specified in terms of their "overall Grms" (ISTA, 2013). This is a number which gives the intensity, in G, averaged with the root-mean-square calculation, over the entire frequency band of interest (ISTA, 2013). Graphically it is proportional to the area under the PSD profile (ISTA, 2013).

Several studies have been conducted to study the vibration levels produced by different mode of transport. Singh et al. (2010) have conducted extensive research to study the vibration levels observed for truck and rail shipments. Specifically, this research was conducted in Thailand to analyze the vibration levels in three axes (vertical, lateral, and longitudinal) of a truck and rail. They concluded that the vertical vibration levels measured in both truck and rail shipments were the highest, followed by lateral and longitudinal levels.

Another study conducted by Singh, Singh, and Joneson (2006), mentioned that the vibration levels inside a tractor-trailer are a function of the road surface, the speed of the vehicle, the type of suspension and the structure of the trailer.

In addition, Singh et al. (2007) captured the vibration levels for several material handling equipment. The study measured the vibration levels experienced by four commonly used manual push carts and a manually operated pallet jack, and two types of powered forklift trucks. The study concluded that vibration levels were higher in the outside track as compared to the inside track because of the surface irregularities. Additionally, the vibration level and frequencies measured

from the material handling equipment occur at a higher frequency (8-30 Hz) as compared to most transportation vehicle vibrations (2-8 Hz) (Singh S. P., Singh, Gaur, & Saha, 2007).

3.10. Package-Pallet Interaction

Unit load interactions can be analyzed in two different ways. The first method is by determining the effect of the pallet on the packages and the second method is by determining the effect of the packages on the pallet. There are several factors such as the box overhang (Monaghan and Marcondes, 1992), deckboard gap (Monaghan and Marcondes, 1992 and Baker, 2016), deckboard stiffness (Baker, 2016, Phanthanousy, 2017), stacking configuration (Singh et al., 2011 and Meng et al. 2007), and the contents of the packages (Frank et al., 2010) affect the strength of corrugated boxes.

Recent studies have focused on understanding how packages affect the performance of the pallet. For design and testing methods, a uniformly distributed loading on the pallets is assumed, commonly using airbags as load applicators as shown in Figure 14. But in real case scenarios, the actual load on pallets differs from airbags and do not distribute uniformly.

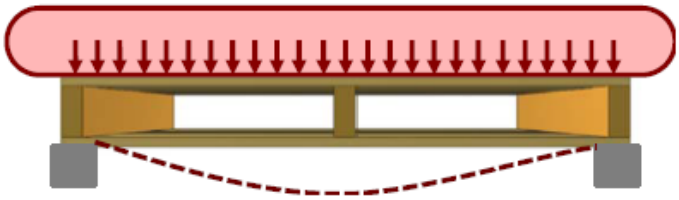

Figure 14. Pallet racked across the width under uniformly distributed loading with an airbag *(Molina, 2017)*

3.10.1. Support conditions

The most common support conditions that can be observed in a warehouse are floor support, fork tine support, rack support and conveyor support. Molina (2017) conducted a research to analyze the effect of pallet stacking pattern on unit load bridging in four support conditions: floor support, pallet bending racked across the width, pallet bending racked across the length, and pallet bending using forklift support across the width. In the case of the fork tine support, it was observed

that the highest deflection occurs in lowest stiffness pallet. Figure 15 shows a scheme of how the load is transferred in a column stacked unit load on a forklift support condition.

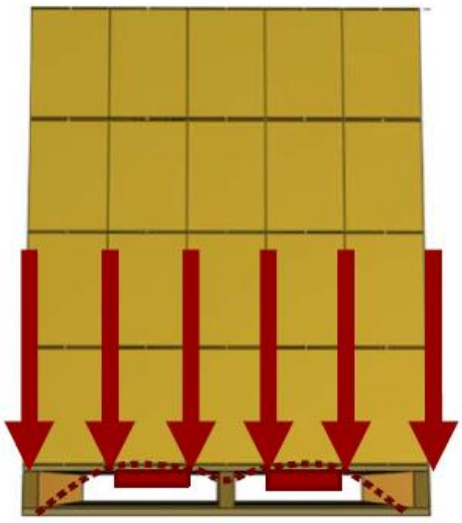

Figure 15. Load transfer schematic of a column stacked Unit Load on a forklift support across the width *(Molina, 2017)*

When unbound unit loads are loaded on pallet, there is a tendency of the boxes to bend toward the outside of the pallet due to the bending of the pallet, as shown in Figure 16.

Figure 16. Example of a column stacked unit load supported on a forklift.

3.11. BIBLIOGRAPHY

1. Adaptalift. (2013). *Pallet Design Types*. Retrieved from Logistics & Materials Handling: https://www.aalhysterforklifts.com.au/index.php/about/blog-post/pallet_design_types
2. ANSI MH2. (1991). *American National Standard for Materials Handling (Containers) - Steel Drums and Pails.* United States of America: American National Standards Institute.
3. ASTM D1185. (2009). *ASTM D1185-98a: Standard Test Methods for Pallets and Related Structures Employed in Materials Handling and Shipping.*
4. ASTM D4649. (2009). *Standard Guide for Selection and Use of Stretch Wrap Films.* Pennsylvania: ASTM International.
5. Athens. (n.d.). *Athens: Paper, Packaging, Wide Format*. Retrieved from Containment Force: http://www.athenspaper.com/containment-force/
6. Bisha, V. J. (2012). *Correlation of the Elastic Properties of Stretch Film on Unit Load Containment.* (Doctoral dissertation). Virginia Polytechnic Institute and State University: Blacksburg, VA.
7. Bottle & Packaging, Inc. (n.d.). *Plastic Bottles*. Retrieved from SKS: Bottle & Packaging: https://www.sks-bottle.com/340c/SearchIndexPlastic.html
8. Chonhenchob, V., Singh, S. P., Singh, J. J., Sittipod, S., Swasdee, D., & Pratheepthinthong, S. (2010). Measurement and Analysis of Truck and Rail Vibration Levels in Thailand. *Packaging Technology and Science*, 91-100.
9. Clarke, J. (2004). *Pallets 101: Industry Overview and Wood, Plastic, Paper & Metal Options*. Retrieved from https://abe.psu.edu/research/bio-based-products/wood-packaging/publications/articles-from-non-penn-state-authors/pallets-101-industry-overview-and-wood-plastic-paper-metal-options
10. Conner Industries. (2019). *Block pallet vs stringer pallet*. Retrieved from Conner Industries: https://www.connerindustries.com/block-pallet-vs-stringer-pallet/
11. Daggar, J. (2019). *Corrugated board grades explained: types of cardboard*. Retrieved from GWPGroup: https://www.gwp.co.uk/guides/corrugated-board-grades-explained/
12. Deprintedbox. (n.d.). *Corrugated Board for Corrugated Box*. Retrieved from Deprintedbox: https://www.deprintedbox.com/corrugated-board-for-corrugated-box.php
13. Diff, J. (2019). *The complete buyer's guide to plastic* . Retrieved from Reusable Transport Packaging agriculture containers: https://reusabletranspack.com/2019/05/the-complete-buyers-guide-to-plastic-agriculture-bins/
14. East Riding Sacks Limited. (n.d.). *Valve Paper Sacks*. Retrieved from East Riding Sacks Limited: http://www.eastridingsacks.com/valve-paper-sacks/
15. FEFCO. (2007). *International fibreboard case code.* Belgium: FEFCO.
16. Fibre Box Association. (2019). *What is Corrugated*. Retrieved from Fibre Box Association: https://www.fibrebox.org/info/WhatIsCorrugated.aspx
17. Freedonia. (2015). *Pallets*. Retrieved from Freedonia: https://www.freedoniagroup.com/industry-study/pallets-3033.htm
18. Gerber, N., Horvath, L., Araman, P., & Gething, B. (2020). Investigation of New and Recovered Wood Shipping Platforms in the United States. *BioResources*, 2818-2838.
19. Gordon, G. (2009). Drums, Fiber. In K. Yam, *The Wiley Encyclopedia of Packaging Technology* (pp. 368-382). Massachusetts: Wiley Publication.
20. Herbert, G. (1977). *United States Patent No. US4014452A.* Retrieved from https://patents.google.com/patent/US4014452A/en

21. Holocene Solutions Inc. (n.d.). *Pallets*. Retrieved from Holocene Solutions Inc.: http://holocene.biz/pallet/
22. iPS Packaging. (2016). *Packaging 101: The Corrugated Box*. Retrieved from iPS Packaging: https://www.ipack.com/solutions/packaging-101-the-corrugated-box/
23. ISO 21898. (2004). *ISO 21898: Packaging — Flexible intermediate bulk.*
24. ISO 6780. (2003). ISO 6780:2003. *Flat Pallets for Intercontinental Materials Handling - Principal Dimensions and Tolerances*.
25. ISO 8611. (2011). *Pallets for materials handling - Flat pallets - Part 2.*
26. ISTA. (2013). *CPLP Technologist: Package Vibration Testing.* ISTA.
27. Kirwan, M. J. (2012). *Paper and Paperboard Packaging Technology.* Oxford, UK: Blackwell Publishing Ltd.
28. Kitinoja, L. (2013). *Returnable Plastic Crate (RPC) systems can reduce postharvest losses and improve earnings for fresh produce operations.* Oregon: The Postharvest Education Foundation.
29. Leblanc, R. (2019, July 15). *Introduction to Pallet Usage*. Retrieved from Packaging Revolution: https://packagingrevolution.net/pallets-introduction-to-pallet-usage/
30. Leblanc, R. (2019, July 30). *Pallet Uses and Design*. Retrieved from Sustainable Businesses: https://www.thebalancesmb.com/what-is-a-pallet-2877860
31. Li, J., Wang, J., & Zhou, J. (2018). The reliability-based design and optimization procedures for a heavy-duty pallet system. *Sage Journals*, 1-11.
32. Loferski, J. R. (1985). *A Reliability Based Design Procedure for Wood Pallets.* Virginia Polytechnic Institute and State University, Blacksburg, VA.
33. Material Motion. (n.d.). *FIBC Bulk Bags*. Retrieved from Material Motion, Inc: https://www.materialmotion.com/industrial/bulk-bags
34. McCrea, B. (2016). *Pallet Usage Report: Remain Critical in the Modern-Day Warehouse*. Retrieved from Modern Materials Handling: https://www.mmh.com/article/pallets_remain_critical_in_the_modern_day_warehouse
35. MH1. (2016). *MH1-2005 Pallets, Slip Sheets, and Other Bases for Unit Loads.*
36. Modern Materials Handling. (2018). *The Pallet Report*. Retrieved from Modern Materials Handling: https://www.mmh.com/article/the_pallet_report_users_want_more_service_support
37. Molina, E. (2017). *Investigation of Pallet Stacking Pattern on Unit Load Bridging.* Virginia Polytechnic Institute and State University, Blacksburg, VA.
38. NWPCA. (2014). *Uniform Standard for Wood Pallets*. Retrieved from https://www.palletcentral
39. OSHA. (2018). *Types of Pallets and When to Use Them*. Retrieved from OSHA: https://www.certifyme.net/osha-blog/types-of-pallets-and-when-to-use-them/
40. Packsize. (2013). *Corrugated Cardboard for Packaging and Shipping Boxes*. Retrieved from Packsize: on demand packaging: https://www.packsize.com/know-your-different-types-of-corrugated-cardboard/
41. PCA. (n.d.). *Basic Designs*. Retrieved from Packagingcorp: https://www.packagingcorp.com/basic-designs
42. Plastic2go. (n.d.). *Vented Plastic Crate*. Retrieved from Plastic2go: https://www.plastic2go.com.au/products/plastic-crates/600x400/vented-iso-crate/c2g6418u/
43. Primorsk Supply. (2019). *Pallet's Manufacture*. Retrieved from Primorsk Supply: https://primorsksupply.com/manufacture/

44. Rapusas, R., & Rolle, R. (2009). *Management of reusable plastic crates in fresh produce supply chains - A technical guide.* RAP Publication.
45. Raymond. (n.d.). *One Sided Pallet*. Retrieved from Raymond: Handling Concepts Corporation: https://raymondhandling.com/dictionary/one-sided-pallet/
46. Singh, J., Singh, P., & Joneson, E. (2006). Measurement and Analysis of US Truck Vibration for Leaf Spring and Air Ride Suspensions, and Development of Tests to Simulate these Conditions. *Packaging Technology and Science*, 309-323.
47. Singh, S. P., Singh, J., Gaur, P., & Saha, K. (2007). Measurement and Analysis of Vibration Levels on Warehouse and Retail Store Material Handling. *Applied Packaging Research*.
48. Smurfit Kappa. (n.d.). *Open Mouth Sacks*. Retrieved from Smurfit Kappa: https://www.smurfitkappa.com/products-and-services/packaging/open-mouth-sacks
49. The Solid Waste Management Coordinating Board and the Reusable Pallet & Coalition. (n.d.). *Reusables 102: A Cost Comparison Model for Reusable Transport Packaging.* Minneapolis & Washington D.C.
50. TranPack. (n.d.). *Returnable Plastic Crates*. Retrieved from TranPack: https://www.tranpak.com/handheld-plastic-crates/returnable/
51. United States Department of Agriculture Forest Service. (2005). *Reusable flexible intermediate bulk containers*. Retrieved from United States Department of Agriculture Forest Service: https://www.fs.fed.us/t-d/pubs/pdf/hi_res/05571304hi.pdf
52. United States Department of Agriculture Forest Service. (2010). *Wood Handbook.* Wisconsin: Forest Products Laboratory.
53. Vigneault, C., Thompson, J., & Wu, S. (2009). Chapter 2: Designing container for handling fresh horticultural produce. In C. Vigneault, J. Thompson, & S. Wu, *Postharvest Technologies for Horticultural Crops* (pp. 25-47). Noureddine Benkeblia.
54. Vocabulary. (n.d.). *Bottle*. Retrieved from Vocabulary: https://www.vocabulary.com/dictionary/bottle
55. Wiemann, M. (2010). Characteristics and Availability of Commercially Important Woods. In U. Agriculture, *Wood Handbook* (pp. 16-55). Wisconsin: United States Department of Agriculture.

5. Study # 1. Measurement and Analysis of Industrial Forklifts Vibration Levels for Unit Load Testing Purposes

Yu Yang Huang[1], Laszlo Horvath[1], and Péter Börocz[2]

[1] Department of Sustainable Biomaterials, Virginia Tech; 1650 Research Center Dr, Blacksburg VA 24060, USA

[2] Department of Logistics and Forwarding, Széchenyi István University, Egyetem tér 1, Hungary 9026, Győr

Keywords: vibration; forklift; PSD (power spectral density)

Reference: Y.Y. Huang, L. Horvath, P. Böröcz, "Measurement and Analysis of Industrial Forklifts Vibration Levels for Unit Load Testing Purposes." Applied Sciences 11, no. 7 (March 2021): 2901. https://doi.org/10.3390/app11072901.

5.1. Abstract

Forklifts are one of the most common types of material handling equipment used in warehouses and distribution centers. Vibration generated by forklifts may have an effect on the performance of unit loads and product damage rates. Historical research projects focused predominantly on the measurement of vibration for over-the-road transportation. Thus, there is still a lack of understanding of the level of vibration caused by forklifts. The goal of this study was to understand how the vibration that is experienced by unit loads while being transported by forklifts is affected by factors such as speed, road condition, unit load weight, type of forklift, and sensor location.

For the study, power spectral density (PSD) measurements were collected using a Lansmont Saver 9X30 data logger. Vibration levels were measured for three different industrial forklifts on two different surface types. The forklifts were driven at two different speeds while carrying two different unit load weights. For all of these conditions, the vibration levels were measured at the forklift carriage, at the back of the fork tine heel, and at the fork tine tips. The results obtained showed that the highest vibrational intensity occurred at 3 – 4 Hz, while the highest overall Grms value observed was 0.145 G^2/Hz (between 1 – 200 Hz). An increase in the forklift speed caused an increase in vibration intensity. In contrast, an increase in the unit load weight carried by the forklift caused a decrease in vibration intensity. Among the three forklifts studied, the gas-powered forklift had the highest vibration intensity, and all forklifts, when driven on asphalt, experienced more vibration.

5.2. Introduction

In recent decades, an increase in free trade across all regions of the world has al-lowed the global distribution of products. Products that are produced for domestic markets now face the challenge of having to compete in international markets. Current global manufacturing and distribution systems force products and materials to be moved through poorly understood distribution environments (Böröcz, 2019).

In most cases, damage to products and packages can be attributed to the various vibration forces that occur during distribution. Vibration is an important factor to product survivability. Truck vibration during transport has been recognized as a source of product damage (Brandenburg & Lee, 2001; Kipp, 2008).

Vibration is a mechanical phenomenon produced by transport vehicles, forklifts, conveyors, etc., that affects every packaged product during the handling and transportation process. This phenomenon consists of a periodic motion that repeats itself after a certain interval of time. Vibration produced by these types of material handling equipment is not a smooth oscillatory motion; it is a shaped mix of frequencies and amplitudes that are constantly changing. Since vibration is a continuously occurring phenomenon, it may produce mechanical failures, a fatigue failure, cosmetic damages, undesirable settling of contents, the breaking of solid/liquid suspensions, static charge buildup, bottle-closure cap back-off causing leak of fluids and powdered products (Garcia-Romeu-Martinez et al., 2008).

In most of the studies conducted, vibration data is often collected in a time-domain, where the horizontal axis is the time. However, it is difficult to describe the characteristics of the motion or use it as a control target for the random vibration test system. Thus, the Power Spectral Density (PSD) plots are used instead for data analysis. PSD plots chart the average intensity of the vibration against the frequency of the vibration (Brandenburg & Lee, 2001). This form is called frequency-domain representation, where the horizonal axis is frequency. Random vibration PSD plots are also specified in terms of their “overall Grms.” This root- mean-square (RMS) calculation is used to average the PSD plots to obtain a number which gives the intensity, in G, over the frequency spectrum of interest.

Many studies have been conducted previously to study the vibration levels produced by different modes of transport in multiple countries, such as heavy trailer-truck and railcars (Böröcz & Singh, 2017; Singh et al., 2007; Chonhenchob et al., 2010; Singh et al., 2012; Park et al., 2020) and medium and small trucks (Böröcz & Singh, 2018; Chonhenchob et al., 2012; Böröcz & Molnár, 2020). Some of the former studies measured the effect of distribution circumstances to vibration as a function of road conditions, truck speeds, suspension systems, or payloads (Garcia-Romeu-Martinez et al., 2008; Lu et al., 2010; Böröcz, 2017; Singh et al., 2006). In addition, these studies revealed that intensity of vibration in transportation is related to various factors such as speed and driving performance, road conditions and quality, load conditions, and truck suspension systems.

Materials and products are also moved around within warehouses. Warehousing is becoming a critical activity in trade enterprises in order to outperform competitors on productivity, lead time, and customer service (Burinskiene, 2012). The most common type of material handling equipment in a warehouse is the forklift (Mejias, 2020; Singh & Marcondes, 1992).

Forklifts play an important role in the global distribution of packaged products. Moreover, they have a major impact in the economic growth of the industry. There are more than 540,000 powered industrial truck operators currently employed in the United States alone, operating in all 50 states, and working in more than 300 different industries. According to the needs of the user, forklifts can come in a variety of designs, sizes, engine types, and load capacities. Forklift vibration levels are mainly dependent on the type of forklift structure, speed, payload, and road roughness, respectively.

Although many published papers have focused on the exposure of vibration to the human body in forklift operators, these papers primarily observed and analyzed the vibration circumstances over the seat location (Blood et al., 2010; Motmans, 2012; Botelho & Matos, 2017). There are no studies that have been conducted with the aim of packaging testing purposes that have obtained vibration data at or around the fork tines. Therefore, the purpose of this study was to measure and analyze the vibration levels of common forklift types using different handling conditions. The research was developed in a laboratory environment that simulated different handling environments. The main objective of this project was to analyze the vibration levels experienced by different industrial forklifts under different conditions.

5.3. Objectives

- Measure vibration levels experienced by a gas-powered forklift, electric-powered forklift, and a reach truck.
- Analyze the effects of road conditions, unit load weight, speed, forklift type, and sensor location on the vibration levels.
- Determine the most conservative vibration profile to create a testing procedure in order to measure pallet deflection in a dynamic environment.

5.4. Materials

Study 1 consisted of determining the vibration levels experienced by industrial forklifts under different conditions. A comprehensive analysis was conducted in under to determine the effect of factors such as forklift types, sensor locations, speed, unit load payload, and road conditions in forklift vibration levels. The analysis of the vibration levels collected from the forklifts was performed using MICROSOFT EXCEL (Microsoft Corporation, Redmond, Washington, USA) and MATLAB R2020a (MathWorks Inc., Massachusetts, USA). Additionally, the analysis was done using power spectral density (PSD) plots and G_{rms} values to analyze the effects of speed, road conditions, forklift type, unit load weight, and sensor location on forklift vibration levels.

PSD plots were prepared from the measured vibration data using fast Fourier transformation (FFT) of Xware software and MATLAB R2020a (MathWorks Inc, Natick, Massachusetts, USA). The values of the power density (PD) levels are presented between 1–200 Hz. This frequency range represents the vibration events that do not have enough intensity to influence the integrity of the product-package systems in general industry use. For easier comparability, the spectrum of the International Safe Transport Association (ISTA) 3B test procedure's (ISTA Procedure 3B, 2011) vibration profile is also shown in the figures.

Furthermore, this frequency range contains vibration responses that can be observed in small vehicle delivery from the vehicle body structure, suspension system, tire type, etc. Additionally, the overall G_{rms} were calculated from the PSD spectra in each case and layer between

1–200 Hz. This way each vibration environment could be compared by the vibration intensity in the frequency range between 1–200 Hz that was generated by each of the three industrial forklifts under the different handling scenarios.

Statistical analyses of the collected vibration events were performed with the MATLAB R2014a software to find the calculated G_{rms} values, which helped to more thoroughly understand the nature of the vibrations. These statistical characteristics show the kurtosis (K) of the probability distribution functions for these events using a 95% confidence interval (CI). The definition of kurtosis is as follows: when the standard normal distribution has a kurtosis of zero, then a positive kurtosis indicates a "heavy-tailed" distribution, compared to a normal Gaussian distribution. Presenting kurtosis values is very important because the random vibration testing controller in the laboratory, when engineers want to simulate vibration circumstances, mostly generates a control signal from normal distribution so that field measured kurtosis can be used as an input parameter to perform realistic variability for the random signal during vibration simulation in the laboratory.

4.1. Forklifts

Three types of forklifts were investigated including a CLARK CQ30L, CLARK TMG15, and a CROWN 5200 Series, as shown in Figure 17. The CLARK CQ30L is a four wheeled, sit-down cantilever, gas propane powered forklift with pneumatic tires and 4,800 lbs maximum load capacity. The CLARK TMG15 is a three wheeled, sit-down cantilever, electric powered forklift with solid tires and 2,600 lbs maximum load capacity. The CROWN 5200 Series is an electric powered reach truck with solid tires and 3,500 lbs maximum load capacity. The study was conducted using 42 in. long fork tines on each of the industrial forklifts. Table 5 presents the characteristics of the forklifts used in the study.

Figure 17. Representative pictures of the investigated forklifts: a) gas-powered forklift, b) electric-powered forklift, c) reach truck.

Table 5. Characterization of the forklifts used in the study

Characteristic	Gas-powered forklift	Electric-powered forklift	Reach truck
Model	CLARK CQ30L	CLARK TMG15	CROWN 5200
Production year	2009	1999	2006
Load capacity (lbs)	6,600	3,500	4,000
Any Suspension	None	None	None
Wheels (front / back)	2 / 2	2 / 1	4 / 2
Diameter (in.) (front / back)	27 / 22	18 / 18	5 / 13 & 8
Tire pressure (bar) (front / back)	10 / 8.8	None	None

4.2. Road conditions

To capture the vibration levels experienced by the three types of forklifts on different operation surfaces, the study was conducted both inside and outside the laboratory facility. The internal floor surface used for this study comprised of concrete flooring. On the other hand, the external surface analyzed comprised of asphalt flooring, as shown in Figure 18.

Figure 18. Investigated road conditions: a) concrete, b) asphalt

4.3. Load conditions and forklift speed

The vibration levels of the forklifts were recorded according to the load carried. Two levels of semi rigid payloads were used in this study (1,500 lbs and 2,500 lbs) The load was carried on top of a 48 in. x 40 in. block class, 4-way, non-reversible, perimeter base wooden pallet. Each of these were driven at two different travel speeds (2mph and 3mph).

5.5. Methods

The intensity of vibration caused by forklifts were measured using a Lansmont SAVER 9X30 data logger (Lansmont Corporation, Monterey, California, USA) under different handling scenarios. The data recorder is a battery-powered instrument capable of measuring and recording shock (impact/drop), vibration, temperature, and humidity conditions. Two three-axis accelerometers (DYTRAN 3443C, Chatsworth, California, USA) were connected to the Saver 9x30 data logger to record data in three different positions of the forklift.

All SAVER 9X30s were configured with the following recording setup:

- Sampling rate: 1000 Hz
- Recording window for PSD: 15 s
- Total recording period: 15 min
- Anti-Aliasing filter frequency: 200 Hz
- Sample size: 15,000
- PSD resolution: 0.066 Hz

Additional details of the recording setup for SAVER 9x30 are provided in Figure 19.

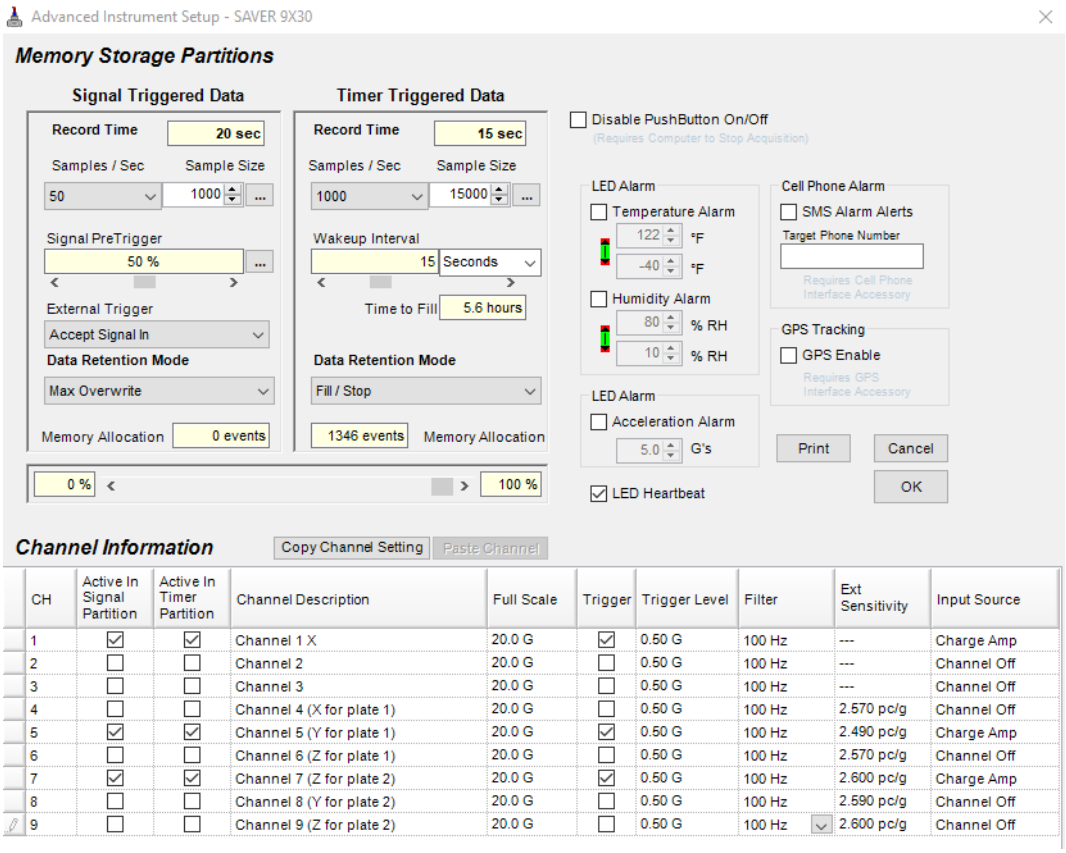

Figure 19. SAVER recording setup

Vibration profiles were collected from three different positions, as shown in Figure 20. Sensor 1 was placed on the carriage of the forklift. Sensor 2 was placed on the back of the heel of the fork tines, and sensor 3 was placed on the tip of the fork tines. The Saver 9X30 was mounted to the carriage using a magnetic mount. The two three-axis accelerometers were connected to the back of the fork tine heel and the fork tine tip using wax and tape to provide extra security. To collect the vibration data, the forklifts were driven on the different road conditions for 15 min, and recording was conducted only when the forklifts were in motion.

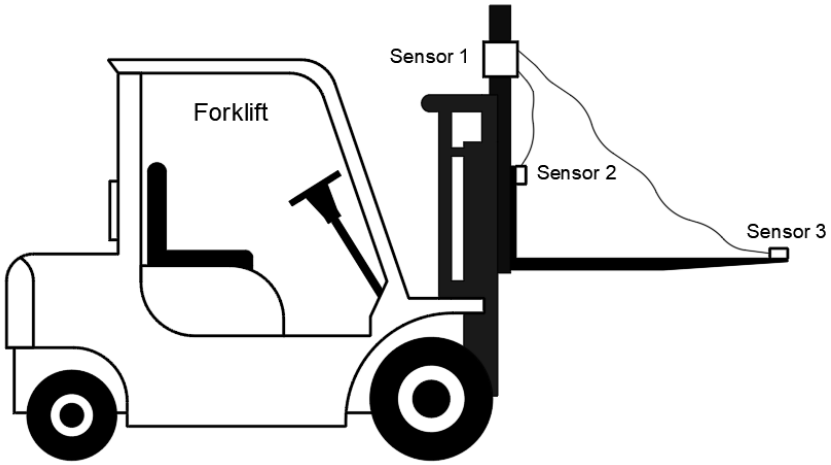

Figure 20. Sensor locations for vibration data collection

5.6. Experimental Design

The experimental design used in order to study the different forklift vibration intensities is stated on Table 6.

Table 6. Experimental design used in order to measure forklift vibration levels

Road Condition	Forklift Type	Load Weight	Speed	Sensor Location
Asphalt	Electric Forklift	1,500	2	Carriage
				Tip
			3	Carriage
				Tip
		2,500	2	Carriage
				Tip
			3	Carriage
				Tip
	Gas Forklift	1,500	2	Carriage
				Tip
			3	Carriage
				Tip
		2,500	2	Carriage
				Tip
			3	Carriage
				Tip
Concrete	Reach Truck	1,500	2	Carriage

				Tip
			3	Carriage
				Tip
		2,500	2	Carriage
				Tip
			3	Carriage
				Tip
	Electric Forklift	1,500	2	Carriage
				Tip
			3	Carriage
				Tip
		2,500	2	Carriage
				Tip
			3	Carriage
				Tip
	Gas Forklift	1,500	2	Carriage
				Tip
			3	Carriage
				Tip
		2,500	2	Carriage
				Tip
			3	Carriage
				Tip

5.7. Results and Discussion

The overall G_{rms} (1-200 Hz) and the kurtosis values for distributions of G_{rms} values are presented in Table 7, while the trends in overall G_{rms} for the carriage and the tip of the forklift tines are presented in Figure 21 and Figure 22. Out of the three locations investigated, the data obtained for the carriage and the back of the fork tine heel was identical. Thus, only the data obtained for the carriage and the tip of the fork tines was further analyzed. Based on the overall G_{rms} values, forklifts experience higher vibrations on the tip of the fork tine compared to the carriage.

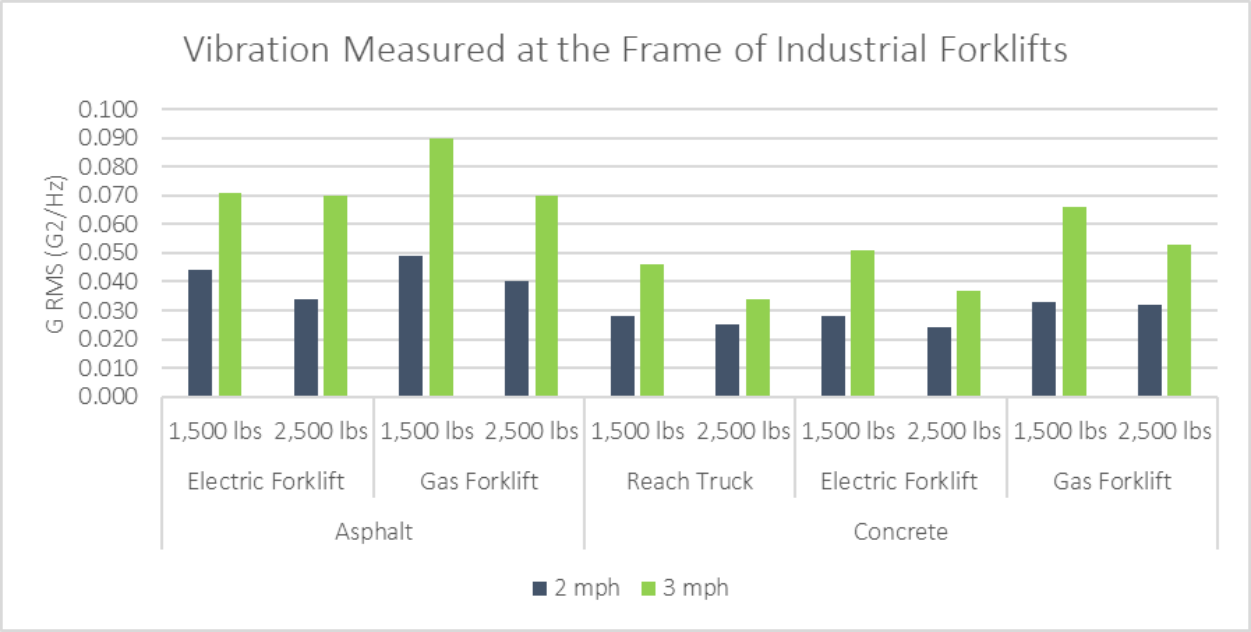

Figure 21. Overall vibration intensity measured at the carriage for each of the three forklifts (1 – 200 Hz).

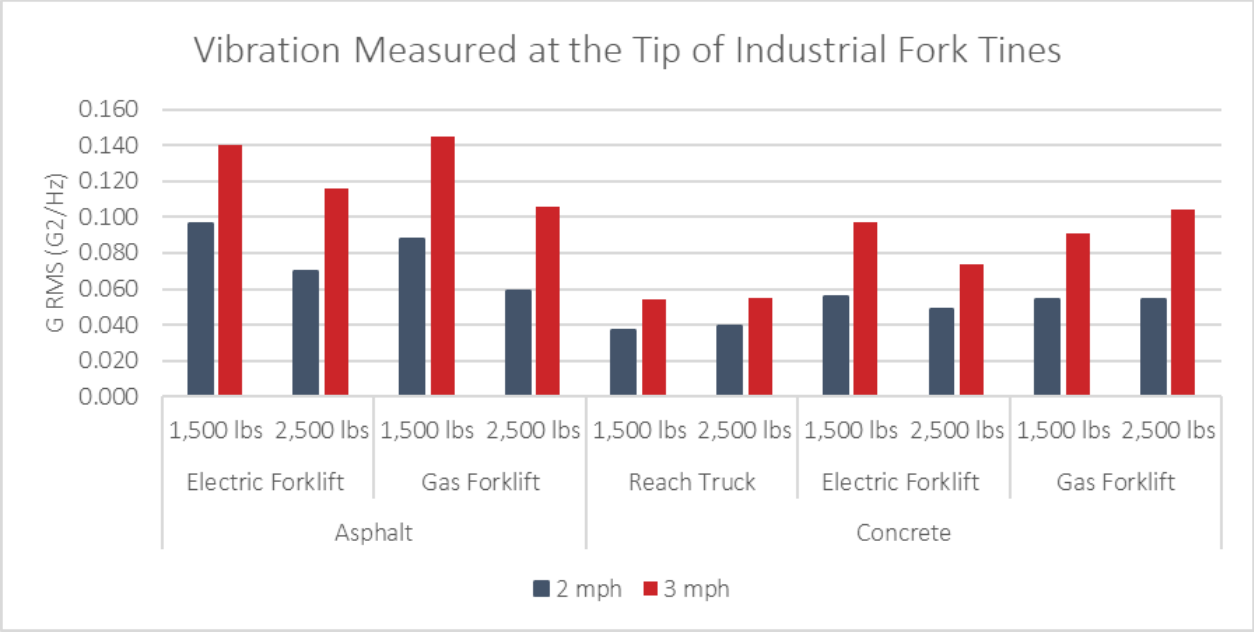

Figure 22. Overall vibration intensity measured at the tip of the fork tines for each of the three forklifts (1 – 200 Hz).

Table 7. Overall G_{rms} (G^2/Hz) and kurtosis values for distributions of recorded events obtained for this study.

Road Condition	Forklift Type	Sensor Location	Unit Load Weight (lbs)	Speed (2 mph)		Speed (3 mph)	
				G_{rms} (G^2/Hz)	Kurtosis	G_{rms} (G^2/Hz)	Kurtosis
Asphalt	Electric Forklift	Carriage	1,500	0.044	3.40	0.071	2.28
		Tip	1,500	0.096	2.03	0.140	2.36
		Carriage	2,500	0.034	9.15	0.070	3.12
		Tip	2,500	0.070	1.95	0.116	1.43
	Gas Forklift	Carriage	1,500	0.049	6.49	0.090	1.87
		Tip	1,500	0.088	6.71	0.145	1.26
		Carriage	2,500	0.040	11.43	0.070	1.91
		Tip	2,500	0.059	2.77	0.106	2.58
Concrete	Reach Truck	Carriage	1,500	0.028	4.68	0.046	4.22
		Tip	1,500	0.037	3.62	0.054	1.05
		Carriage	2,500	0.025	10.28	0.034	8.32
		Tip	2,500	0.039	2.91	0.055	2.01
	Electric Forklift	Carriage	1,500	0.028	9.78	0.051	1.26
		Tip	1,500	0.056	5.05	0.097	11.21
		Carriage	2,500	0.024	6.42	0.037	5.00
		Tip	2,500	0.049	10.34	0.074	3.64
	Gas Forklift	Carriage	1,500	0.033	8.63	0.066	8.56
		Tip	1,500	0.054	2.04	0.091	11.17
		Carriage	2,500	0.032	2.47	0.053	6.33
		Tip	2,500	0.054	13.81	0.104	9.21

Note, that the maximum acceleration level observed while recording measurements was 1.73 G (with a duration of 8ms); it was observed for the electric forklift on asphalt while carrying a payload of 2,500 lbs and driven at 3 mph. The kurtosis values of the probability distribution functions of recorded acceleration events at the back of the fork tine heel, fork tine tips, and forklift

carriage were 0.51 to 6.59, 1.05 to 13.81, and 1.26 to 10.28, respectively. It should be noted here that timer-triggered data should not automatically be considered random vibration with normal distributions as stated in previous studies (Rouillard & Lamb, 2008; Lu et al., 2010; Rouillard, 2007; Otari et al., 2011; Lu et al., 2008). This study revealed that, similar to other modes of transportation, the random vibration observed for forklifts was non-Gaussian in nature.

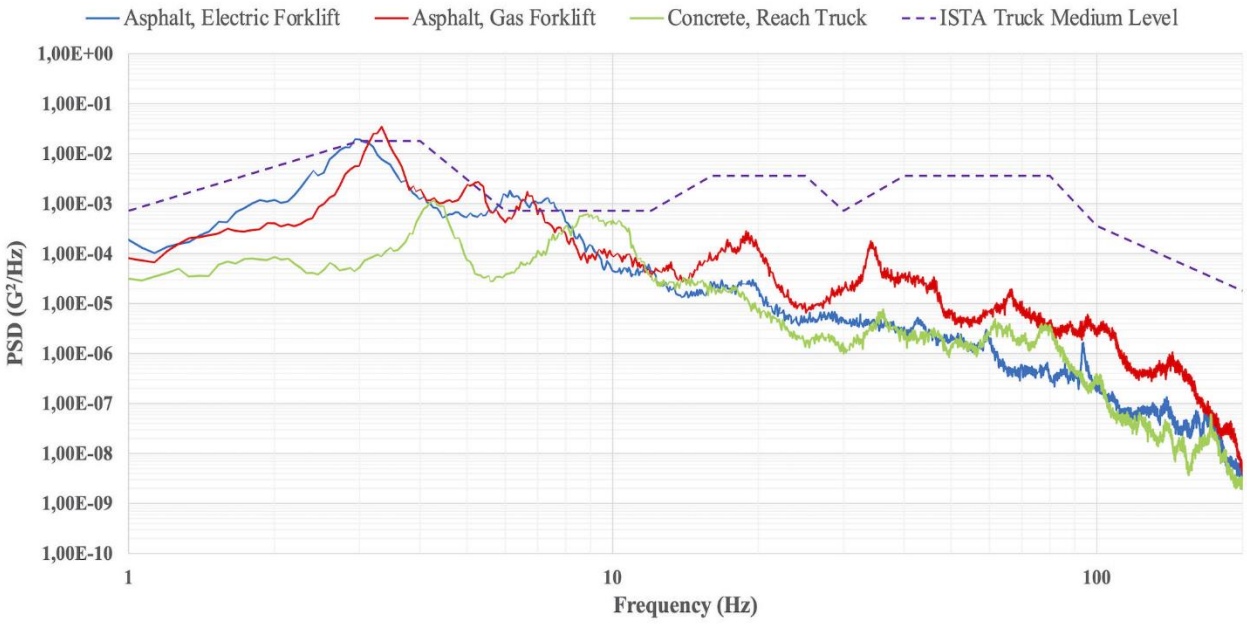

Figure 23. The highest intensity PSD plot for each of the studies forklift types compared to the ISTA truck test vibration level PSD (payload: 1,500 lbs, speed: 3 mph).

A second analysis was done using the PSD plots to analyze in more detail the effects of speed, road quality, forklift type, unit load weight, and sensor location on forklift vibration levels. Furthermore, a comparison of vibration levels was performed between the ISTA truck vibration profile and these forklifts, as shown in Figure 23. The PSD plot with the highest G_{rms} value for each forklift type is also presented in Figure 23. The highest intensity peaks were observed for the gas and electric forklifts and were between 3-4 Hz. Meanwhile, the peak shifted to 4-5 Hz for the reach truck indicating that its suspension system is much stiffer than the suspension of the other two forklifts. When compared to the PSD plot of the ISTA-recommended vibration test spectrum, it was observed that trucks experienced higher vibration levels, when compared to forklifts, especially for the higher frequency regions above 10 Hz.

Additionally, based on the PSD profiles and the overall G_{rms} values, it was observed that the gas-powered forklift presented the highest vibration intensity. The electric forklift presented the second highest vibration intensity, and the reach truck showed the least intensity. Forklifts driven on asphalt were found to experience higher levels of vibration compared to forklifts driven on concrete. These findings are similar to other truck and rail vibration measurement studies done in the past (Chonhenchob et al., 2010; Singh et al. 2012; Park et al. 2020; Garcia-Romeu-Martinez et al. 2008; Lu et al. 2010).

The results revealed that, for both the carriage and the fork tine tip, vibration levels increased with increasing speed. The highest G_{rms} observed at 2 mph was 0.096 while the lowest overall G_{rms} was 0.024. Similarly, the highest G_{rms} observed at 3 mph was 0.145 while the lowest G_{rms} was 0.034.

Additionally, it was observed that the vibration levels decreased with the unit load weight carried by the forklift. The highest overall G_{rms} observed at 1,500 lbs was 0.145 while the lowest overall G_{rms} was 0.028. Similarly, the highest overall G_{rms} observed at 2,500 lbs was 0.116 while the lowest G_{rms} was 0.024.

Overall, the gas-powered forklift driving on the asphalt condition, at 3 mph, while supporting a 1,500 lbs payload, experienced the highest vibration among the three forklifts studied with an overall G_{rms} of 0.145. This G_{rms} level is much smaller than what is generally observed for trucks and small vehicles such vans or motor cars; however, it is only marginally smaller than what is observed for railcars.

5.7.1. The effect of speed to the PSD

To determine the effect of speed on the vibration levels, PSD spectra were collected and analyzed for the three forklifts, as shown in Figure 24. A comparison of the speed effect was conducted based on the forklift and road type. Since the highest intensity vibration was observed at the fork tine tips, data analysis was conducted using vibration levels obtained at the tips of the fork tines while carrying a 1,500 lbs payload.

For all three types of forklifts, it was observed that increasing the speed of the forklift increases the vibration intensity with around 2 dB. This change was consistent for both investigated road types.

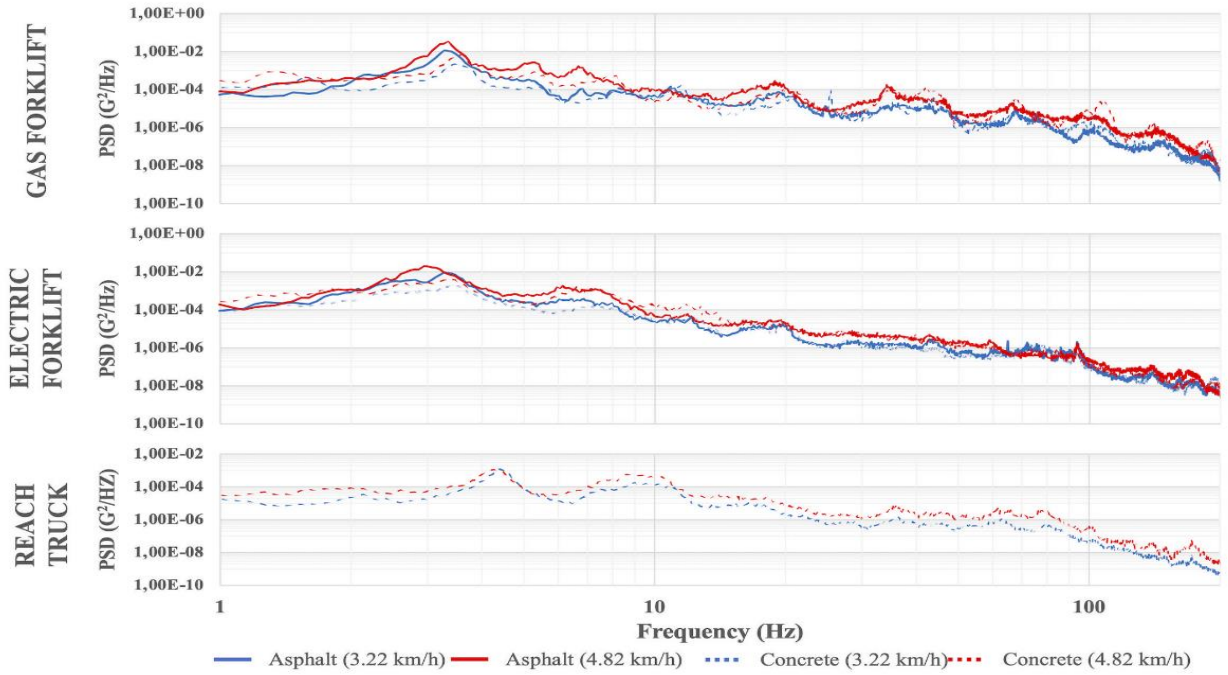

Figure 24. PSD plots of the three investigated forklifts as a function of speed (2 mph, 3 mph).

5.7.2. The effect of payload to the PSD

To determine the payload weight's effect on the vibration levels, PSD profiles were collected and analyzed for the three forklifts, as shown in Figure 25. The comparison was conducted using vibration data measured at the fork tine tip while traveling at a speed of 3 mph since that speed is the one that created the highest intensity vibration. The results showed that in forklift, more payload probably suppressed the vibration to lower levels, mainly at lower speeds. It was also found that the 3-4 Hz peak, which is generally attributed to the suspension system of the vehicles, shifted to a lower frequency as a consequence of the increase in weight. It was observed that the peaks for overloaded trucks shifted to a lower frequency in comparison to normally loaded trucks. This observed behavior is expected because the natural frequency of an object tends to decrease with the increasing weight of the spring mass system. In addition, increases in the high frequency region were observed for the electric forklift and the reach truck but not for the gas forklift.

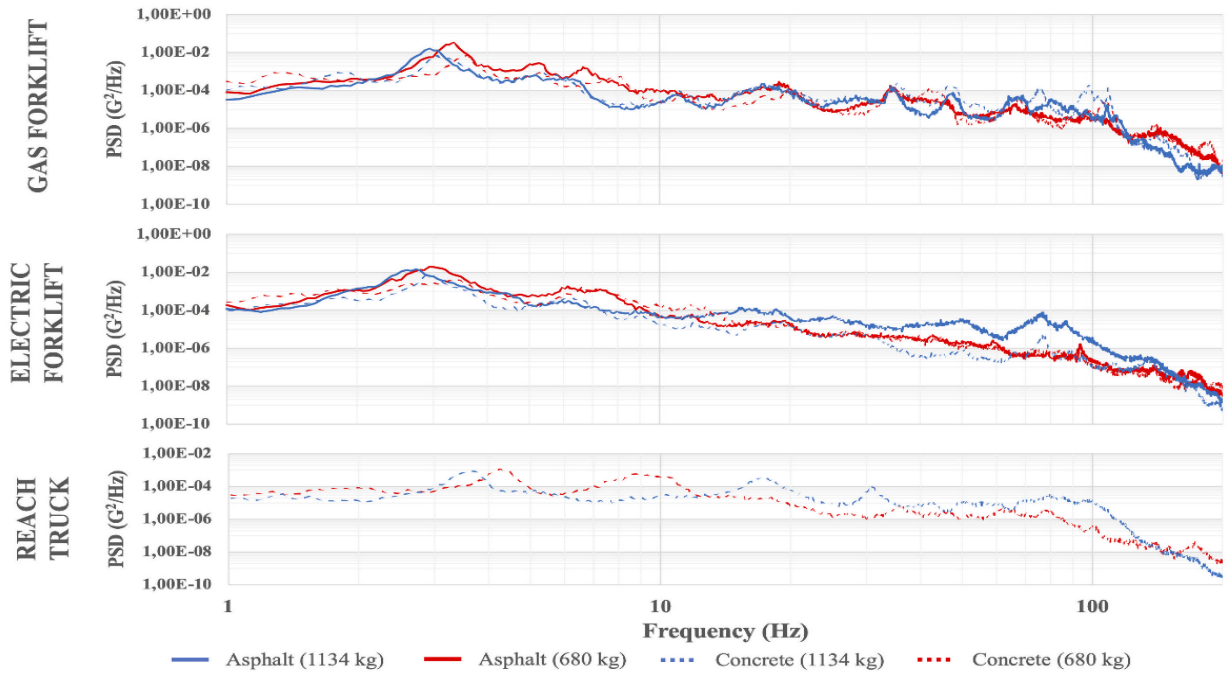

Figure 25. PSD of the three investigated forklifts as a function of payload (1,500 lbs and 2,500 lbs).

5.7.3. The effect of road condition to the PSD

To determine how the road surface affects vibration levels, PSD profiles were collected and analyzed for only two of the forklift types, as shown in Figure 26. Because the reach truck is generally not driven outside, thus was not part of this analysis. The comparison was conducted using vibration data measured at the fork tine tips using the parameters that resulted in the highest vibration intensity, which was a speed of 3 mph and a weight of 1,500 lbs. The intensity of vibration increased with the increasing roughness of the road, as shown in Figure 21 and Figure 22. The greatest change was observed for the first peak of the PSD observed at 3-4 Hz. The intensity of the peak increased and slightly shifted towards the lower frequency region when the forklift is driven on asphalt compared to concrete.

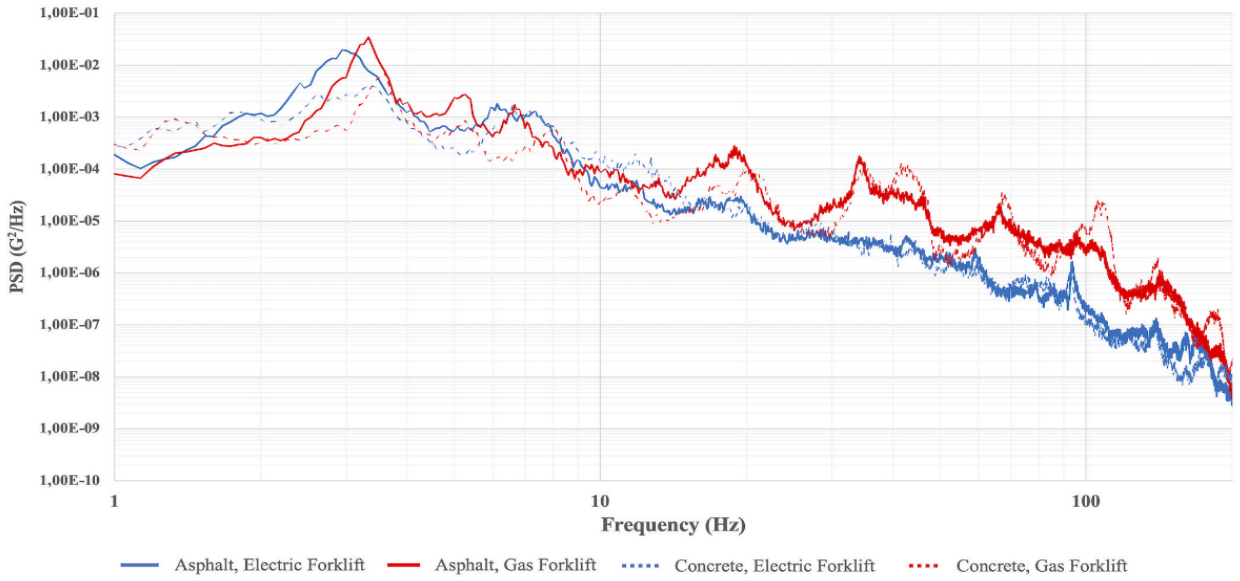

Figure 26. PSD plots of the three investigated forklifts as a function of road roughness (concrete and asphalt).

5.7.4. Effect of forklift type to the PSD

To determine how vibration levels varied due to the type of forklift, PSD profiles were collected and analyzed for all three forklifts, as shown in Figure 27. The comparison was conducted using vibration data measured at the fork tine tips, using the parameters that resulted the highest vibration intensity, which was a speed of 3 mph and a weight of 1,500 lbs. The concrete road condition was chosen for the comparison because the reach truck was not driven on the asphalt during this study. The gas forklift presented the highest vibration intensity, as shown in Figure 27. The electric forklift presented the second highest vibration intensity, while the reach truck showed the least intensity. The highest peak was observed around 3-4 Hz while the presence of a second peak was observed at 5-8 Hz region for both the gas and the electric forklifts. Meanwhile, for the reach truck, the peaks were shifted to 4-5 Hz and 8-11 Hz, indicating that the reach truck has a stiffer suspension and/or tires. Similar results were observed in a study conducted in the United States that measured truck vibration for both leaf spring and air ride suspensions (Böröcz, 2017). It was observed that, for trucks with air ride suspensions, peaks occurred at lower frequencies in comparison to trucks with leaf spring suspensions.

In addition, both the gas and the electric forklift have wheels under the mast while the reach truck does not, as shown in Figure *17*. The wheels of the outrigger arms of the reach truck are also smaller which could have contributed in shifting the peaks to the higher frequency region.

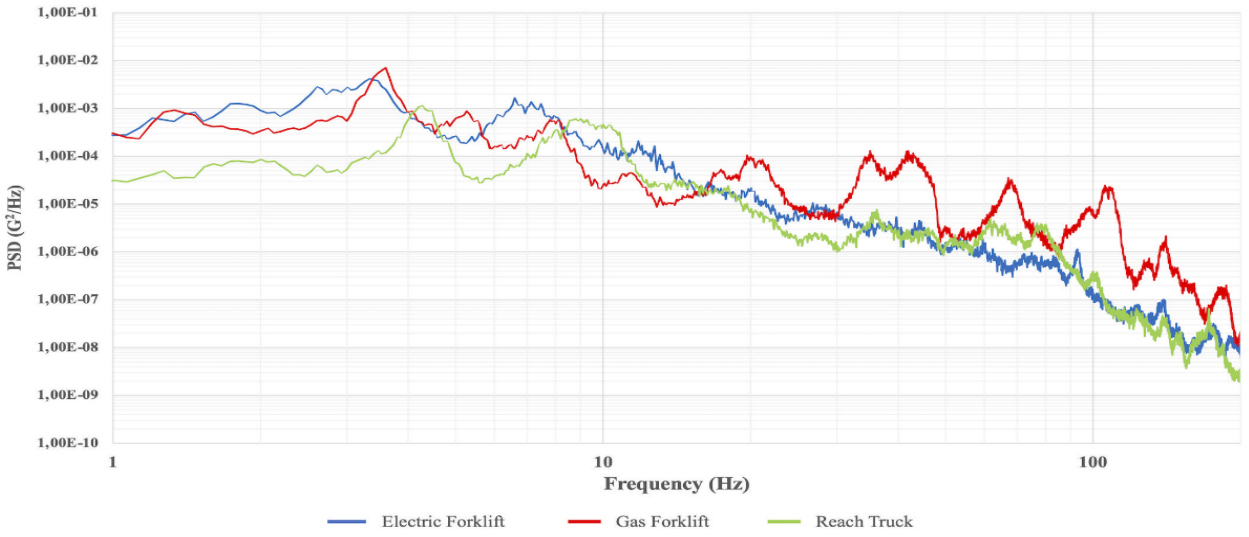

Figure 27. PSD plots of the three investigated forklifts: gas-powered forklift, electric forklift and reach truck.

5.7.5. The effect of sensor location to the PSD

To determine if there was a difference in vibration that occurs at the fork tine tip, the heel of the fork tines, and at the carriage of the forklift, PSD profiles were collected and analyzed for the three forklifts, as shown in Figure 28. The comparison was conducted using the parameters that resulted the highest vibration intensity, which was a speed of 3 mph and a weight of 1,500 lbs. It was observed that the PSD plots at the carriage and at the back of the fork tine heel were almost identical. The PSD measured at the tip of the fork tines showed a higher intensity especially in the lower frequency region. The location of the peaks did not change as a function of the measurement location.

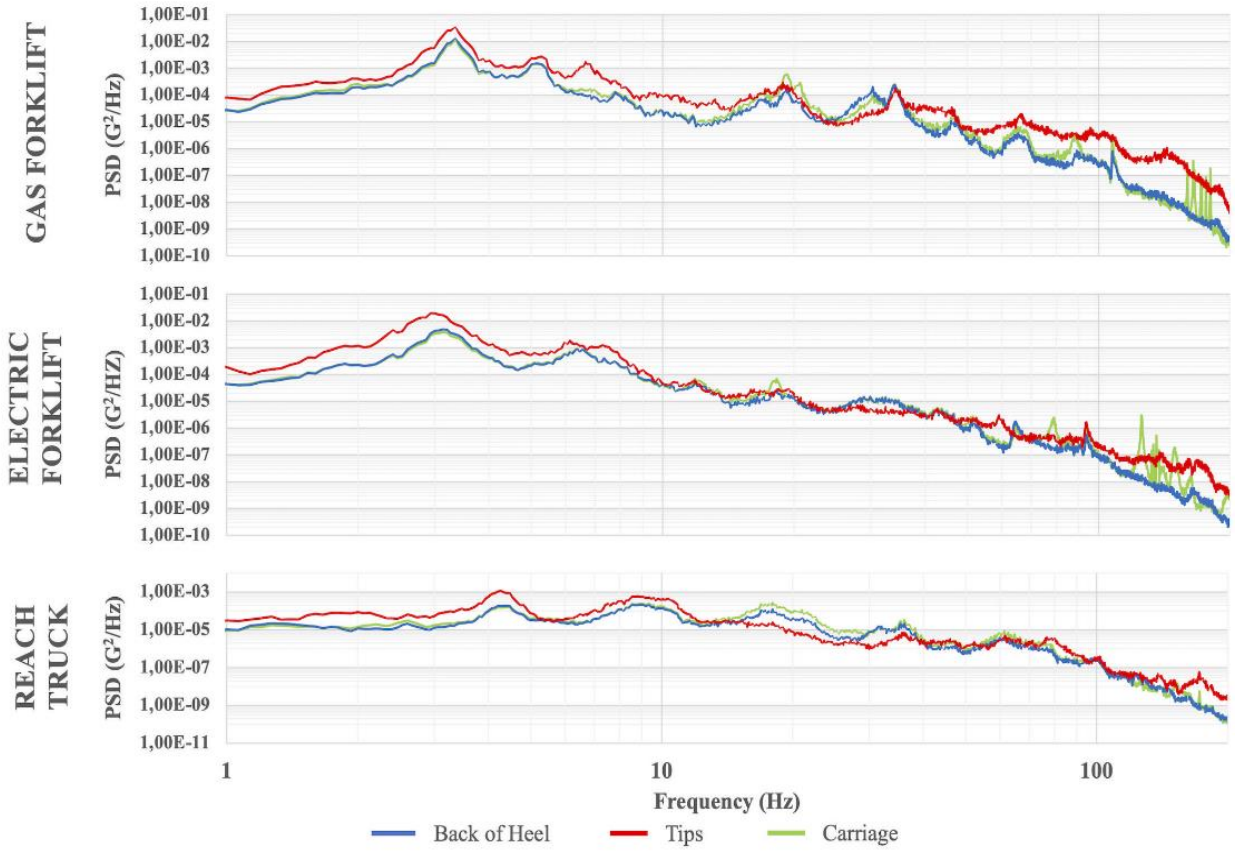

Figure 28. PSD plots of the three investigated forklifts as a function of sensor location (carriage, heel, and tip).

5.8. Limitations

It must be noted here that in laboratory processes, the vibration tests are time-accelerated, with an artificial increase in intensity to shorten the tests' duration. At the same time, forklift transport is in fact short in nature. Therefore, if the laboratory simulation is time-compressed, the test time will be even shorter, so the kurtosis value set during the test time can have little effect on the test results due to the time that it takes for the signal generation to occur in the vibration controller. This way, the time-acceleration is presumably not recommended.

5.9. Conclusions

The highest vibration intensity occurred at low frequencies, around 3-4 Hz. Vibration levels at the tip of the fork tines were higher than those at the carriage and the fork tine heels. An increase in speed of the forklift resulted in an increase in the vibration intensity while an increase in the weight carried by the forklift resulted in a decrease in the vibration intensity. Vibration levels were higher on asphalt compared to concrete due to the surface irregularities. The gas-powered forklift presented the highest vibration intensity, followed by the electric forklift, and then, the reach truck. The highest vibration intensity in the frequency range of 1 – 200 Hz was 0.145 Grms which is much lower than vibrations observed during truck transport. The maximum acceleration level observed was 1.73 G with a duration of 8ms. Random vibration events observed for forklifts followed a non-Gaussian distribution.

5.10. References

1. Blood, R. P.; Ploger, J. D.; & Johnson, P. W. Whole body vibration exposures in forklift operators: comparison of a mechanical and air suspension seat. *Ergonomics* **2010**; *19*, 1385-1394.
2. Böröcz, P. Vibration and acceleration levels of multimodal container shipping physical environment. *Packag. Technol. Sci.* **2019**, *32*, 269-277.
3. Böröcz, P. Vibration levels in vans as a function of payload and leaf spring sheet number. *J Test Eval* **2017**, *46*, 236-243. https://doi.org/10.1520/JTE20160538
4. Böröcz, P.; Molnár, B. Measurement and Analysis of Vibration Levels in Stacked Small Package Shipments in Delivery Vans as a Function of Free Movement Space. *Appl. Sci.* **2020**, *10*, 7821.
5. Böröcz, P.; Singh, S.P. Measurement and analysis of delivery van vibration levels to simulate package testing for parcel delivery in Hungary. *Packag. Technol. Sci.* **2018**, *31*, 342-352.
6. Böröcz, P.; Singh, S.P. Measurement and analysis of vibration levels in rail transport in central Europe. *Packag. Technol. Sci.* **2017**, *30*, 361-371.
7. Botelho, C.; Matos, M. L. Whole-body vibration exposure in forklift operators—a short review. In Occupational Safety and Hygiene V: Selected papers from the International Symposium on Occupational Safety and Hygiene (SHO 2017), April 10-11, 2017, Guimarães, Portugal (p. 127). CRC Press.
8. Brandenburg, R.K.; Lee, J.J. *Fundamentals of Packaging Dynamics*. L.A.B. Equipment, Inc.: Itasca, USA, 2001.
9. Burinskiene A. Operations by Forklifts in Warehouses. European Modeling and Simulation Symposium. Proceedings of European Modeling and Simulation. 2012; pp. 402-407
10. Chonhenchob, V.; Singh, S.P.; Singh, J.; Sittipod, S.; Swasdee, D.; Pratheepthinthong, S. Measurement and analysis of truck and rail vibration level in Thailand. *Packag. Technol. Sci.* **2010**, *23*, 91–100.
11. Chonhenchob, V.; Singh, S.P.; Singh, J.; Stallings, J.; Grewal, G. Measurement and analysis of vehicle vibration for delivering packages in small-sized and medium-sized trucks and automobiles. *Packag. Technol. Sci.* **2012**, *25*, 31–38.
12. Garcia-Romeu-Martinez, M.-A., Singh, S.P. and Cloquell-Ballester, V.-A. Measurement and analysis of vibration levels for truck transport in Spain as a function of payload, suspension and speed. *Packag. Technol. Sci.* **2008**, *21*, 439-451. doi:10.1002/pts.798
13. Garcia-Romeu-Martinez, M.A., Singh, S.P., Cloquell-Ballester, V.A. Measurement and Analysis of Vibration Levels for Truck Transport in Spain as a Function of Payload, Suspension and Speed. *Packag. Technol. Sci.* **2008**, *21(8)*, 439–451.
14. ISTA Procedure 3B. Packaged-Products for Less-Than-Truckload (LTL) Shipment. East Lansing: International Safe Transit Association; 2011.
15. Kipp B. Environmental Data Recording, Analysis and Simulation of Transport Vibrations. *Packag. Technol. Sci.* **2008**, *9*, 437-438.
16. Lu, F., Ishikawa, Y., Kitazawa, H. and Satake, T. Effect of vehicle speed on shock and vibration levels in truck transport. *Packag. Technol. Sci.* **2010**, *23*, 101-109. doi:10.1002/pts.882
17. Lu, F.; Ishikawa, Y.; Shiina, T.; Satake, T. Analysis of Shock and Vibration in Truck Transport in Japan. *Packag. Technol. Sci.* **2008**, *21*, 479-489.

18. Lu, F.; Ishikawa, Y.; Shiina, T.; Satake, T. Effect of Sampling Parameters on Shock and Vibration Levels in Truck Transport. Proceedings of 17th IAPRI World Conference on Packaging, Scientific Research Publishing, 2010, pp. 129-135
19. Mejias, A. Effect of Pallet Design on the Performance of Semi-Automatic & Fully-Automatic Warehouse. M.S. Thesis, Virginia Tech, **2020** p. 66.
20. Motmans, R. Reducing whole body vibration in forklift drivers. *Work* **2012**, *41*(Supplement 1), 2476-2481.
21. Otari, S.; Odof, S.; Nolot, J.B.; Vasseur, P.; Pellot, J.; Krajka, N.; Erre, D. Statistical characterization of acceleration levels of random vibrations during transport. *Packag. Technol. Sci.* **2011**, *24*. 177–188. DOI: 10.1002/pts.926
22. Park, J.; Choi, S.; Jung, H.M. Measurement and Analysis of Vibration Levels for Truck Transport Environment in Korea, *Appl. Sci.* **2020**, *10*, 6754
23. Rouillard, V. On the Non-Gaussian Nature of Random Vehicle Vibrations. World Congress on Engineering. 2007.
24. Rouillard, V.; Lamb, M. On the effects of sampling parameters when surveying distribution vibrations. *Packag. Technol. Sci.* **2008**, *21*, 467–477.
25. Singh, J.; Singh, P.; Joneson, E. Measurement and Analysis of US Truck Vibration for Leaf Spring and Air Ride Suspensions, and Development of Tests to Simulate these Conditions. *Packag. Technol. Sci.* **2006**; *19*, 309-323.
26. Singh, S.P.; Marcondes, J.A. Vibration levels in commercial truck shipments as a function of suspension and payload. *J Test Eval* **1992**, *20*, 466–469.
27. Singh, S.P.; Saha, K.; Singh, J.; Sandhu, A.P.S. Measurement and analysis of vibration and temperature levels in global intermodal container shipments on truck, rail and ship. *Packag. Technol. Sci.* **2012**, *25*, 149–160.
28. Singh, S.P.; Sandhu, A.P.S., Singh, J.; Joneson, E. Measurement and analysis of truck and rail shipping environment in India. *Packag. Technol. Sci.* **2007**, *20*, 381–392.

6. Study # 2. Evaluation of Pallet Deflection under Forklift Handling Conditions

Yu Yang Huang[1], Laszlo Horvath[1], John Bouldin[1], and Marshall White[1]

[1] Department of Sustainable Biomaterials, Virginia Tech; 1650 Research Center Dr, Blacksburg VA 24060, USA

Keywords: pallet deflection; dynamic and static test; forklift handling; vibration; ISO 8611

6.1. Abstract

Industrial forklifts are one of the most common types of handling equipment for pallets in warehouses and distribution centers. Pallets deflect while they are being transported by forklifts due to the weight of the unit load. Most of this deflection occurs on the outside edges and corners of the pallet. Limits for the deflection of the pallet during forklift handling can be found in many international standards (ISO 8611, ASTM D1185). However, there is still a lack of understanding about the maximum allowed bending of the pallet that would influence the safety and performance of the pallet during forklift handling. Understanding pallet bending during the dynamic forklift movement and how it affects the stability of a unit load will help improve the industry testing standards and will help to design safer and more cost-effective pallets.

For this study, pallet deflection was measured and analyzed based on different simulated forklift handling conditions. These conditions included fork tines orientation (leveled and 4° angle), unit load condition (bound and unbound), pallet orientation (across width and across length), and type of forklift handling condition (static and dynamic).

The results showed that when unit loads were handled in a static condition, no failure was observed throughout the entire 30 minutes of testing. However, when they were tested under a dynamic conditions, and specifically, with the unbound unit loads, unit load instability was observed. In addition, unit loads that were tested with the 4° angle fork tines configuration tended to survive longer during the dynamic testing. It was observed that vibration increased pallet bending due to the magnification of the movement. The results revealed that, the deflection limit proposed in the ISO 8611 standard is appropriate and potentially even too conservative for bound loads but not appropriate for unbound unit load.

6.2. Introduction

Industrial forklifts are one of the most commonly used material handling equipment in the warehouse system (Mejias, 2020). Pallets are the most common platforms for unitized loads. There are approximately 2.6 billion pallets in circulation in the U.S. (Freedonia, 2015). The majority of companies are using wooden pallets (94%) but about the third of the companies uses plastic pallets (MMH, 2020). There are several international standards used to measure the performance of pallets, including ISO 8611 (ISO 8611, 2011), and ASTM D1185 (ASTM D1185-98a, 2009). During the performance evaluation, the load capacity of pallets is measured for stacking, racking, and forklifting. Additionally, the deflection of the pallet is monitored and cannot exceed the performance limit published in the standard. Plastic pallets, due to their low, stiffness, tend to bend more in comparison to pallets made of other materials such as wood. Therefore, their deflection is often a limiting factor during the assessment of their performance.

When unit loads are transported through the supply chain, the vibration caused by the different transportation modes has a major effect of the damage observed for the products transported (Brandenburg & Lee, 2011; Kipp, 2008). Therefore, the vibration caused by the different transportation modes is well characterized, such as heavy trailer-truck (Singh et al. 2007; Chonhenchob et al. 2010; Singh et al. 2012; Park et al. 2020), and medium and small trucks (Böröcz & Singh, 2018; Chonhenchob et al. 2012; Böröcz & Molnár, 2020). Despite the popularity of the forklift, there are only a limited number of studies that focused on the vibration caused by the forklift (Huang et al., 2021). A recent study published by Huang et al. (2021) investigated the vibration caused by different types of forklift and multiple operational factors such as road conditions, speed, and unit load weight.

Although the movement of the pallet during a forklift handling is dynamic in nature, there are no testing standards that contains guidelines for dynamic testing of pallets on a forklift support. In addition, there is not published information on how the deflection limit published in the different testing standards was determined.

Therefore, the goal of this study was to evaluate pallet deflection during a static and dynamic environment and investigate how these values are affected by factors such as forklift fork

tines orientation (leveled and 4° angle), unit load condition (bound and unbound), and pallet orientation (across width and across length).

6.3. Objectives

- Investigate the effect of factors such as fork tines configuration, unit load condition, pallet orientation and forklift handling condition on pallet deflection.
- Analyze the correlation between the static and dynamic pallet deflection.
- Evaluate the correlation between the ISO nominal load deflection limit with a forklift support condition and unit load stability.

6.4. Materials

4.1. Pallet Design

One design of plastic pallet was used to conduct the experiments of the study. The pallet consisted of a 48 in. x 40 in. nestable, block class, non-reversible plastic pallet used for grocery distribution. The average weight of the pallet was 24.66 lb. The pallet was provided by the Orbis Corporation (website: https://www.orbiscorporation.com/en-us/). Representative pictures of the pallet are shown in Figure 29.

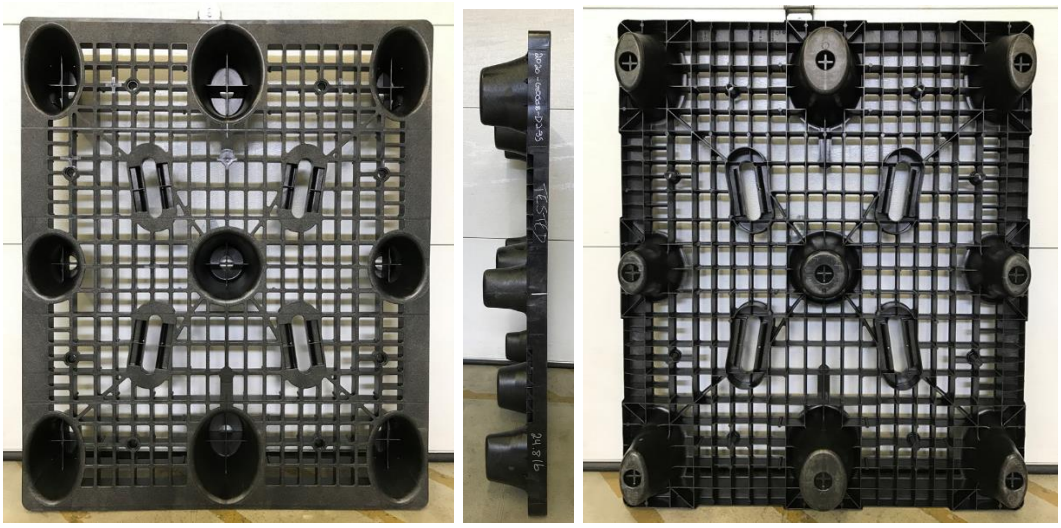

Figure 29. Representative pictures of the investigated pallet.

4.2. Corrugated boxes

Regular slotted container (RSC) style corrugated boxes were used for this study. The boxes were manufactured with a Kongsberg computerized cutting table (Esko, Miamisburg, Ohio, USA), as shown in Figure 30. The boxes were constructed using C-Flute, single wall corrugated board with 32 lb/in nominal Edge Crush Test (ECT) value. The external dimensions of the boxes were 8 in. x 8 in. x 10 in. in an effort to create the most conservative setup. To ensure consistency of the center of gravity for each of the box, they were filled with evenly distributed weight using wood pellets and the weight of each box was based on the load capacity of the pallet as determine in the ISO nominal fork tine test. A 7.688 in. x 7.500 in. x 2.750 in. corrugated insert was placed on the top and bottom of each box to ensure that the overall weight of the filled box was 6.3 lbs.

The boxes were erected using a jig to ensure 90-degree corners and the top and bottom of the box was taped shut using a nominal 2 in. package tape (Scotch, St. Paul, Minnesota, USA).

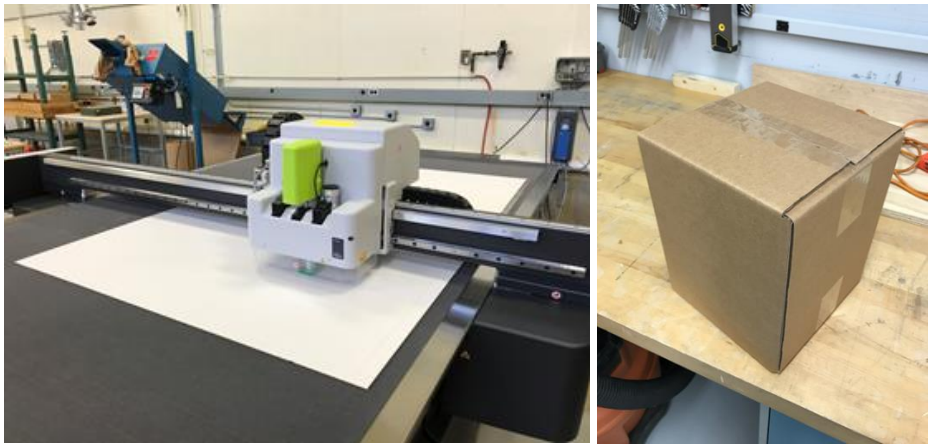

Figure 30. Representative pictures of the corrugated boxes used to construct the unit load.

4.3. Unit Load

The study was conducted using both a stretch (bound) and unwrapped (unbound) unit load, as presented in Figure 31. Both unit loads were constructed with four layers tall, in a column stacked pattern, with thirty boxes per layer.

One unit load was stretch wrapped to reduce the instability of the boxes during the vibration tests. The stretch film was purchased from U-line and with model number S-1524. The thickness of the film was 80 gauge, and the film width was 20 in. The film was made of linear low-density polyethylene (LLDPE). The Highlight Synergy 4 stretch wrapper was used for the application of the stretch film. The containment force of the applied stretch wrap was 12 lbs measured using a Highlight Film Force Pull Kit (PTC-919) based on the guidelines of ASTM D4649-03: Standard Guide for Selection and Use of Stretch Wrap Films. The film was pre-stretched 200% before application and three top and three bottom layers were applied with a 40% overlap in the middle. The film force multiplier was set at 125%. The carriage speed was set at 15% while the turntable speed was 6rpm.

Figure 31. Representative pictures of the unit loads used to conduct the experiments in the across the length orientation: (a) unbounded unit load, (b) bounded unit load

6.5. Methods

5.1. Coefficient of Friction testing

The coefficient of friction (CoF) of the pallet was determined for each of the pallets. The test method was based on a study conducted by O'Dell et al. (1998). The pallet was exposed to the test surface (corrugated), and a horizontal force was applied to the pallet at a constant rate of 1.0

in. / minute, as presented in Figure 32. Force was applied until motion was achieved and that force was recorded as F_h. The static coefficient of friction was determined using the following equation:

$$\mu_s = F_h/F_n$$

Where μ_s=static coefficient of friction, F_h=horizontal force required to cause motion, F_n=weight of the pallet.

Figure 32. Test setup for top deck Coefficient of Friction testing on corrugated board. (O'Dell et al. 1998)

5.2. Pallet load capacity

The bending stiffness and strength of the deck were tested using fork tine support conditions based on the proposed guidelines of ISO 8611 testing standard. A Tinius Olson compression testing equipment, equipped with four 24,000 lbs. load cells was used for the testing, as presented in Figure 33. During the test two (2) 4 in. wide steel beams were positioned under the top deck halfway between the blocks. To determine the weakest orientation, three (3) pallets were tested to failure racked across the length (RAL) and three were tested to failure racked across the width (RAW). A thirty (30) minutes creep test was performed at the calculated creep test load using three (3) specimens from each design. The load was provided by a set of rigid beams defined by ISO 8611-2011 situated on the top of the pallet. A 40 lbs. datum load was applied to the top of the pallet prior to the application of the creep load. The datum load included the weight of the loading-beams. The maximum allowed pallet bending was based on the proposed deflection limit of 4.5° angle of the cantilevers. The deflection was monitored using string potentiometers.

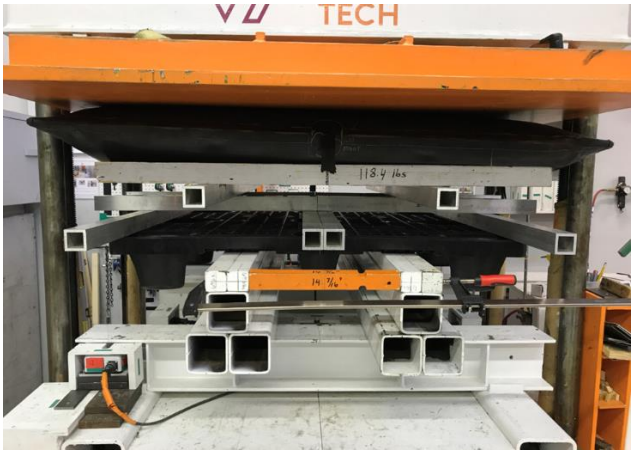

Figure 33. Test setup used to determine the load capacity of the plastic pallet.

5.3. Dynamic unit load bending using fork tine support

A custom jig was created to support the loaded pallet during the dynamic testing. The test setup is presented in Figure 34. The detailed dimensions of the jig are published in Appendix 0. The custom jig consisted of a metal forklift carriage bolted to a steel assembly and a set of two 42 in. long fork tines (Atlas Companies, Atlas Forklift Forks) that were hung from the carriage. The custom jig was secured to the vibration tester using bolts. The internal free span between the two fork tines was 14.438 in. based on the ISO 8611 (ISO 8611, 2011) standard. The jig was designed to allow the fork tines either to be leveled with the table or to be tilted upwards by 4 degrees.

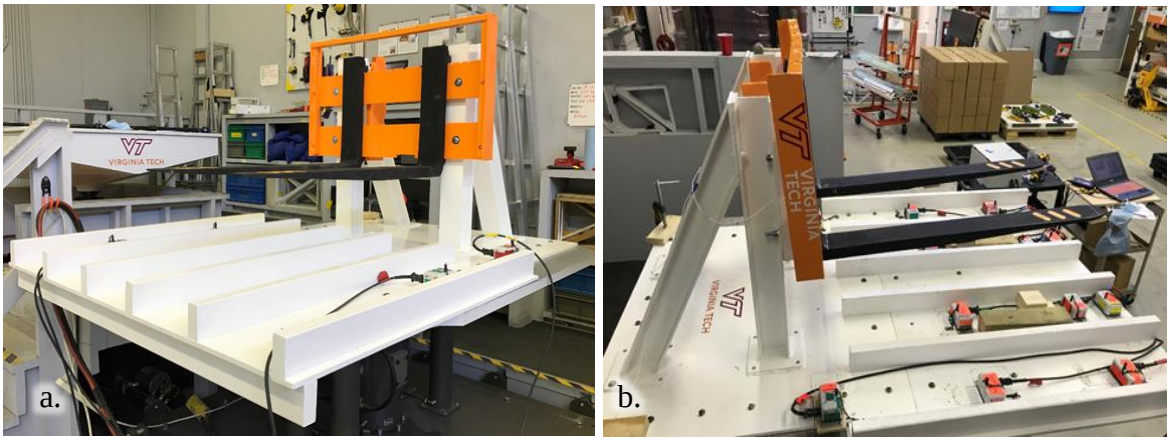

Figure 34. Representative pictures of the forklift simulator jig: a) leveled orientation, and b) tilted upwards by 4 degrees.

A vertical linear vibration table (Model 10000, Lansmont Corporation, Monterey, CA, USA) with a 60 in. x 60 in. platen was used for the dynamic testing. The most conservative vibration profile that was collected from Study 1 was used to simulate a dynamic forklift handling condition, as presented in Figure 35. The collected PSD was directly transferred from the Lansmont Saver 9x30 data logger with any additional processing. The vibration test was conducted for 30 min or until unit load instability was observed.

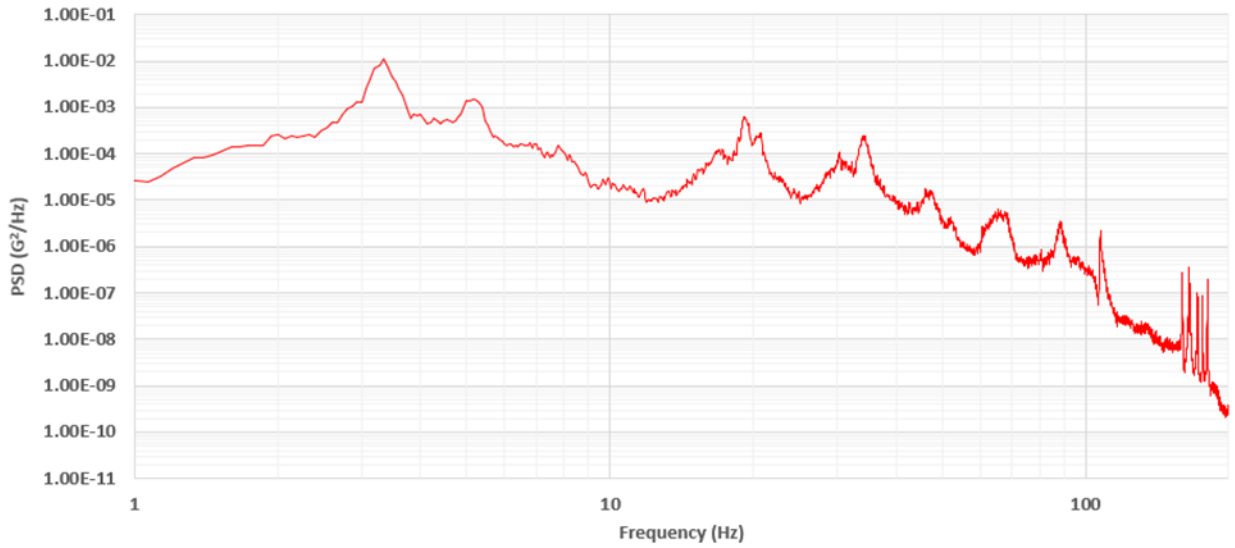

Figure 35. PSD vibration profile used for the vibration simulation. *Profile: Gas-powered forklift driven at 3 mph on asphalt while carrying a unit load of 1,500 lbs measured at the carriage of the forklift.*

To measure the deflection that the pallet experienced during the vibration test, ten (for the across the length orientation) and twelve (for the across the width orientation) string potentiometers (P510-5-S10-NOS-30K, UniMeasure Inc., Corvallis, Oregon, USA) were connected to the pallet and to the fork tines of the forklift simulator. For the across the length orientation, six of these ten string potentiometers were connected to each side of the pallet, while the remaining four string potentiometers were connected to each of the two fork tines. Additionally, for the across the width orientation, two extra string potentiometers were connected to the end of the pallet (Pot 11, and Pot 12), as presented in Figure 36. The deflection of the pallet was measured right after load application (initial deflection), and throughout the 30 min of testing. Deflection

values were recorded through a period of 30 min or until the unit load collapsed. The unit load was also assessed for stability at the end of the testing.

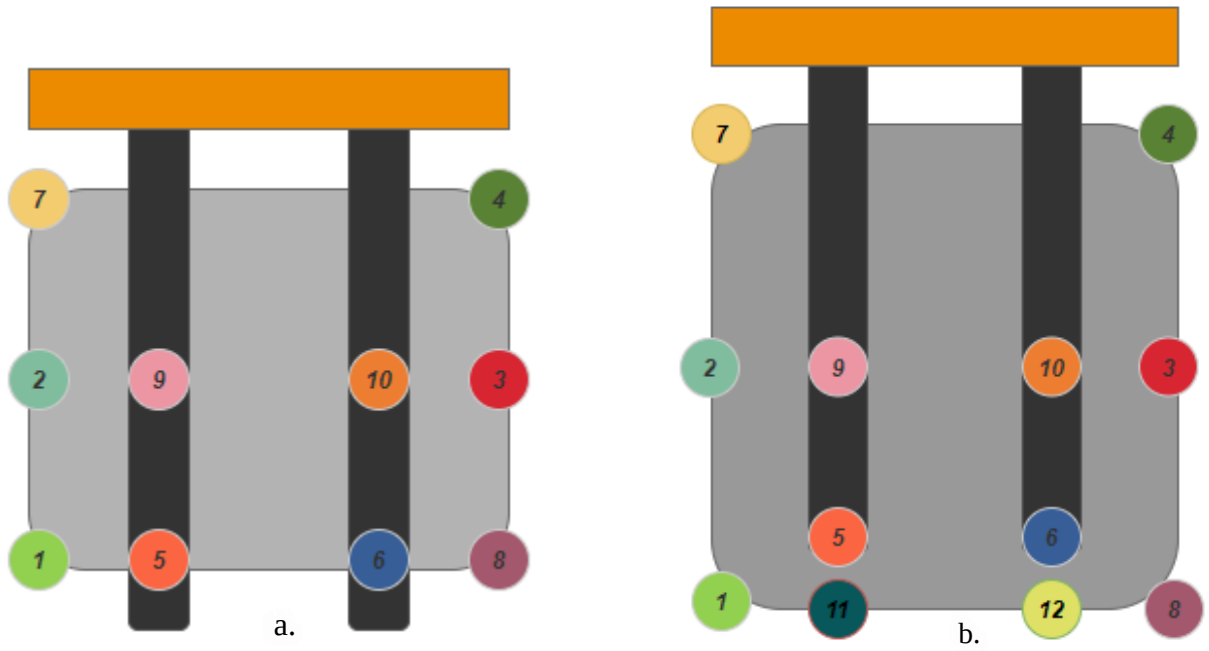

Figure 36. Representative pictures of the string potentiometers location based on: (a) across the length, (b) across the width orientation.

5.4. Static unit load bending using fork tine support

The same custom jig used for the dynamic test was used for the static testing. The main difference between the two tests was that the unit load was not vibration.

6.6. Experimental Design

The experimental design used to determine the effect of dynamic vibration on pallet the deflection is shown in Table 8. The pallet deflection was measured and analyzed using three different variables (pallet orientation, unit load containment, and fork tine configuration). Based on the variables, eight different scenarios were conducted. Three replicates were performed for each of the eight scenarios.

Table 8. Experimental design for each of the unit load and testing conditions.

Fork tines Configuration	Unit Load Condition	Orientation	Static Test	Dynamic Test
Level	Bound	Across length	3	3
	Unbound	Across length	3	3
		Across width	-	3
4° Angle	Unbound	Across length	3	3
		Across width	-	3

6.7. Results and Discussion

An analysis of pallet deflection was conducted for each of the tested scenarios. For each of the analysis, a representative graph was provided showing the deflection observed during the 30 minutes of testing. Additionally, a summary table was provided with all the deflections observed at the beginning ("Initial Deflection"), at 3 minutes ("At 3 min"), and at 30 minutes ("At 30 min") of testing for those cases that the unit load survived for that amount of time. For those cases that the unit load did not survive through the entire test (30 minutes), the reported deflection was based on the time in which the unit load collapsed (box falling off from the unit load).

The deflection reported in each summary table consisted of the average value of the three samples. An upper, middle, and lower deflection was reported for each of the cases. As shown in Figure 37, the upper and lower deflection values consisted of the average of the ten minimum and ten maximum points of the recorded peaks observed during a period of 10 s. The data was extracted using the findpeak function available in MATLAB R2020a (MathWorks Inc, Natick, Massachusetts, USA). Finally, the middle deflection consisted of the average of all the data points observed during a period of 10 s.

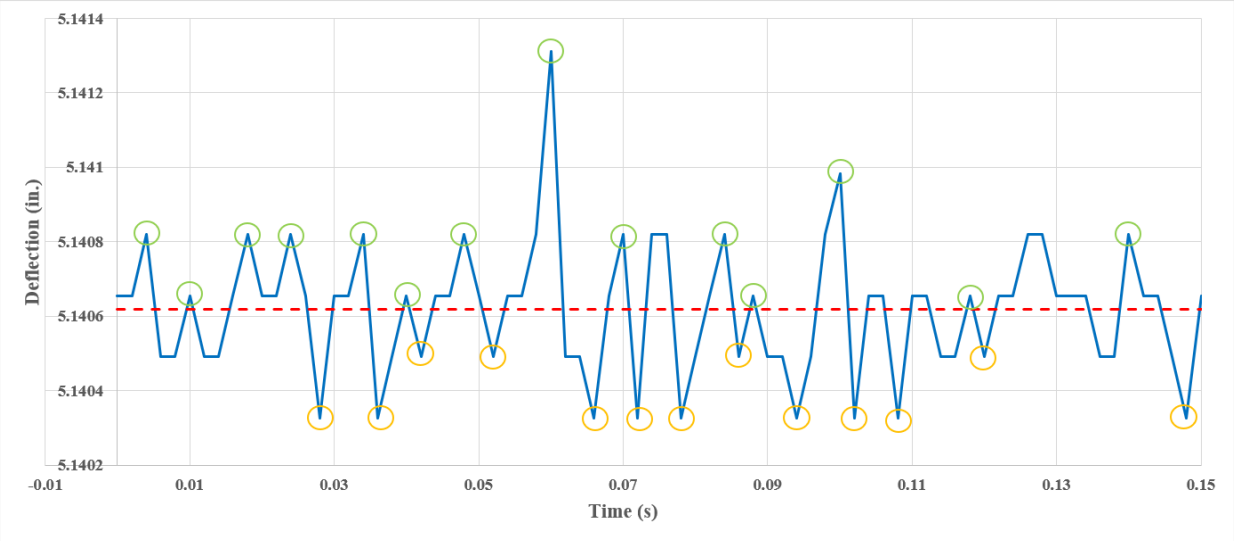

Figure 37. Representative picture of the upper, middle, and lower deflection reported for each experiment.

6.7.1. Effect of a bound unit load under static handling in the across the length orientation with initially leveled fork tines

The bound unit load under static handling in the across the length orientation with initial leveled fork tines survived the 30-minute creep test for all three tested replicates without any boxes falling off from the unit load. The condition of the unit load after the creep test is presented in Figure 38. The deflection values collected during the static testing for the bound unit load are presented in Table 9 and Figure 39. The final deflection of the pallet and the fork tines are presented in Figure 40.

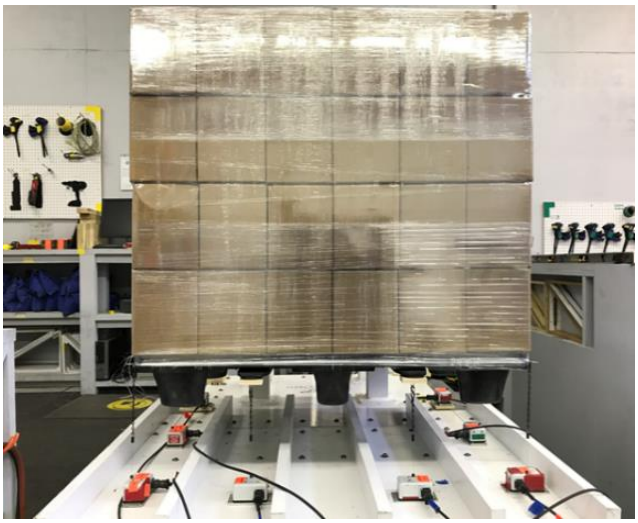

Figure 38. Representative picture of the unit load after the static test in the across the length orientation with level fork tines.

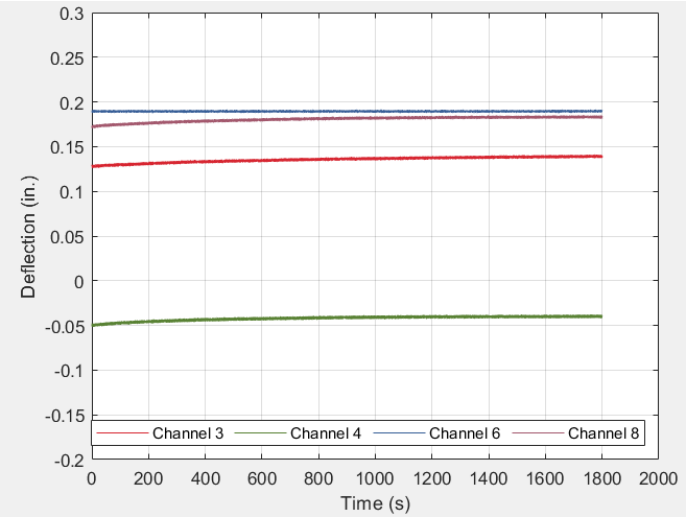

Figure 39. Pallet deflection measured for the bound unit load during the static test.

As observed in Figure 39, when comparing the final deflection at 30 minutes of testing against the initial deflection, the creep observed on the two fork tines ranged from 0.3% – 1.1%. This observed behavior is due to the material characteristics of the fork tines. The fork tines are made of steel which has high stiffness. In contrast, the creep amount observed on the pallet ranged from 6% - 13%. Additionally, it was observed that the corners of the pallet were bending upward in comparison to the fork tines. This behavior might be attributed to the effect of the stretch film.

Table 9. Summary of the deflections measured using a bound unit load during the static handling in the across the length orientation.

		Pallet and Fork Tines Deflection (in.) for Each Pot									
		1	**2**	**3**	**4**	**5**	**6**	**7**	**8**	**9**	**10**
Initial Deflection		0.0873	0.1296	0.1227	-0.0530	0.1780	0.1810	-0.0926	0.1373	0.1005	0.0924
At 3 min	**Upper**	0.0935	0.1359	0.1276	-0.0484	0.1791	0.1813	-0.0875	0.1421	0.1153	0.1070
	Average	0.0934	0.1354	0.1275	-0.0486	0.1789	0.1810	-0.0880	0.1418	0.0552	0.0478
	Lower	0.0931	0.1353	0.1272	-0.0487	0.1788	0.1805	-0.0882	0.1415	0.0006	-0.0031
At 30 min	**Upper**	0.1022	0.1458	0.1356	-0.0422	0.1805	0.1817	-0.0802	0.1494	0.1157	0.1068
	Average	0.1017	0.1456	0.1355	-0.0424	0.1800	0.1815	-0.0806	0.1493	0.0560	0.0481
	Lower	0.1016	0.1455	0.1353	-0.0425	0.1799	0.1810	-0.0808	0.1492	0.0013	-0.0026

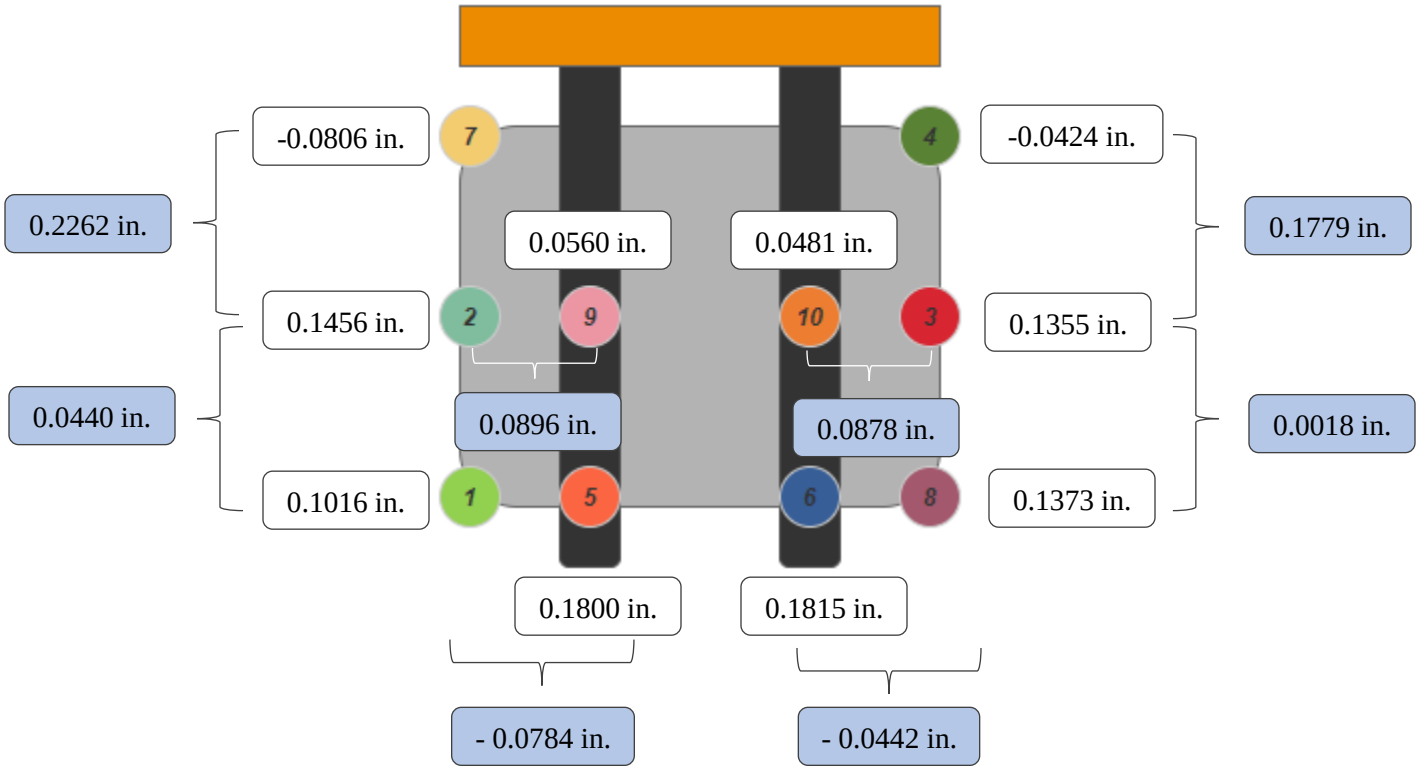

Figure 40. Average deflection (in.) measured at 30 minutes from the bound unit load during the static test for the across the length orientation with initially leveled fork tines. *White balloons: measurement of the deflection at the stated location. Blue balloons: deflection difference between the two stated locations.*

Figure 40 shows that higher initial deflection was observed at the end of the fork tines (Pot 5 and Pot 6) in comparison to the middle point of the fork tines (Pot 9 and Pot 10) due to the increase of the length of the cantilever and the changing geometry of the fork tines. When the pallet deflection was investigated, it was found that the lowest deflection was observed at the rear

of the pallet (Pots 4 and 7) followed by the front (Pots 1 and 8) and the greatest deflection was observed in the middle of the pallet (Pots 2 and 3). However, the high deflection results for the mid-section of the pallet were not consistent on both sides of the pallet. It could be presumed that the deflection at the rear of the pallet is not affected by the bending of the fork tines as no cantilever is present. The increased deflection in the middle of the sides could be explained with the greater tributary area that distributed load to this region of the pallet. Higher deflection difference was observed between Pot 2 and Pot 7 (0.2262 in.) in comparison to Pot 1 and Pot 2 (0.0440 in.) which could indicate that the fork tines are bending more closer to the heel than the tip.

6.7.2. Effect of bound unit load under dynamic handling in the across the length orientation with initially leveled fork tines

The bound unit load under dynamic conditions in the across the length orientation with level fork tines survived the 30 minutes of test for all three tested replicates without any boxes falling from the unit load. The deflection values collected during the dynamic testing for the bound unit load are presented in Figure 41 and Table 10. The final deflection of the pallet and the fork tines are presented in Figure 42.

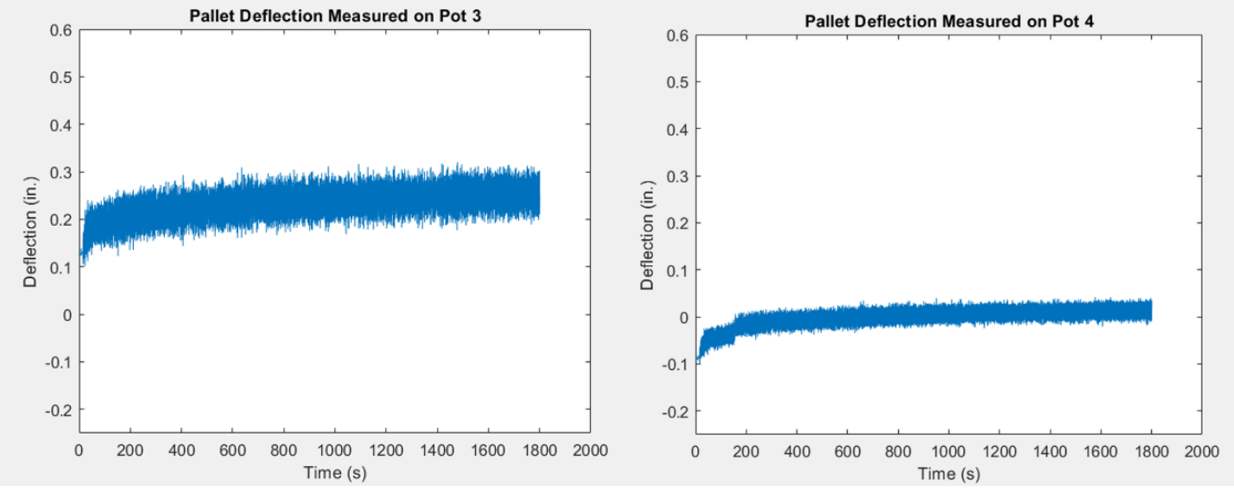

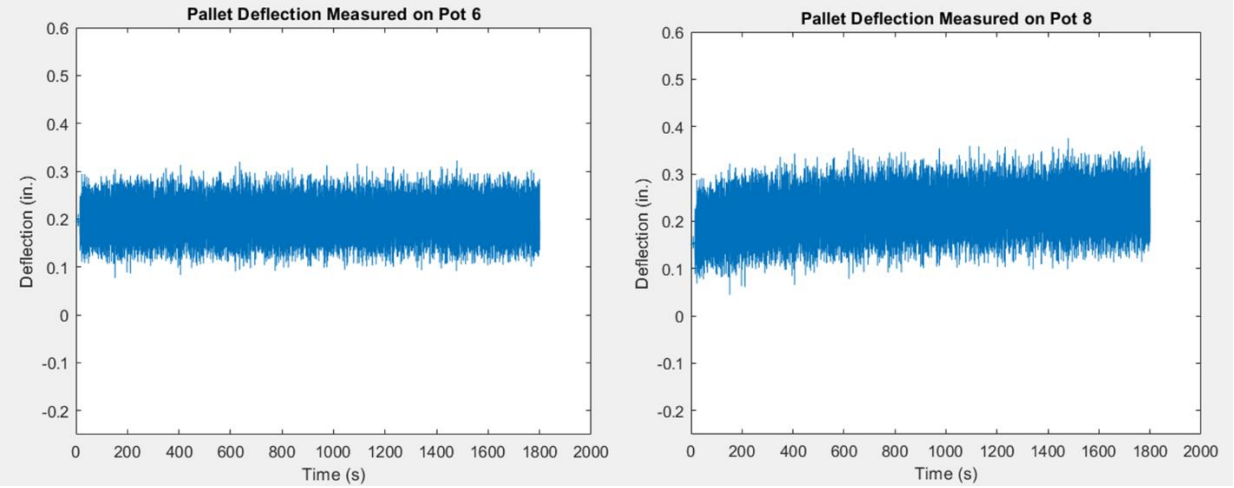

Figure 41. Pallet and fork tine deflection measured for the bound unit load during the dynamic test.

As observed in Figure 41, the vibration of the unit load magnifies the deflection, as well as the range of movement of the pallet in comparison to the unit load in static condition.

Table 10. Summary of the deflections measured for the bound unit load during the dynamic condition in the across the length orientation.

		Pallet and Fork Tines Deflection (in.) for Each Pot									
		1	2	3	4	5	6	7	8	9	10
Initial Deflection		0.0327	0.0985	0.1507	-0.0671	0.1823	0.1841	-0.1222	0.1443	0.08167	0.0852
At 3 min	**Upper**	0.1957	0.2301	0.2828	0.0282	0.2610	0.2578	-0.0326	0.2889	0.2200	0.2181
	Average	0.1168	0.1889	0.2387	0.0071	0.1931	0.1885	-0.0592	0.2055	0.1218	0.1222
	Lower	0.0378	0.1468	0.1963	-0.0165	0.1298	0.1208	-0.0883	0.1244	0.0337	0.0385
At 30 min	**Upper**	0.2318	0.2800	0.3275	0.0625	0.2615	0.2593	0.0022	0.3142	0.2201	0.2171
	Average	0.1559	0.2407	0.2859	0.0423	0.1964	0.1898	-0.0219	0.2360	0.1238	0.1231
	Lower	0.0824	0.2028	0.2457	0.0210	0.1364	0.1258	-0.0496	0.1598	0.0380	0.0414

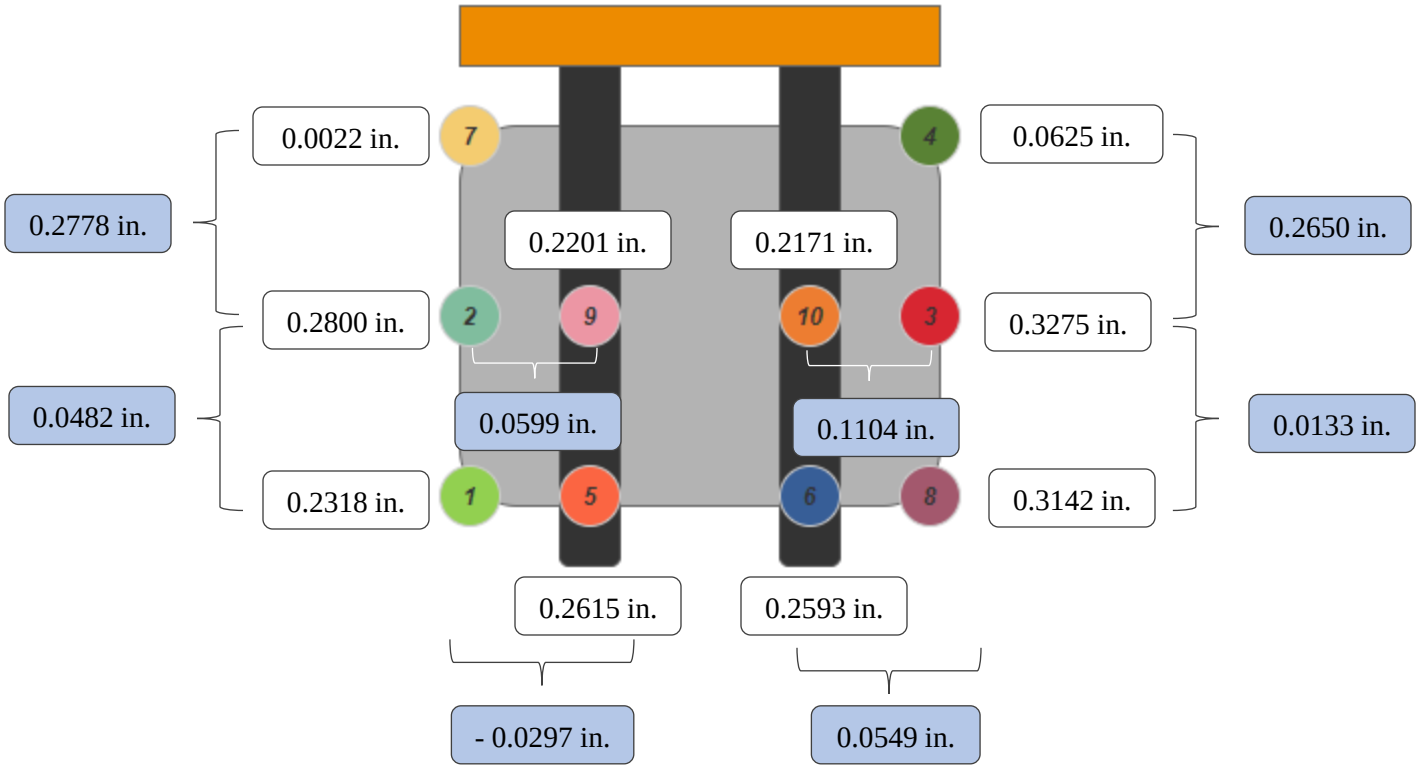

Figure 42. Upper deflection (in.) measured at 30 minutes from the bound unit load during the static test for the across the length orientation with initially leveled fork tines. *White balloons: measurement of the deflection at the stated location. Blue balloons: deflection difference between the two stated locations.*

Similarly to the static condition, higher initial deflection was recorded at the end of the fork tines (Pot 5 and Pot 6) in comparison to the middle point of the fork tines (Pot 9 and Pot 10) due to the increasing length of the cantilever and the changing geometry of the fork tines. Additionally, less deflection was observed at the corners of the pallet (Pots 1, 4, 7, and 8) in comparison to the center of the pallet (Pots 2, and 3) due to the geometry of the pallet, as well as the effect of the stretch film.

After 30 minutes of test, the creep amount observed on the fork tines was around 3%. In contrast, the creep amount observed on the pallet ranged from 15% - 33%. The creep deflection observed for the dynamic testing was much greater than the static testing. This indicated that the additional dynamic movement increased the creep and deflection of the pallet. A study conducted by Neville (1957) showed that when mechanical vibrations is applied to material, it reduces the stress necessary to initiate yield strength in materials. As a result, vibration reduces the strength of the materials. Additionally, as observed in Figure 41, when vibration motion was applied to the

unit load, it was observed that there was a jump in deflection measurements. This phenomenon was not observed for the static testing. Thus, the creep amount increased from 6% - 13% during the static testing to 15% - 33% during the dynamic testing. The highest deflection (0.3275 in.) observed was on Pot 3 after the 30 minutes of testing.

Table 11. Summary of the average pallet and fork tine movement measured for the bound unit load during the dynamic condition in the across the length orientation

		Pallet and Fork Tines Movement (in.) for Each Pot									
		1	2	3	4	5	6	7	8	9	10
At 3 min	**Upper**	0.0789	0.0412	0.0442	0.0211	0.0679	0.0693	0.0266	0.0834	0.0982	0.0958
	Lower	0.0790	0.0421	0.0424	0.0237	0.0634	0.0677	0.0291	0.0810	0.0881	0.0838
At 30 min	**Upper**	0.0758	0.0393	0.0415	0.0201	0.0651	0.0695	0.0241	0.0782	0.0963	0.0940
	Lower	0.0735	0.0380	0.0402	0.0214	0.0600	0.0640	0.0277	0.0763	0.0858	0.0817

When the dynamic motion of the pallet and the fork tines were investigated, it was found that the amount of up and down motion was similar. It was also observed that the dynamic flexing of the fork tines ranged between 0.06 – 0.07 in. at the end and 0.08 – 0.09 in. at the middle of the fork tines. This indicates that the fork tines are following a sinusoidal flexing with peaks in the mid-length of the fork tines.

Additionally, when comparing the movement between the front and the rear corners of the pallet, it was observed that the front corners presented more motion (0.0735 in. – 0.0782 in.). More flexing was observed at the front of the pallet, which could be explained by the additional flexing of the fork tines.

When comparing the deflection observed between the static and dynamic test for the bound unit loads in the across the length orientation with initial leveled fork tines, it was observed that there was higher deflection in the unit loads that experienced vibration.

6.7.3. Effect of unbound unit load under static handling in the across the length orientation with initially leveled fork tines

The unbound unit load under static condition across the length orientation with level fork tines survived the 30 minutes of test for all three tested replicates without any boxes falling from the unit load. The condition of the unit load after the creep test is presented in Figure 43. The deflection of the fork tines and the pallet is presented in Table 12, Figure 44, and Figure 45.

When the unit load does not have stretch film, as shown in Figure 43, two columns on both sides of the pallet were observed to be bending towards the outside of the unit load due to the combine deflection of the pallet, and fork tines.

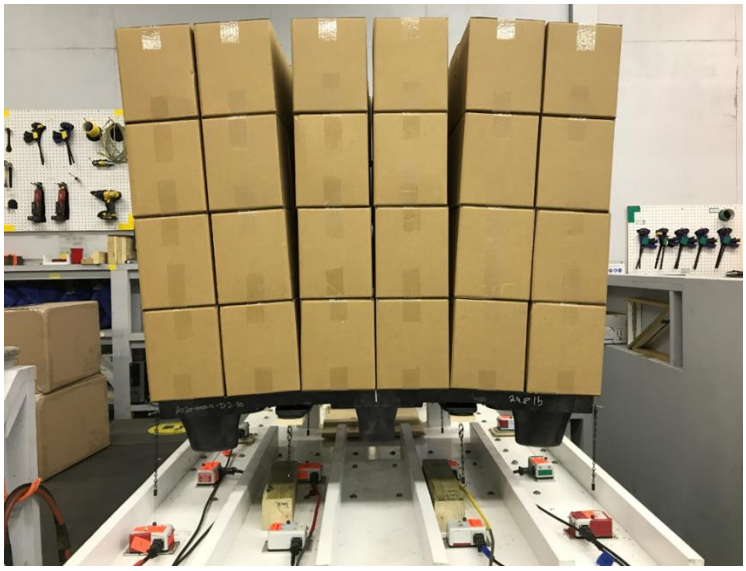

Figure 43. Representative picture of the unbound unit load after the static test in the across the width orientation with level fork tines.

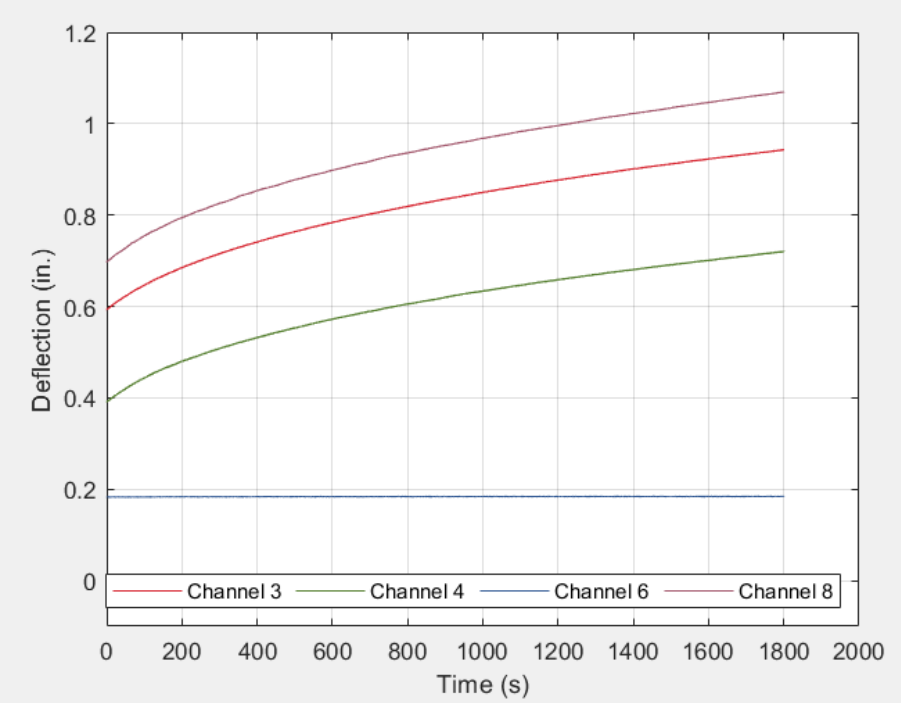

Figure 44. Pallet and fork tine deflection measured for the unbound unit load during the static test.

As presented in Figure 44, the creep amount for the pallet ranged from 36% - 50% which is much higher than what was observed during the static condition of the bound unit load. This can be explained by the fact that the stretch film used for the bound unit load constraints the movement of the boxes, as well as the bending of the pallet. The creep amount for the fork tines ranged from 0.9% - 1.0%, which was similar to what was observed for the bound unit load. Contrary to the static testing of the bound unit load, the pallet corners and edges deflected more compared to the fork tines. This could be explained by the lack of pulling effect of the stretch film.

Table 12. Summary of the deflections (in.) measured for the unbound unit load during the static condition in the across the length orientation.

		Pallet and Fork Tines Deflection (in.) for Each Pot									
		1	2	3	4	5	6	7	8	9	10
Initial Deflection		0.5776	0.5209	0.5703	0.3964	0.1858	0.1781	0.3713	0.6601	0.1065	0.1032
At 3 min	**Upper**	0.6984	0.6320	0.6829	0.5020	0.1870	0.1795	0.4768	0.7789	0.1978	0.1925
	Middle	0.6975	0.6310	0.6819	0.5010	0.1866	0.1791	0.4759	0.7778	0.1411	0.1368
	Lower	0.6964	0.6300	0.6809	0.5001	0.1864	0.1789	0.4753	0.7766	0.0867	0.0865
At 30 min	**Upper**	0.9739	0.8868	0.9425	0.7377	0.1880	0.1799	0.7130	1.0607	0.1986	0.1939
	Middle	0.9737	0.8862	0.9419	0.7375	0.1875	0.1798	0.7127	1.0605	0.1415	0.1379
	Lower	0.9735	0.8859	0.9417	0.7369	0.1873	0.1796	0.7125	1.0599	0.0868	0.0871

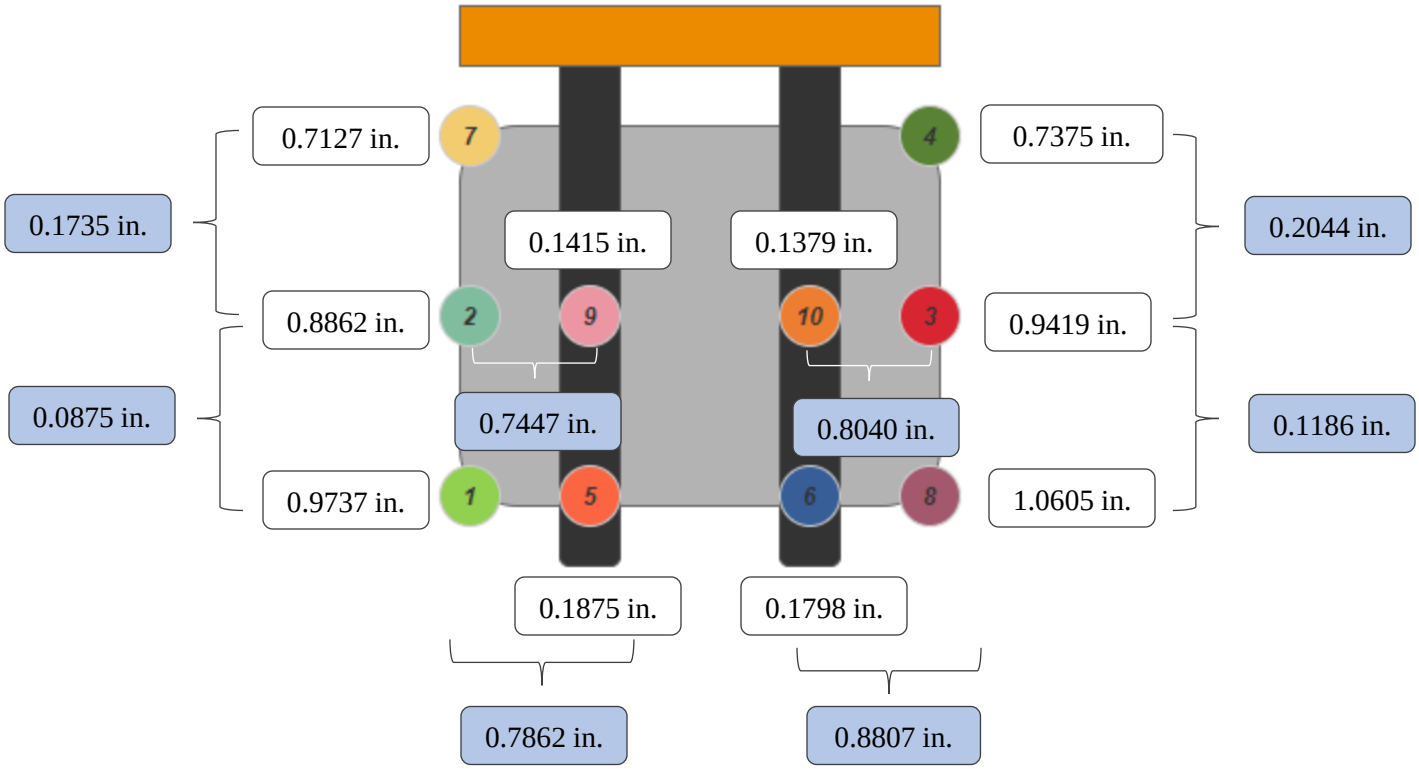

Figure 45. Average deflection (in.) measured at 30 minutes from the unbound unit load during the static test for the across the length orientation with initially leveled fork tines. *White balloons: measurement of the deflection at the stated location. Blue balloons: deflection difference between the two stated locations.*

When comparing the deflection observed at the fork tines, it follows a similar trend in comparison to previous testing. Higher initial deflection was observed at the end of the fork tines (Pot 5 and Pot 6) in comparison to the middle point of the fork tines (Pot 9 and Pot 10). The greatest deflections were observed on the front corners of the pallet (Pot1 and Pot 8) followed by the middle (Pot 2 and Pot 3), and rear corners of the pallet (Pot 7 and Pot 8). This indicates that increasing the length of the cantilever has greater effect in the deflection of the pallet.

The highest deflection of the fork tines was ranging from 0.1798 in. – 0.1875 in. which was similar to what was observed for the bound unit load. It seems like that the deflection of the fork tine is mainly affected by the weight and not the overall stiffness of the unit load. The highest deflection after 30 minutes of testing was observed on Pot 8 (1.0605 in.). The overall deflection of the pallet increased significantly compared to the bound unit load indicating that packages not secured by stretch film are resulting a less stiff unit load and cause more deflection for the same pallet.

6.7.4. Effect of unbound unit load under dynamic handling in the across the length orientation with initially leveled fork tines

The unbound unit load under dynamic condition did not survive the 30 minute tests for all three tested replicates. Boxes fell off from the unit load at different timestamps. The first unit load collapsed at 140 seconds, the second unit load collapsed at 135 seconds, and the third unit load collapsed at 620 seconds. The condition of the unit load after the dynamic testing is presented in Figure 46. It can be observed that the failure of the unit load was usually observed on both sides of the pallet. The combined effect of the pallet and fork tines bending creates instability of the unit load. The deflection of the fork tines and the pallet is presented in Table 13, Figure 47, and Figure 48. The data presented in Table 13 corresponds to the average deflection of the three replicates at the shortest time mark at which the unit loads failed (at 135s).

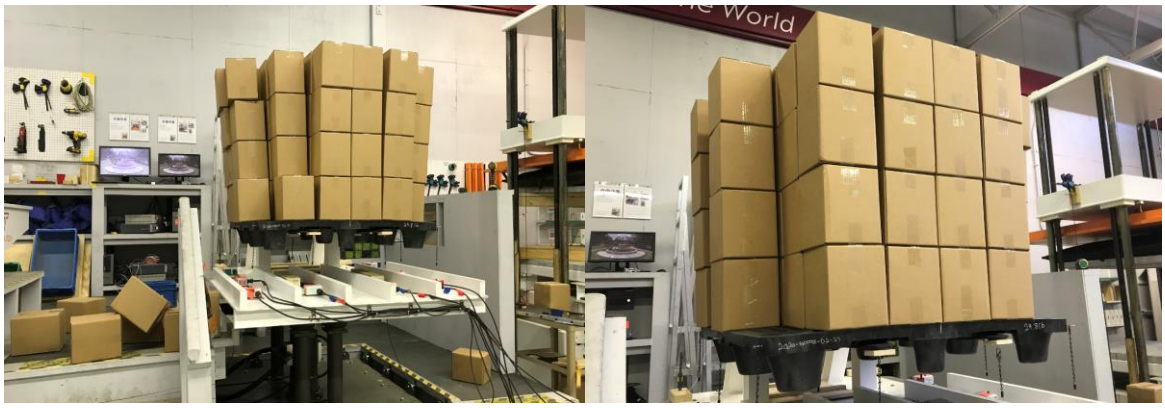

Figure 46. Representative pictures of two of the unbound unit loads after testing.

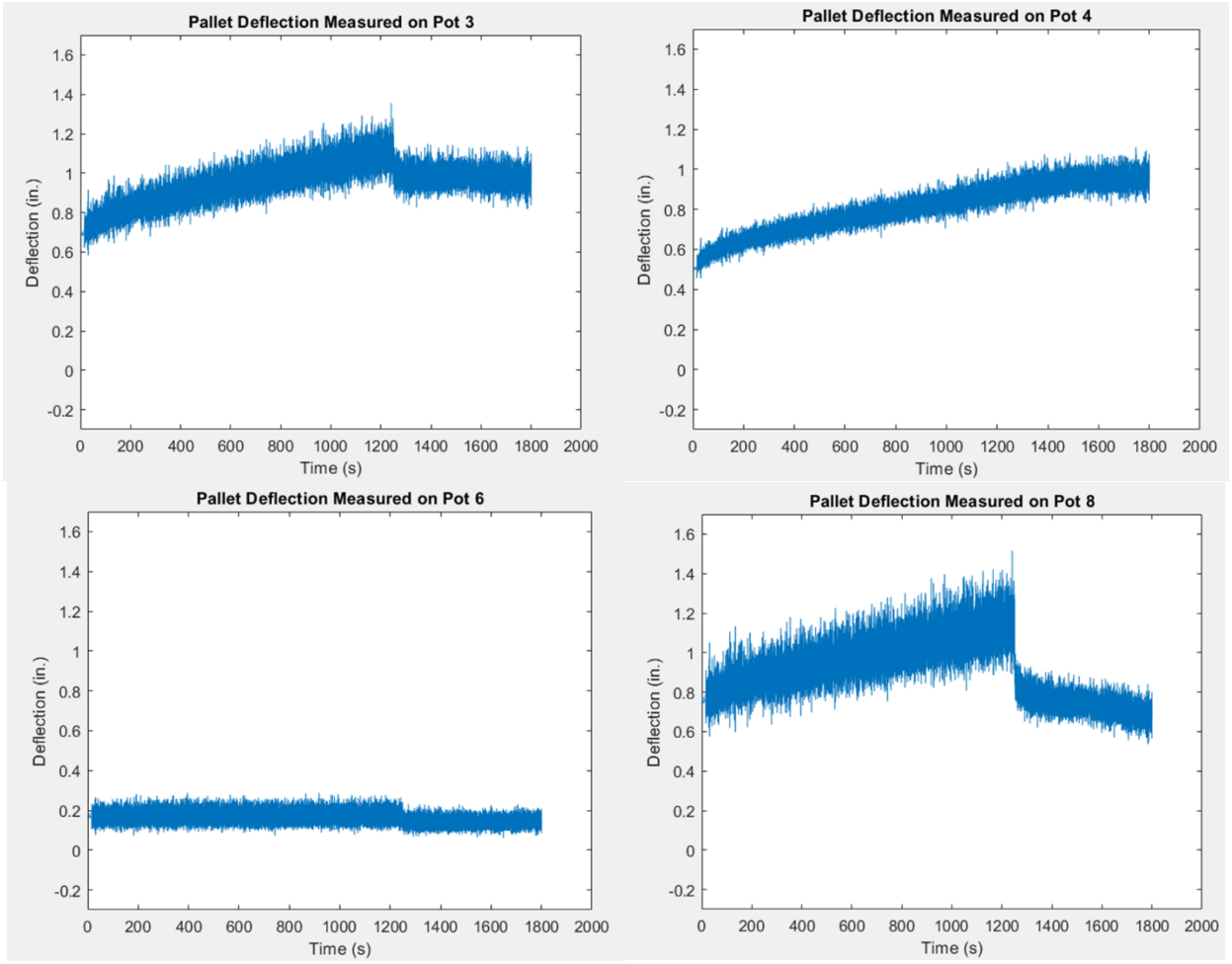

Figure 47. Pallet and fork tine deflection measured for the unbound unit load during the dynamic test.

Table 13. Summary of the deflections measured at 135 s for the unbound unit load during the dynamic condition in the across the length orientation.

		Pallet and Fork Tines Deflection (in.) for Each Pot									
		1	2	3	4	5	6	7	8	9	10
Initial Deflection		0.6154	0.5323	0.6253	0.4475	0.1881	0.1800	0.4055	0.7005	0.0946	0.0823
At 135s	**Upper**	0.9250	0.7807	0.8736	0.6686	0.2551	0.2481	0.6250	0.9792	0.2016	0.1867
	Middle	0.7872	0.6942	0.7833	0.6136	0.1913	0.1834	0.5797	0.8345	0.1101	0.0973
	Lower	0.6622	0.6146	0.7005	0.5609	0.1345	0.1208	0.5263	0.7084	0.0225	0.0142

When analyzing the deflection measured at the fork tines, similar behavior was observed compared to the previous tests. Higher deflection was presented at the tip of the fork tine (Pot 5 and Pot 6) in comparison to the middle point of the fork tines (Pot 9 and Pot 10). The deflection of the fork tines ranged from 0.1834 in. – 0.1913 in. In addition, more deflection was observed on

the front corners of the pallet (Pot1 and Pot 8) in comparison to those observed at the middle (Pot 2 and Pot 3), and inner corners of the pallet (Pot 7 and Pot 8). When analyzing the creep deflection that occurred during the 135 s of testing, greater creep deflection occurred on the rear corners (Pot 4 and Pot 7) of the pallet. The creep amount of the pallet ranged from 19% - 43%.

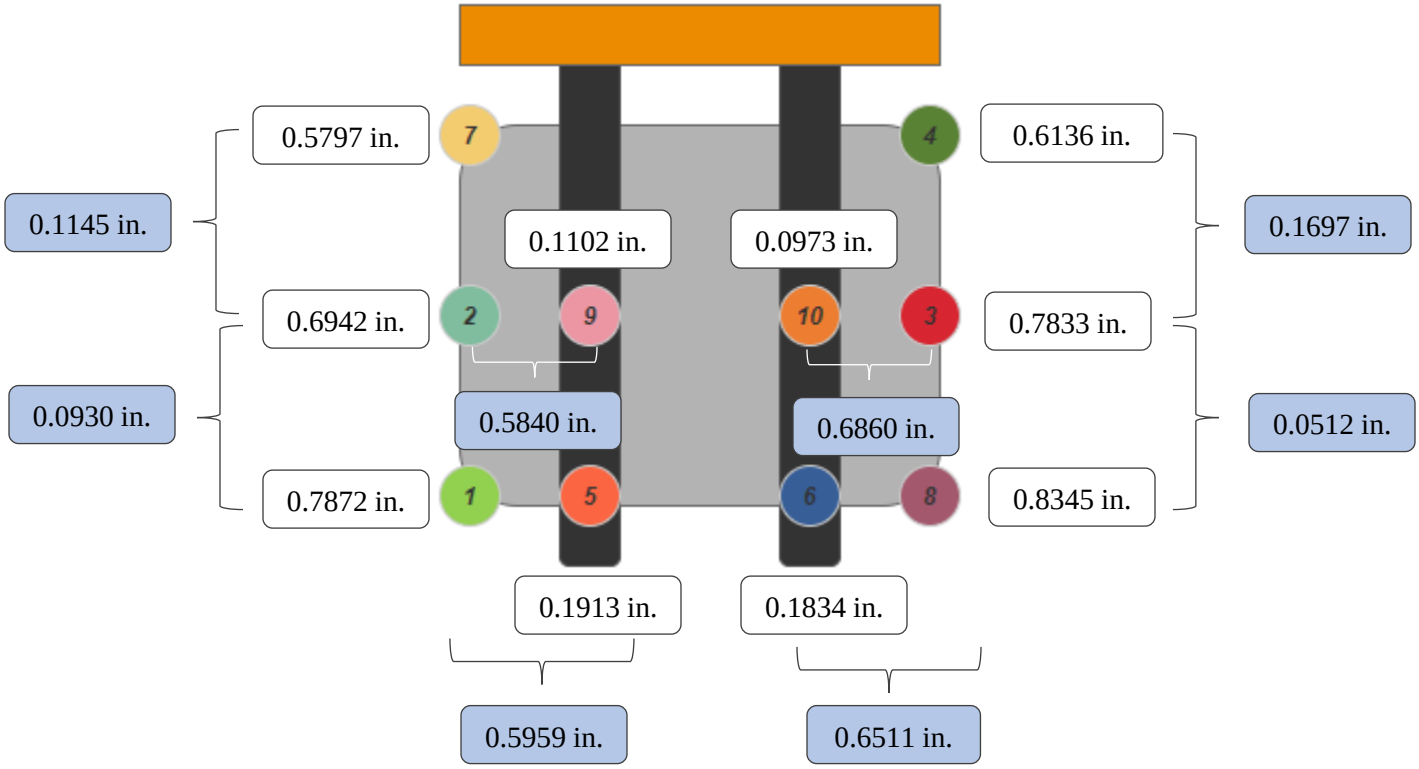

Figure 48. Average deflection measured at failure (135s) for the unbound unit load during the dynamic test for the across the length orientation with level fork tines. *White balloons: measurement of the deflection at the stated location. Blue balloons: deflection difference between the two stated locations.*

Equation 1 presents the angle at which boxes start to fall from the unit load. The angle was calculated based on the highest deflection measured on the pallet (without the influence of the bending of the fork tines). The estimated angle at which the boxes started to fall from the unit load was 3.28°. This angle is lower in comparison to the proposed 4.5° deflection limit stated in the ISO 8611. Therefore, this deflection limit is not appropriate for unbound unit loads.

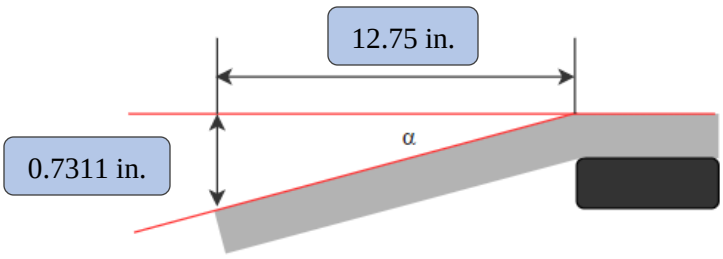

Figure 49. Schematic of the angle at which the boxes started to fall from the unit load.

$$\tan(\alpha) = \frac{0.7311\ in.}{12.75\ in.} => \arctan\left(\frac{0.7311\ in.}{12.75\ in.}\right) = \alpha => \ \alpha = 3.28°$$

Equation 1. Calculation of the angle at which the boxes started to fall from the unit load.

Table 14. Summary of the average pallet and fork tine movement (in.) measured for the unbound unit load during the dynamic condition in the across the length orientation

		Pallet and Fork Tine Movement (in.) for Each Pot									
		1	2	3	4	5	6	7	8	9	10
At 135s	**Upper**	0.1378	0.0865	0.0903	0.0550	0.0638	0.0647	0.0454	0.1447	0.0914	0.0894
	Lower	0.1250	0.0797	0.0827	0.0527	0.0568	0.0626	0.0533	0.1261	0.0876	0.0831

When the dynamic motion of the pallet and the fork tines were investigated, it was found that the amount of up and down motion was similar for each individual location. Additionally, when the dynamic movements of the fork tines were investigated, it was also observed that the dynamic flexing of the fork tines ranged between 0.05 – 0.06 in. at the end and 0.08 – 0.09 in. at the middle of the fork tines which is similar to what was observed for the bound unit load. This indicates that the flexibility of the unit load does not affect the bending or the dynamic motion of the fork tines.

Additionally, when comparing the dynamic motion of the pallet between the bound and the unbound unit load, it was found that greater motion occurred on the unbound unit load. The dynamic motion of the pallet increased from 0.7 in. – 0.8 in. to 0.12 in. – 0.14 in. Therefore, the dynamic flexing of the pallet is influenced by the flexibility of the unit load.

6.7.5. Effect of unbound unit load under dynamic handling in the across the width orientation with initially leveled fork tines

The unbound unit load under dynamic condition in the across the width orientation did not survive the 30-minute tests for two out of three tested replicates. The first unit load collapsed at 5:20 minutes, the second unit load collapsed at 11:02 minutes, and the third unit load survived the 30 minutes of testing. The data presented in Table 15 corresponds to the average deflection of the three replicates at the shortest time mark at which the unit loads failed (at 5:20 min).

Figure 50. Representative picture of one of the unbound unit loads after the dynamic test in the across the width orientation with initial leveled fork tines.

Figure 50 presents the condition of one of the unit loads after the dynamic test. When unit loads were tested in the across the width orientation, boxes had a tendency to fall towards the front side of the unit load. This could be explained with the overhang of the pallet from the fork tines. The existing cantilever of the pallet due to the difference in length between the fork tines (Pot 5 and Pot 6) and the pallet (Pot 11 and Pot 12) creates additional bending of the pallet, as shown in Figure 52. When analyzing the differences of the front corners of the pallet (Pot 1 and Pot 8), two cantilevers are involved in the across the length orientation and the three cantilevers are involved in the across the width orientation. The pallet in the across the length orientation is affected by the cantilevers of the fork tines, and both sides (left and right side) of the pallet. In contrast, the pallet in the across the width orientation is affected by the cantilevers of the fork tines, the bending on both sides (left and right side) of the pallet, and the front side of the pallet.

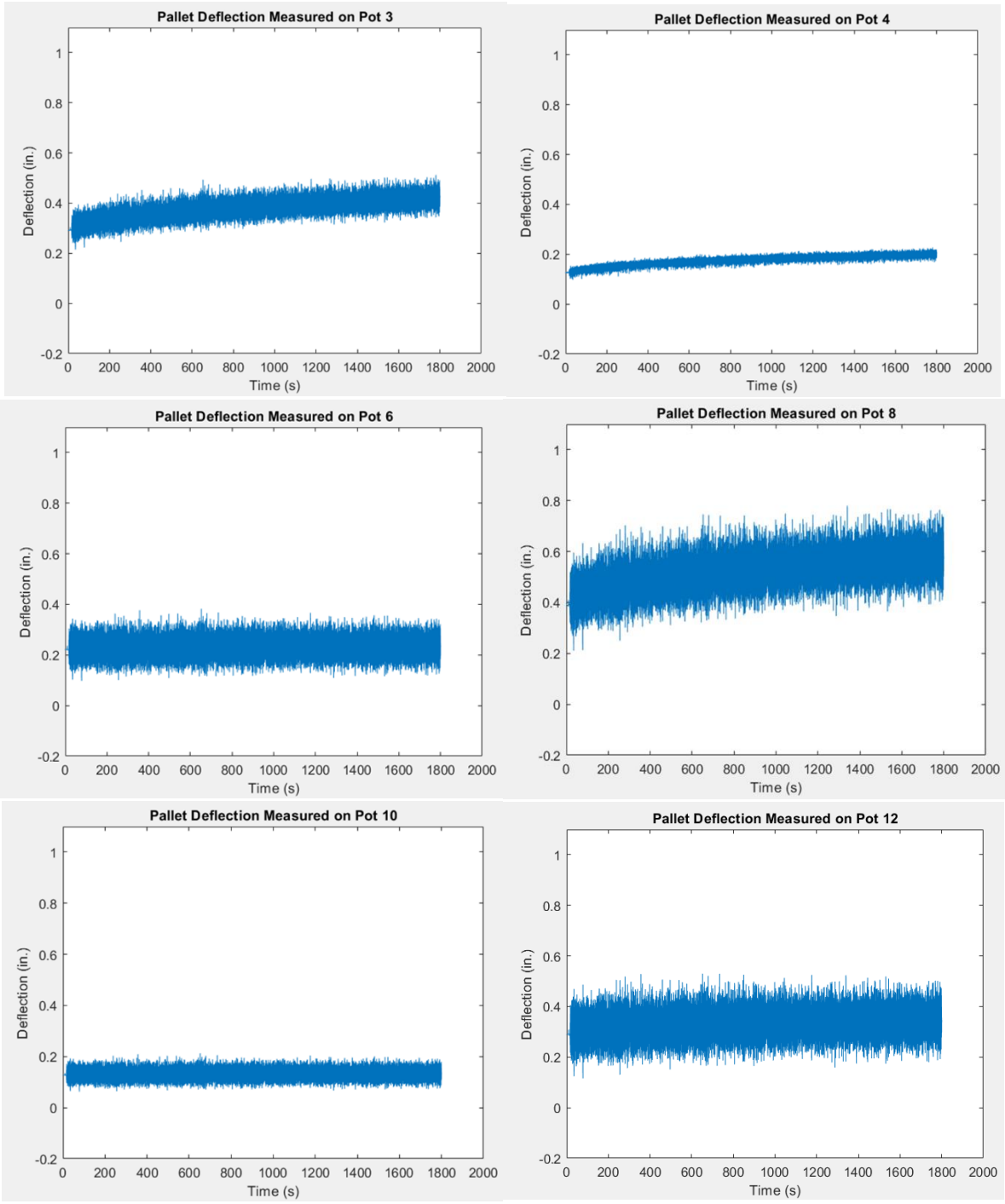

Figure 51. Pallet and fork tine deflection measured for the unbound unit load during the dynamic test across the width orientation

Figure 51 presents the deflection of the pallet and the fork tines during 30 minutes of dynamic testing. It can be observed that less dynamic motion is observed on the rear corner of the pallet (Pot 4), while greater dynamic motion is observed on the front corner of the pallet (Pot 8).

Additionally, it can be observed that the front corners of the pallet (Pot 1 and Pot 8) show greater deflection and dynamic motion when compared to the front side of the pallet (Pot 11 and Pot 12). This effect could be explained by the influence of the combined deflections of the three cantilevers on the front corners of the pallet. The creep amount for the pallet ranged from 2% - 12%.

Table 15. Summary of the average deflections measured for the unbound unit load during the dynamic condition

		Pallet and Fork Tine Deflection (in.) for Each Pot											
		1	2	3	4	5	6	7	8	9	10	11	12
Initial Deflection		0.5253	0.2913	0.2978	0.1448	0.2392	0.2272	0.0656	0.4256	0.0954	0.1042	0.3573	0.3031
At 3 min	**Upper**	0.7221	0.4062	0.3988	0.1953	0.3286	0.3071	0.1366	0.6128	0.1802	0.1826	0.4937	0.4219
	Middle	0.5960	0.3444	0.3416	0.1797	0.2466	0.2312	0.1138	0.4925	0.1168	0.1222	0.3869	0.3272
	Lower	0.4746	0.2846	0.2881	0.1601	0.1707	0.1592	0.0913	0.3746	0.0547	0.0649	0.2807	0.2270
At 5:20 min	**Upper**	0.7604	0.4294	0.4228	0.2066	0.3375	0.3146	0.1509	0.6666	0.1866	0.1881	0.5158	0.4440
	Middle	0.6164	0.3611	0.3606	0.1904	0.2472	0.2325	0.1278	0.5309	0.1176	0.1228	0.3937	0.3394
	Lower	0.4882	0.2994	0.3038	0.1719	0.1667	0.1539	0.1041	0.3980	0.0534	0.0626	0.2750	0.2294

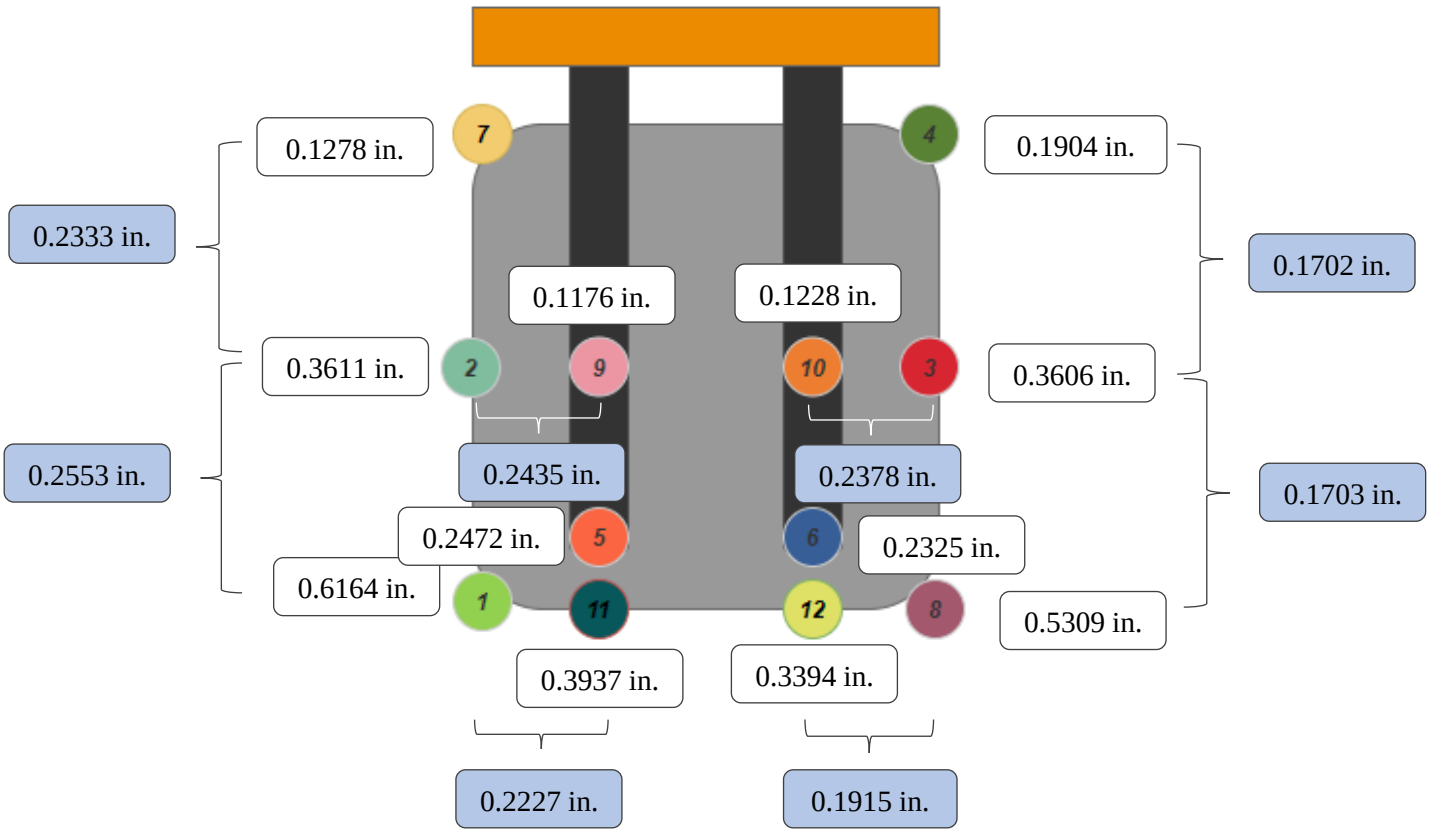

Figure 52. Average deflection measured at failure (5:20 min) for the unbound unit load during the dynamic test for the across the width orientation with level fork tines *White balloons:*

measurement of the deflection at the stated location. Blue balloons: deflection difference between the two stated locations.

Figure 52 shows the shortest time mark at which the unit loads failed (at 5:20 min). As observed, greater deflection occurred on the front corners (Pot 1 and Pot 8) of the pallet, followed by the front side of the pallet (Pot 11 and Pot 12), and the rear corners (Pot 4 and Pot 7) showed the less deflection. The front corners are affected by three cantilevers, the front side of the pallet is affected by two cantilevers, and the rear corners are affected by one cantilever. This shows that increasing the number of cantilevers increases the magnitude in deflection of the pallet.

6.7.6. Effect of unbound unit load under static handling in the across the length orientation with 4° angle fork tines

Forklift drivers have a tendency to tilt up the fork tines in order to create more stability on the unit loads. The maximum tilting of the fork tines measured for the forklifts was around 4°. Thus, in order to simulate this handling condition, unbound unit loads were tested in a static and dynamic condition with in a static and dynamic condition with 4 degree angle fork tines. The unbound unit load under static handling in the across the length orientation with 4° fork tines survived the 30 minutes of test for all three tested replicates, as shown in Figure 53. Figure 54 shows the behavior of pallet deflection during the test. Additionally, the deflections collected during the static test are presented in Table 16, and Figure 55. Similarly to previous tests, no creep deflection was observed on the fork tines.

Figure 53. Representative picture of one of the unbound unit loads after the dynamic test in the across the length orientation with initial leveled fork tines.

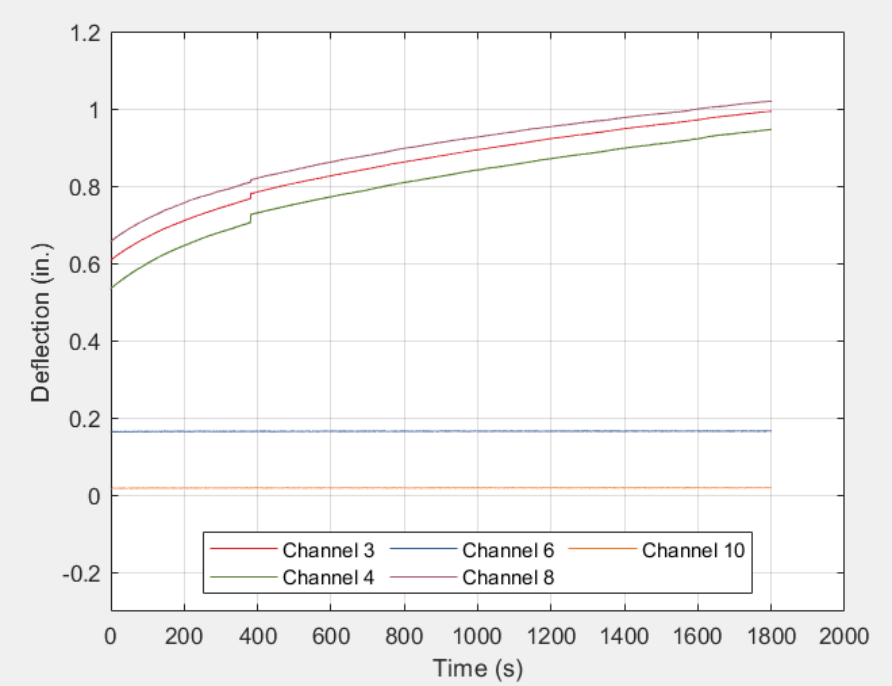

Figure 54. Pallet and fork tine deflection measured for the unbound unit load during the static test across the length orientation with 4° angle fork tines

When comparing the creep deflections between the level and 4-degree fork tines, it was observed that less deflection was measured using 4-degree fork tines in most of the locations on the pallet. This could be explained by the fact that the center of gravity was shifted towards the rear end of the pallet, and since there is no cantilever on the rear side of the fork tines it might have reduced pallet deflection. The creep amount for the pallet ranged from 36% - 50%. Similar creep amount was observed when comparing to the initially leveled fork tines with the unbound unit load during the static testing.

Table 16. Summary of the average deflections measured for the unbound unit load during the static condition in the across the length orientation with 4° angle fork tines

Pallet and Fork Tine Deflection (in.) for Each Pot											
		1	2	3	4	5	6	7	8	9	10
Initial Deflection		0.4315	0.4823	0.6213	0.5346	0.1347	0.1719	0.5611	0.6807	0.0501	0.0186
At 3 min	**Upper**	0.5557	0.5707	0.7145	0.6331	0.1354	0.1726	0.6603	0.7729	0.0503	0.0195
	Middle	0.5548	0.5698	0.7135	0.6320	0.1352	0.1725	0.6592	0.7719	0.0501	0.0192
	Lower	0.5539	0.5688	0.7125	0.6310	0.1350	0.1723	0.6581	0.7708	0.0499	0.0190
At 30 min	**Upper**	0.7967	0.8525	1.0059	0.9440	0.1334	0.1734	0.9778	1.0478	0.0481	0.0199
	Middle	0.7964	0.8522	1.0055	0.9436	0.1332	0.1733	0.9775	1.0475	0.0478	0.0197
	Lower	0.7960	0.8518	1.0051	0.9432	0.1330	0.1730	0.9771	1.0471	0.0476	0.0195

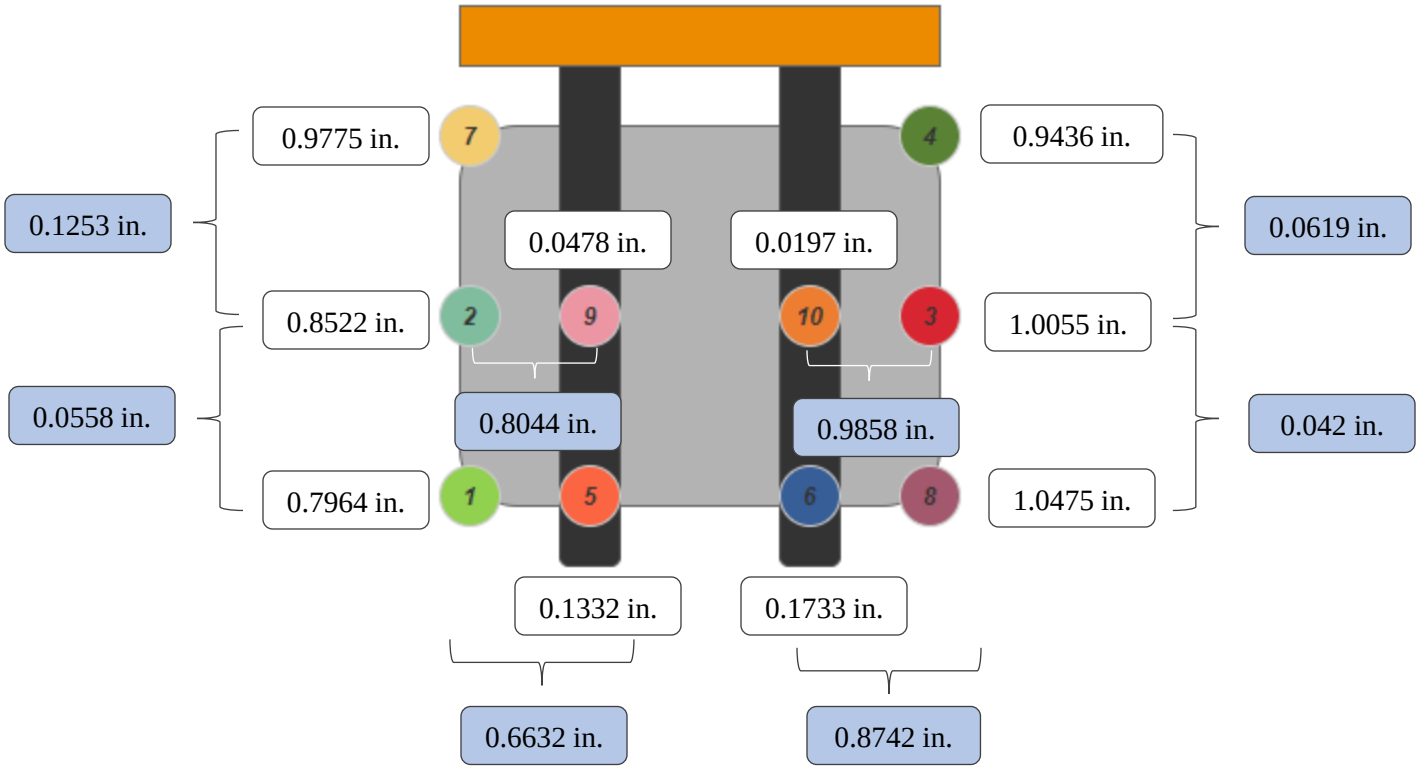

Figure 55. Deflection measured for the unbound unit load during the static test for the across the length orientation with 4-degree fork tines *White balloons: measurement of the deflection at the stated location. Blue balloons: deflection difference between the two stated locations.*

Figure 55 shows the pallet deflection after 30-minute creep test. For this handling condition, greater deflection was observed to occur on one of the rear corners of the pallet (Pot 7). This could be explained by the shifting of the center of gravity towards the rear end of the unit load due to the 4-degree tilting of the fork tines.

6.7.7. Effect of unbound unit load under dynamic handling in the across the length orientation with 4° angle fork tines

The unbound unit load under dynamic condition across the length orientation with 4° fork tines did not survive the 30 minutes of test for two out of the three unit loads. The first unit load collapsed around 25:35 minutes, the second unit load collapsed around 11:10 minutes, while the third unit load survived the test. The condition of one of the unit loads is presented in Figure 56. The deflection of the pallet and fork tines during the dynamic is presented in Table 17, Figure 57, and Figure 58.

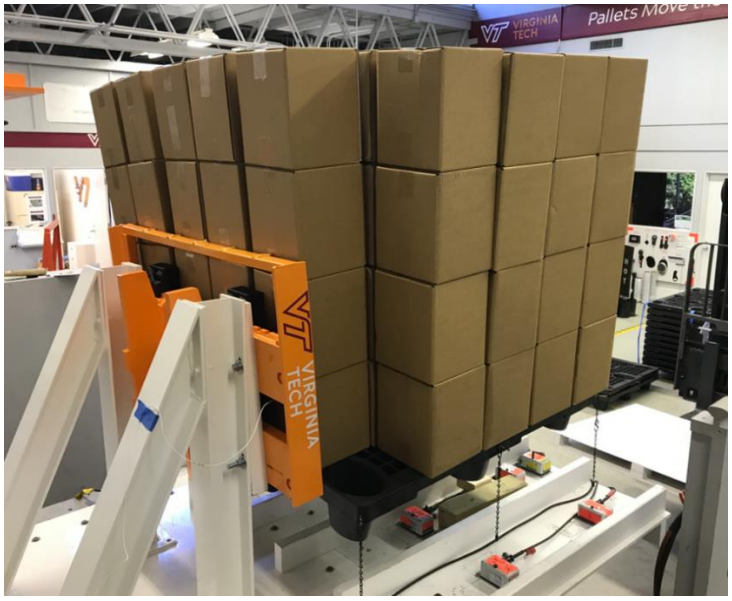

Figure 56. Representative picture of one of the unbound unit loads after the dynamic test in the across the length orientation with initial leveled fork tines.

As observed in Figure 56, boxes tended to fall from the rear corners of the pallet with 4-degree fork tines. While the boxes tended to fall from the sides of the pallet with level fork tines. This could be explained by the shifting of the center of gravity of the unit load towards to rear of the pallet.

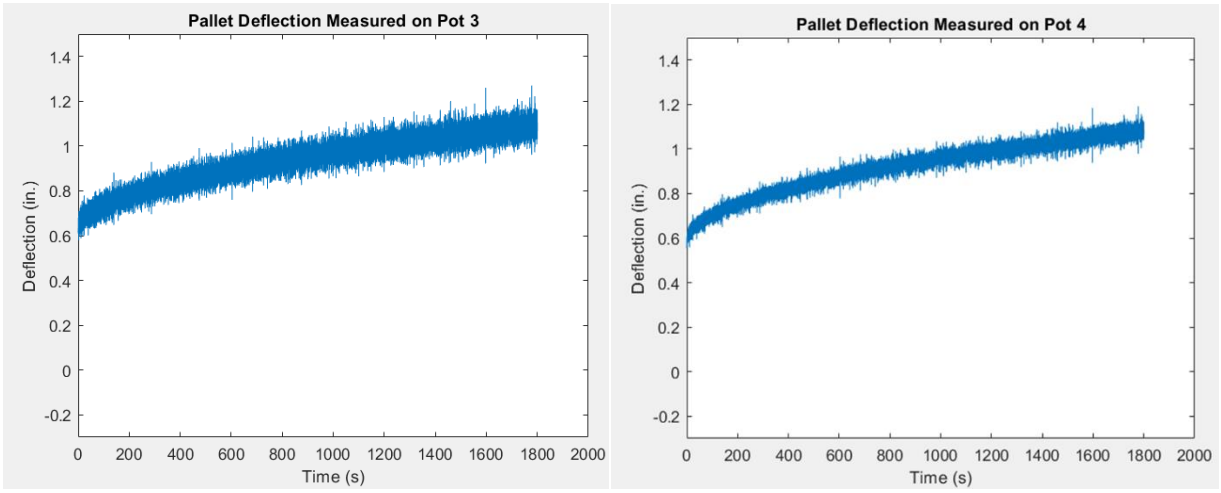

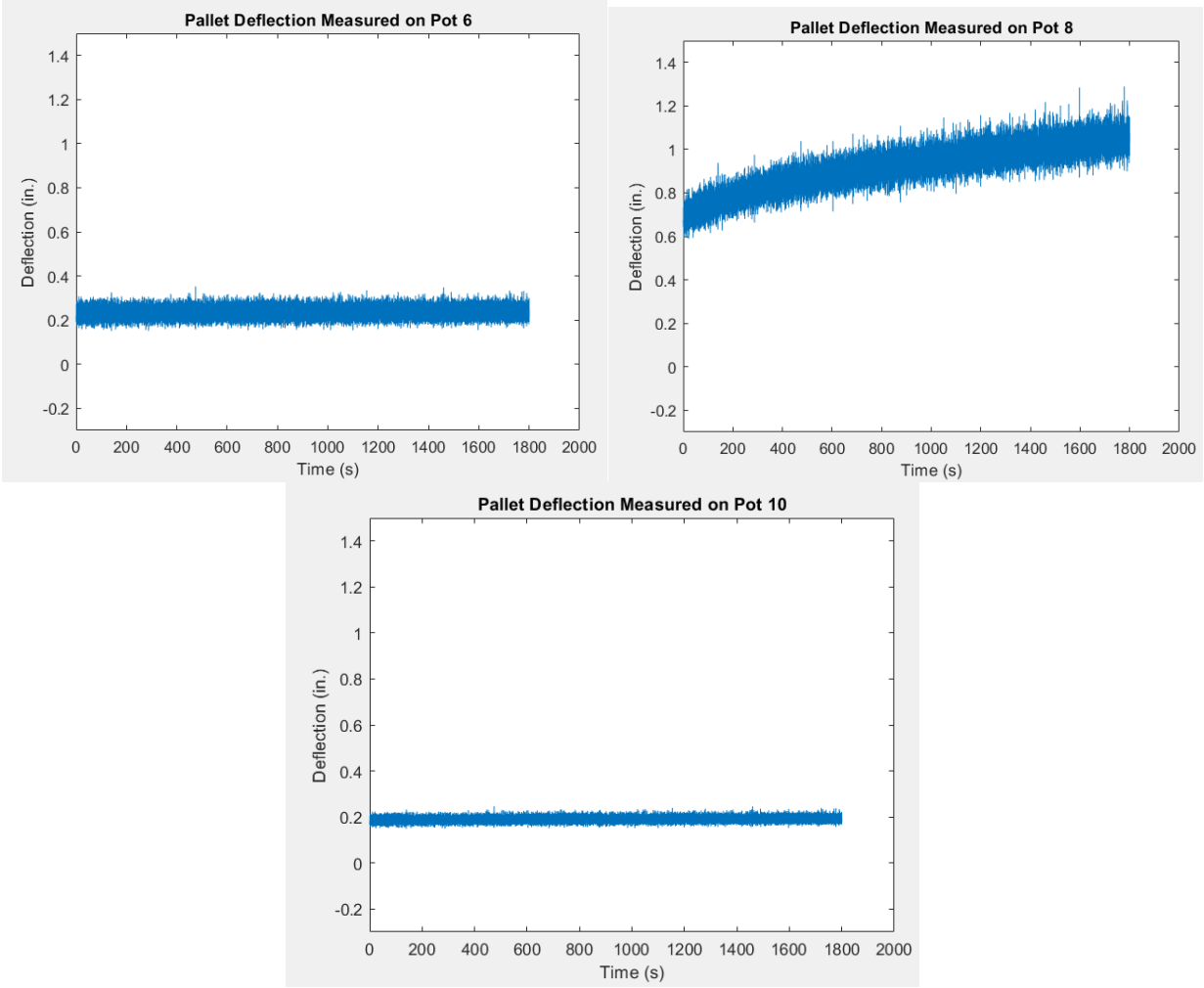

Figure 57. Pallet and fork tine deflection measured for the unbound unit load during the dynamic test across the length orientation with 4° angle fork tines

As shown in Figure 57, greater dynamic motion was observed on the front corners of the pallet (Pot 1 and Pot 8), between 0.0942 in. and 0.1231 in. In addition, the creep deflection of the pallet was between 17% and 23% which is less when comparing to the unit load under dynamic testing with initially leveled fork tines (creep amount ranged from 19% - 43%).

Table 17. Summary of the average deflections measured for the unbound unit load during the dynamic condition in the across the length orientation with 4° angle fork tines

Pallet and Fork Tine Deflection (in.) for Each Pot											
		1	2	3	4	5	6	7	8	9	10
Initial Deflection		0.6008	0.6154	0.6187	0.5620	0.1774	0.1931	0.6593	0.6596	0.1083	0.1169
At 3 min	**Upper**	0.8614	0.8809	0.8566	0.8143	0.2678	0.2785	0.9325	0.8813	0.1554	0.1634
	Middle	0.7365	0.7945	0.7841	0.7690	0.2021	0.2172	0.8800	0.7798	0.1219	0.1323
	Lower	0.6286	0.7156	0.7173	0.7234	0.1459	0.1644	0.8253	0.6875	0.0931	0.1056

At 11:10 min	**Upper**	1.0095	1.0718	1.0189	0.9985	0.2674	0.2773	1.1350	1.0104	0.1554	0.1663
	Middle	0.8864	0.9786	0.9449	0.9477	0.2064	0.2230	1.0744	0.9133	0.1252	0.1381
	Lower	0.7732	0.8921	0.8705	0.8958	0.1504	0.1697	1.0085	0.8191	0.0966	0.1128

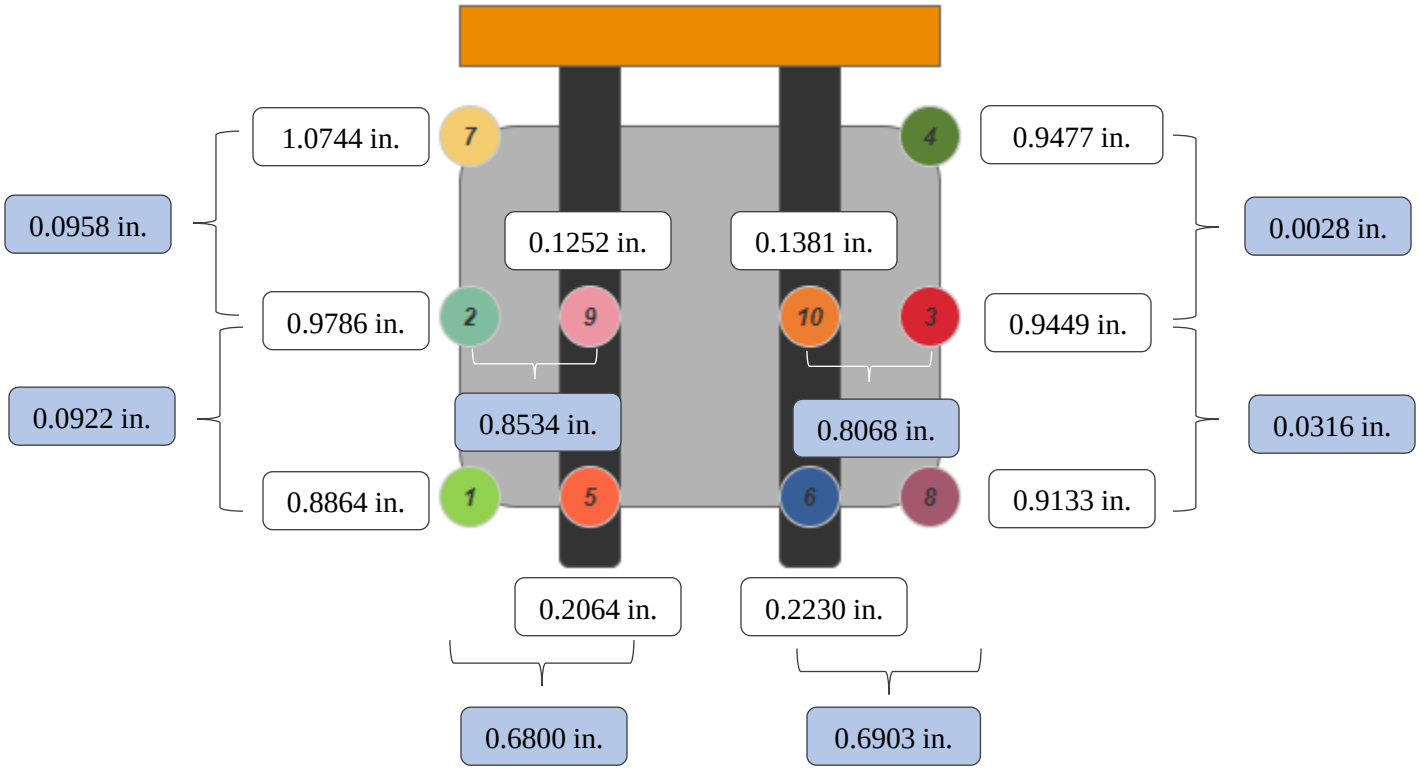

Figure 58. Average deflection measured at failure (11:10 min) for the unbound unit load during the dynamic test for the across the length orientation with 4-degree fork tines. *White balloons: measurement of the deflection at the stated location. Blue balloons: deflection difference between the two stated locations.*

When comparing the dynamic test between level and 4-degree fork tines, unit loads on 4-degree fork tines tended to survive longer. This could be explained by the fact that the center of gravity of the unit load is shifted towards the rear end of the pallet. Therefore, when dynamic motion is applied, part of the side bending of the unit load is distributed towards the rear end. Additionally, when analyzing the dynamic motion for each individual Pot of the pallet and the fork tines, it was found that the amount of up and down motion was similar, as shown in Table 18.

Table 18. Summary of the average of the dynamic motion measured for the unbound unit load during the dynamic condition in the across the length orientation with 4-degree fork tines.

		Pallet and Fork Tine Movement (in.) for Each Pot									
		1	2	3	4	5	6	7	8	9	10
At 11:10 min	**Upper**	0.1231	0.0932	0.074	0.0508	0.061	0.0543	0.0606	0.0971	0.0302	0.0282
	Lower	0.1132	0.0865	0.0744	0.0519	0.056	0.0533	0.0659	0.0942	0.0286	0.0253

6.7.8. Effect of unbound unit load under dynamic handling in the across the width orientation with 4° angle fork tines

The unbound unit load under dynamic handling in the across the width orientation with 4° fork tines survived the 30-minute dynamic test for all three tested replicates. The condition of the unit load after the test is presented in Figure 59. The deflection measured on the pallet and fork tines are presented in Table 19, Table 20, Figure 60, and Figure 61.

Figure 59. Representative picture of one of the unbound unit loads after the dynamic test in the across the width orientation with initial leveled fork tines.

As observed in Figure 59, the three tested replicates survived the 30-minute dynamic testing. Thus, no boxes fell from the unit load. When comparing visually between the across the width and the across the length orientation for the unbound unit load with 4-degree fork tines, the

boxes in the across the width orientation tended to bend less towards the side of the pallet. This could be explained by the difference in cantilever length between these two orientations.

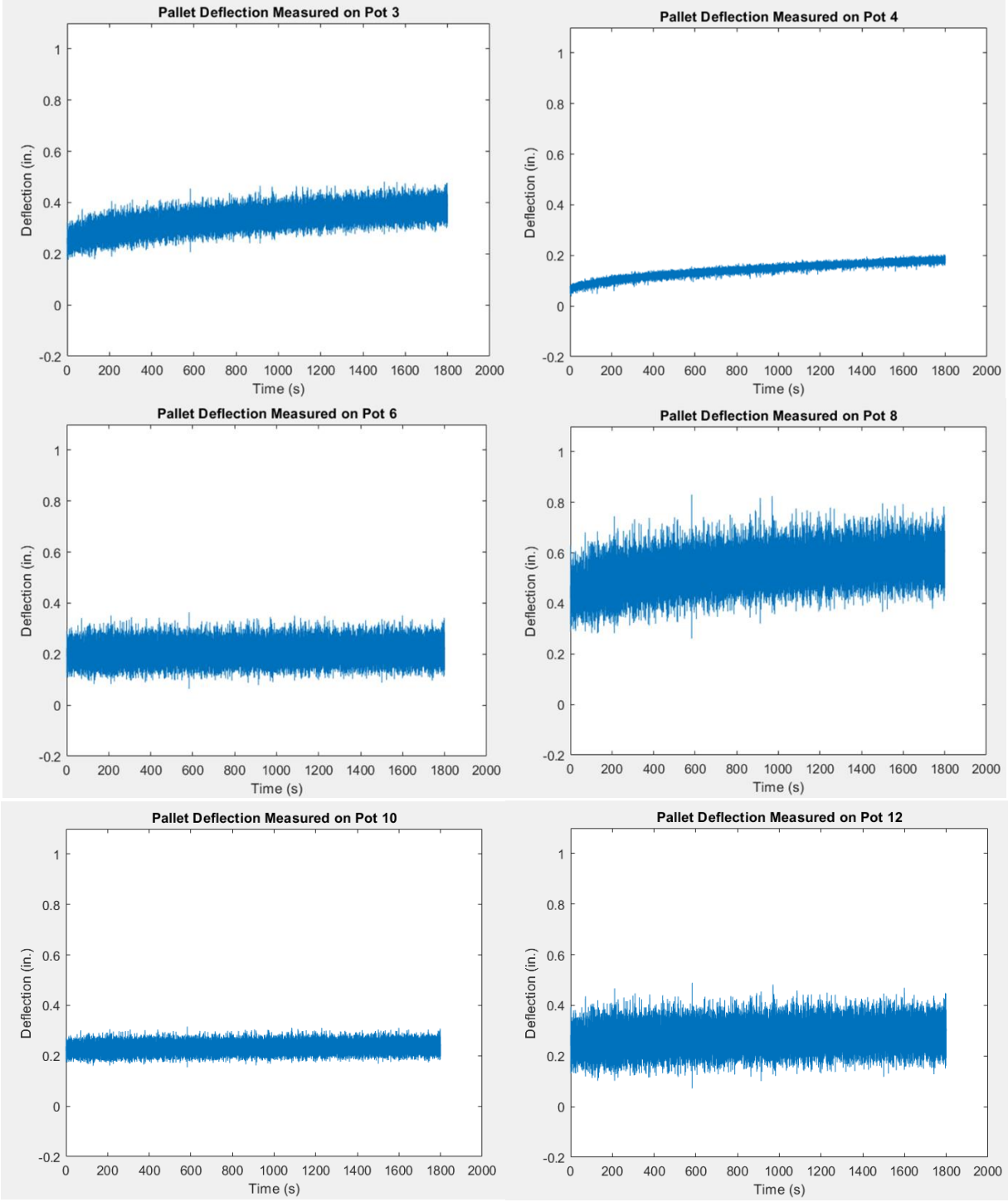

Figure 60. Pallet and fork tine deflection measured for the unbound unit load during the dynamic test across the width orientation with 4° angle fork tines.

As shown in Figure 60, greater dynamic motion was observed on the front corners of the pallet (Pot 1 and Pot 8), between 0.101 in. and 0.1183 in. In addition, the creep amount of the pallet ranged from 25% - 30%. Less motion was observed at the rear corners of the pallet (Pot 4 and Pot 7), between 0.0014 in. and 0.0204 in. This could be explained by the fact that the center of the gravity of the unit load is shifted towards the rear end of the pallet. Therefore, more load is concentrated at the rear of the pallet in comparison to the front corners.

Table 19. Summary of the average deflections measured for the unbound unit load during the dynamic condition in the across the width orientation with 4-degree fork tines.

		Pallet Deflection (in.) for Each Location											
Testing Condition		1	2	3	4	5	6	7	8	9	10	11	12
Initial Deflection		0.4289	0.2677	0.2576	0.0790	0.2256	0.2173	0.1355	0.4182	0.1098	0.2359	0.2454	0.2768
At 3 min	**Upper**	0.5513	0.3659	0.3511	0.1236	0.3015	0.2971	0.1921	0.5737	0.1532	0.2803	0.3506	0.3855
	Middle	0.4430	0.3075	0.2901	0.1081	0.2238	0.2168	0.1701	0.4521	0.1101	0.2366	0.2501	0.2831
	Lower	0.3324	0.2493	0.2334	0.0921	0.1465	0.1414	0.1434	0.3380	0.0661	0.1947	0.1546	0.1864
At 30 min	**Upper**	0.6438	0.4517	0.4365	0.1895	0.3102	0.3065	0.2556	0.6622	0.1616	0.2864	0.3723	0.4081
	Middle	0.5344	0.3931	0.3745	0.1755	0.2306	0.2241	0.2369	0.5439	0.1165	0.2433	0.2736	0.3081
	Lower	0.4334	0.3397	0.3185	0.1595	0.1573	0.1509	0.2165	0.4360	0.0762	0.2027	0.1821	0.2158

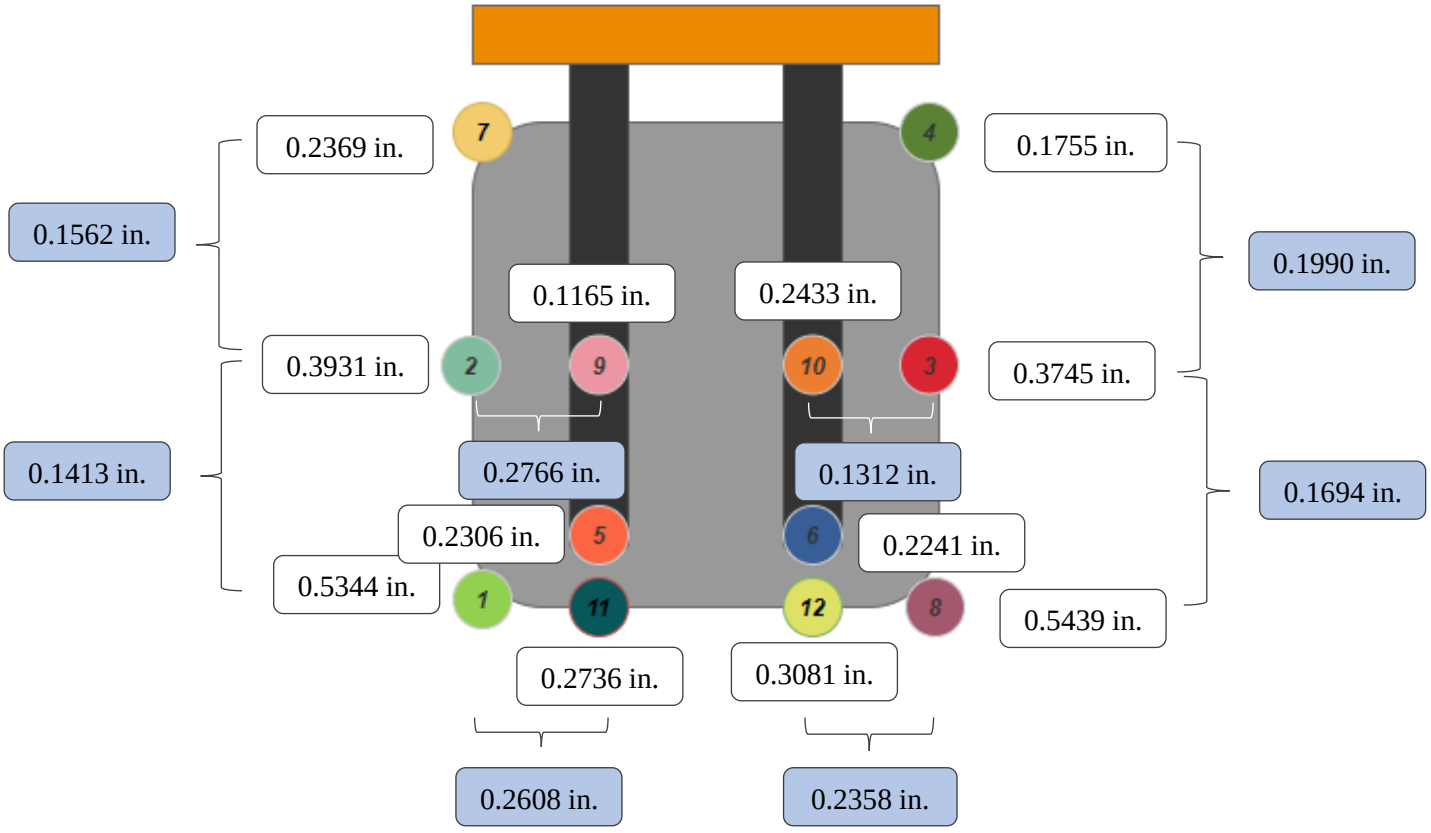

Figure 61. Deflection measured for the unbound unit load during the dynamic test for the across the width orientation with 4-degree fork tines. *White balloons: measurement of the deflection at the stated location. Blue balloons: deflection difference between the two stated locations.*

Similarly to the unbound unit load in the width orientation with initial leveled fork tines, greater deflection was measured on the front corners of the pallet (Pot 1 and Pot 8), followed by the front side of the pallet (Pot 11 and Pot 12), and the rear corners (Pot 4 and Pot 7), as presented in Figure 60 and Figure 61. The front corners of the pallet are affected by three cantilevers, the front side of the pallet is affected by two cantilevers, and the rear corners are affected by one cantilever. This shows that increasing the number of cantilevers increases the magnitude in deflection of the pallet. As presented in Table *21*, when analyzing the each pot individually, it was found that the amount of up and down motion was similar.

Table 20. Summary of the average of the dynamic motion measured for the unbound unit load during the dynamic condition in the across the width orientation with 4-degree fork tines.

		Pallet and Fork Tines Movement (in.) for Each Pot											
		1	2	3	4	5	6	7	8	9	10	11	12
At 3 min	**Upper**	0.1083	0.0584	0.0610	0.0155	0.0777	0.0803	0.0220	0.1216	0.0431	0.0437	0.1005	0.1024
	Lower	0.1106	0.0582	0.0567	0.0160	0.0773	0.0754	0.0267	0.1141	0.0440	0.0419	0.0955	0.0967
At 30 min	**Upper**	0.1094	0.0586	0.0620	0.0140	0.0796	0.0824	0.0187	0.1183	0.0451	0.0431	0.0987	0.1000
	Lower	0.1010	0.0534	0.0560	0.0160	0.0733	0.0732	0.0204	0.1079	0.0403	0.0406	0.0915	0.0923

6.8. Limitations

The results obtained in this study is subject to the specific pallet design used for the experiments, and therefore, any conclusion obtained cannot be generalized to other pallet design. In addition, the vibration profile used to simulate the forklift handling was obtained through a controlled laboratory experiment, therefore, the vibration intensity may not be representative of the real-life handling conditions.

6.9. Conclusions

The conclusions obtained through the study were that highest deflection values were observed to occur on the front corners of the pallet due to the combined effect of deflection due to the cantilever of the fork tines and to the pallet. It was observed that vibration increases bending due to the magnification in the movement of the pallet. In addition, it was observed that fork tines do not creep over the different test due to its rigidity, while pallet creeps over time in the case of

the unbound unit loads. Deflection limit proposed in the ISO 8611 standard is appropriate and potentially even too conservative for bound unit loads but not appropriate for unbound unit loads. When the fork tines are not adjusted to stabilize the load, the unit load of boxes became unstable for both across the width and across the length orientation. In addition, when the operator tilts the fork tines back 4-degrees the unit load was stable for the across the width orientation but not for the across the length orientation. Moreover, the 4-degree tilt might be too much of the unit load since greater deflection was observed towards the rear side of the pallet. Finally, the applicability of the ISO deflection limit depends on how the pallet is handled in the distribution.

6.10. References

1. ASTM International. (2009). *ASTM D1185-98a: Standard Test Methods for Pallets and Related Structures Employed in Materials Handling and Shipping.*
2. Böröcz, P.; Molnár, B. Measurement and Analysis of Vibration Levels in Stacked Small Package Shipments in Delivery Vans as a Function of Free Movement Space. Appl. Sci. **2020**, 10, 7821.
3. Böröcz, P.; Singh, S.P. Measurement and analysis of delivery van vibration levels to simulate package testing for parcel delivery in Hungary. Packag. Technol. Sci. **2018**, 31, 342–352.
4. Brandenburg, R.K.; Lee, J.J. Fundamentals of Packaging Dynamics. L.A.B. Equipment, Inc.: Itasca, USA, 2001.
5. Chonhenchob, V.; Singh, S.P.; Singh, J.; Sittipod, S.; Swasdee, D.; Pratheepthinthong, S. Measurement and analysis of truck and rail vibration level in Thailand. Packag. Technol. Sci. **2010**, 23, 91–100.
6. Chonhenchob, V.; Singh, S.P.; Singh, J.; Stallings, J.; Grewal, G. Measurement and analysis of vehicle vibration for delivering packages in small-sized and medium-sized trucks and automobiles. Packag. Technol. Sci. **2012**, 25, 31–38.
7. Freedonia. (2015). *Pallets*. Retrieved from Freedonia: https://www.freedoniagroup.com/industry-study/pallets-3033.htm
8. Huang, Y., Horvath, L., Böröcz, P., "Measurement and Analysis of Industrial Forklifts Vibration Levels for Unit Load Testing Purposes." Applied Sciences 11, no. 7 (March 2021): 2901. https://doi.org/10.3390/app11072901.
9. ISO 8611. (2011). *Pallets for materials handling - Flat pallets - Part 2.*
10. Kipp B. Environmental Data Recording, Analysis and Simulation of Transport Vibrations. Packag. Technol. Sci. 2008, 9, 437-438.
11. Mejias, A. Effect of Pallet Design on the Performance of Semi-Automatic & Fully-Automatic Warehouse. M.S. Thesis, Virginia Tech, **2020** p. 66.
12. MMH, (2020). Annual Pallet Report: 2020's market evaluation. Retrieved from: https://www.mmh.com/article/annual_pallet_report_2020s_market_evaluation
13. O'Dell, R., Clarke, J.W., White, M.S. (1998) Relationship of Friction Characteristics and Pallet Performance. Retrieved from: https://www.slick.unitload.vt.edu/membership/member-center/slick/uploaded_pdfs/ODell_Clarke_White_1998_Relationship_of_friction_characteristics_and_pallet_performance.pdf

14. Park, J.; Choi, S.; Jung, H.M. Measurement and Analysis of Vibration Levels for Truck Transport Environment in Korea. Appl. Sci. **2020**, 10, 6754.
15. Singh, S.P.; Saha, K.; Singh, J.; Sandhu, A.P.S. Measurement and analysis of vibration and temperature levels in global intermodal container shipments on truck, rail and ship. Packag. Technol. Sci. **2012**, 25, 149–160.
16. Singh, S.P.; Sandhu, A.P.S.; Singh, J.; Joneson, E. Measurement and analysis of truck and rail shipping environment in India. Packag. Technol. Sci. **2007**, 20, 381–392.

7. GENERAL CONCLUSIONS

Forklift vibration intensity is affected by factors such as the speed of the forklift, the carried payload of the unit load, the road conditions, sensor location, and type of forklift. These factors increase or decrease vibration intensities. The most conservative condition was observed to occur with the gas-powered forklift, driven on asphalt condition while driven at 3 mph and carrying a unit load of 1,500 lbs. The highest vibration intensity occurred at low frequencies, around 3-4 Hz. Vibration levels at the tip of the fork tines were higher than those at the carriage and the fork tine heels. An increase in speed of the forklift resulted in an increase in the vibration intensity while an increase in the weight carried by the forklift resulted in a decrease in the vibration intensity. Vibration levels were higher on asphalt compared to concrete due to the surface irregularities. The gas-powered forklift presented the highest vibration intensity, followed by the electric forklift, and then, the reach truck. The highest vibration intensity in the frequency range of 1 – 200 Hz was 0.145 Grms which is much lower than vibrations observed during truck transport. The maximum acceleration level observed was 1.73 G with a duration of 8ms. Random vibration events observed for forklifts followed a non-Gaussian distribution.

Additionally, when measuring pallet bending under a simulated forklift handling condition, it was observed that the highest deflection values were usually observed to occur on the front corners of the pallet due to the combined effect of deflection due to the cantilever of the fork tines and to the pallet. It was observed that vibration increases bending due to the magnification in the movement of the pallet. In addition, it was observed that fork tines do not creep over the different test due to its rigidity, while pallet creeps over time in the case of the unbound unit loads. Deflection limit proposed in the ISO 8611 standard is appropriate and potentially even too conservative for bound unit loads but not appropriate for unbound unit loads. When the fork tines are not adjusted to stabilize the load, the unit load of boxes became unstable for both across the width and across the length orientation. In addition, when the operator tilts the fork tines back 4-degrees the unit load was stable for the across the width orientation but not for the across the length orientation. Moreover, the 4-degree tilt might be too much of the unit load since greater deflection was observed towards the rear side of the pallet. Finally, the applicability of the ISO deflection limit depends on how the pallet is handled in the distribution.

8. RECOMMENDATIONS FOR FUTURE RESEARCH

Additional research should be conducted in order to further understand pallet bending during a forklift handling condition.

- Different unit load weights should be investigated further in order to determine a more accurate pallet deflection limit.
- Different types of plastic pallets should be investigated further since different unit load capacity rating are obtained.
- Different corrugated boxes sizes should be investigated since it way affects the unit load stability.
- Conduct a study in order to map the picking process of a warehouse, since it may determine the success of the dynamic test.
- Further investigate vibration intensities that occur in an actual warehouse or distribution center.
- Further investigated the correlation between static and dynamic bending by performing sinusoidal vibration tests.
- Investigate the natural frequency of the different locations of the pallet during the dynamic testing.

APPENDIX A

Jig Design

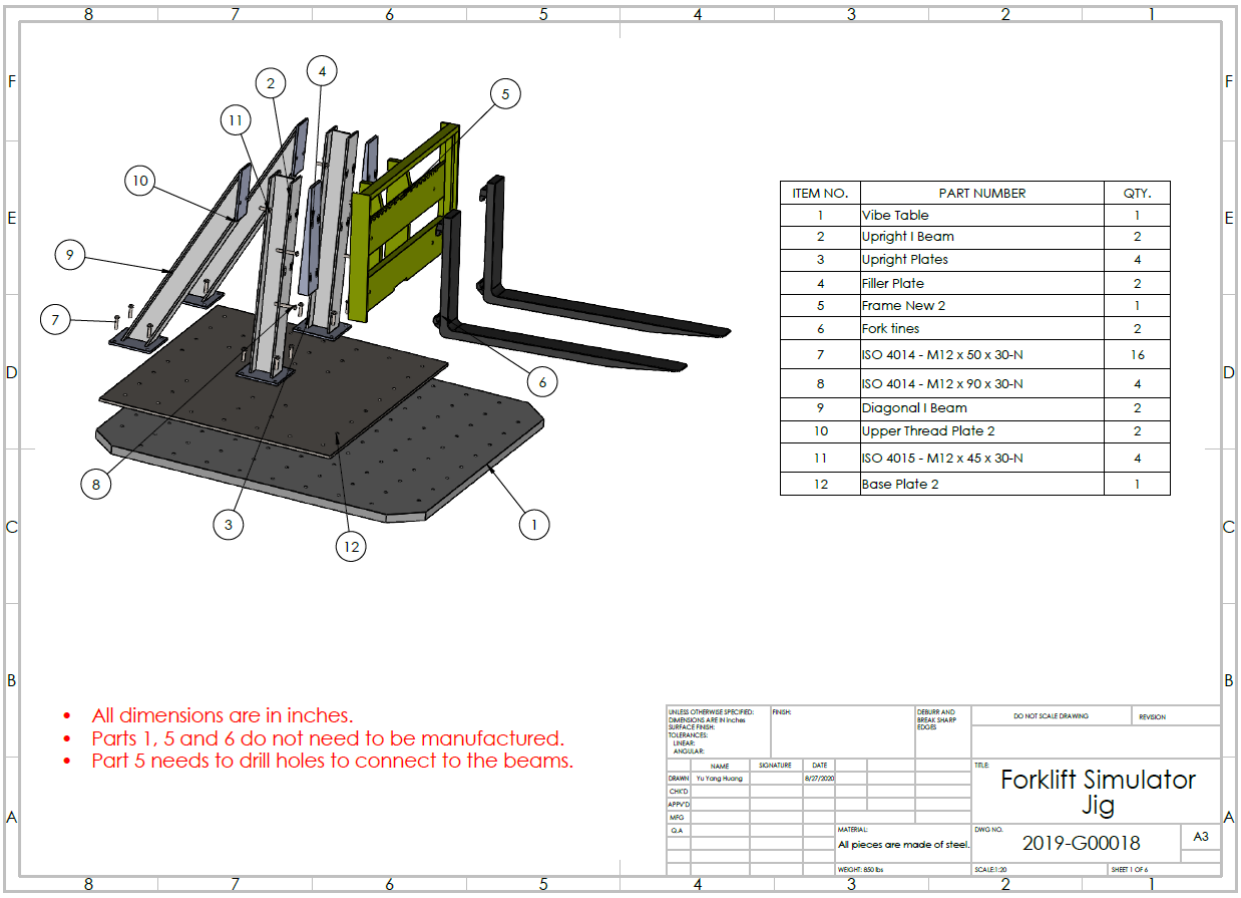

ITEM NO.	PART NUMBER	QTY.
1	Vibe Table	1
2	Upright I Beam	2
3	Upright Plates	4
4	Filler Plate	2
5	Frame New 2	1
6	Fork tines	2
7	ISO 4014 - M12 x 50 x 30-N	16
8	ISO 4014 - M12 x 90 x 30-N	4
9	Diagonal I Beam	2
10	Upper Thread Plate 2	2
11	ISO 4015 - M12 x 45 x 30-N	4
12	Base Plate 2	1

- All dimensions are in inches.
- Parts 1, 5 and 6 do not need to be manufactured.
- Part 5 needs to drill holes to connect to the beams.

UNLESS OTHERWISE SPECIFIED: DIMENSIONS ARE IN Inches SURFACE FINISH: TOLERANCES: LINEAR: ANGULAR:
FINISH:
DEBURR AND BREAK SHARP EDGES
DO NOT SCALE DRAWING
REVISION

	NAME	SIGNATURE	DATE
DRAWN	Yu Yang Huang		8/27/2020
CHK'D			
APP'V'D			
MFG			
Q.A			

TITLE: Forklift Simulator Jig

MATERIAL: All pieces are made of steel.

DWG NO. 2019-G00018

A3

WEIGHT: 850 lbs

SCALE:1:20

SHEET 1 OF 6

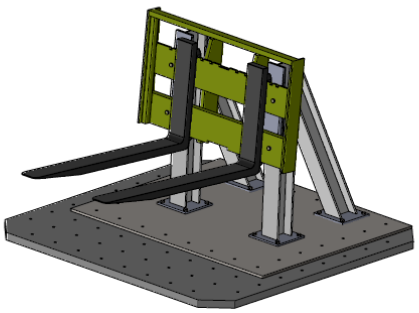

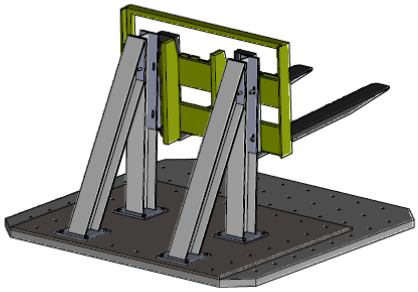

UNLESS OTHERWISE SPECIFIED: DIMENSIONS ARE IN MILLIMETERS SURFACE FINISH: TOLERANCES: LINEAR: ANGULAR:		FINISH:			DEBURR AND BREAK SHARP EDGES	DO NOT SCALE DRAWING	REVISION
	NAME	SIGNATURE	DATE			TITLE: Forklift Simulator Jig	
DRAWN	Yu Yang Huang		8/27/2020				
CHK'D							
APPV'D							
MFG							
Q.A				MATERIAL: All pieces are made of steel.		DWG NO. 2019-G00018	A3
				WEIGHT: 850 lbs		SCALE:1:20	SHEET 2 OF 6

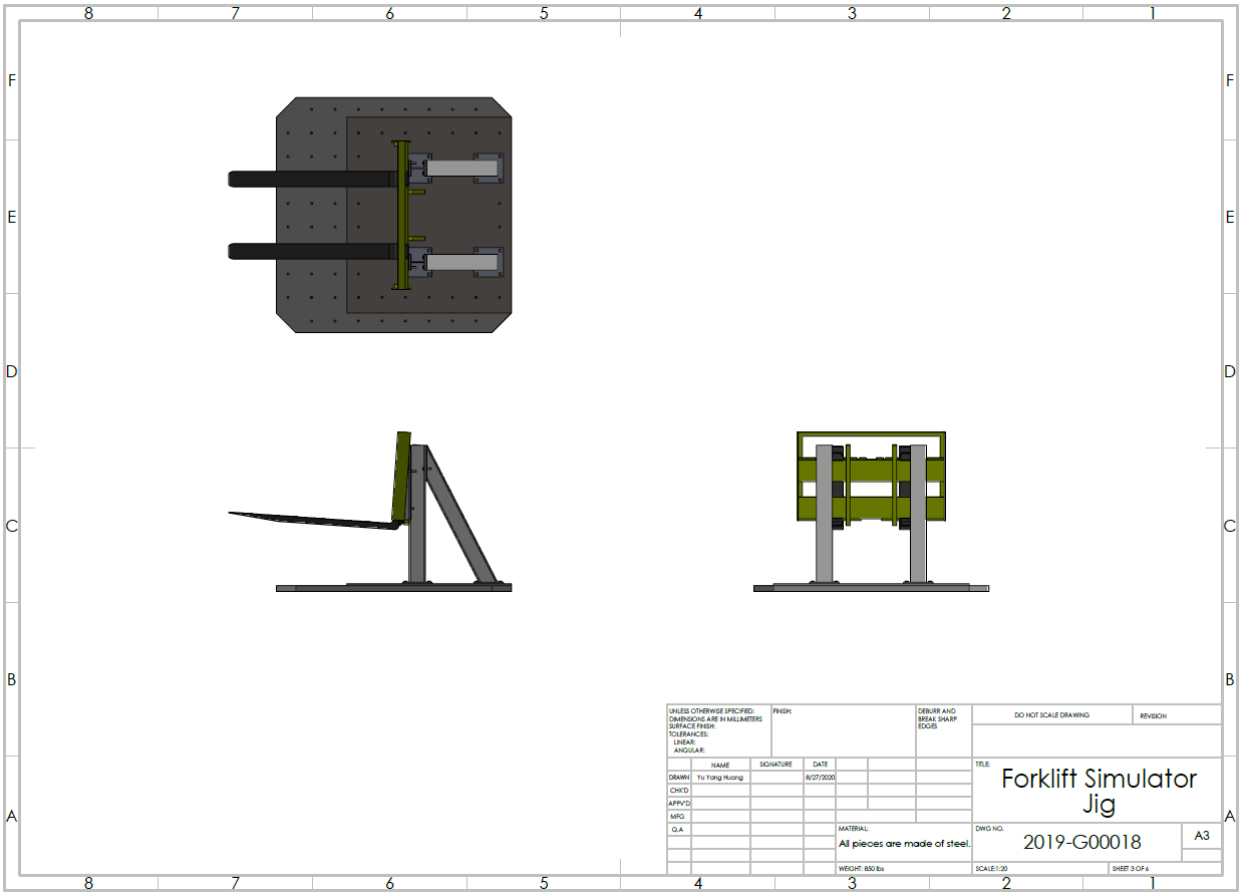
UNLESS OTHERWISE SPECIFIED:
DIMENSIONS ARE IN MILLIMETERS
SURFACE FINISH:
TOLERANCES:
LINEAR:
ANGULAR:
FINISH:
DEBURR AND BREAK SHARP EDGES
DO NOT SCALE DRAWING
REVISION
NAME
SIGNATURE
DATE
DRAWN
Yu Yang Huang
8/27/2020
CHK'D
APPV'D
MFG
Q.A
TITLE:
Forklift Simulator Jig
MATERIAL:
All pieces are made of steel.
DWG NO.
2019-G00018
A3
WEIGHT: 850 lbs
SCALE:1:20
SHEET 3 OF 6

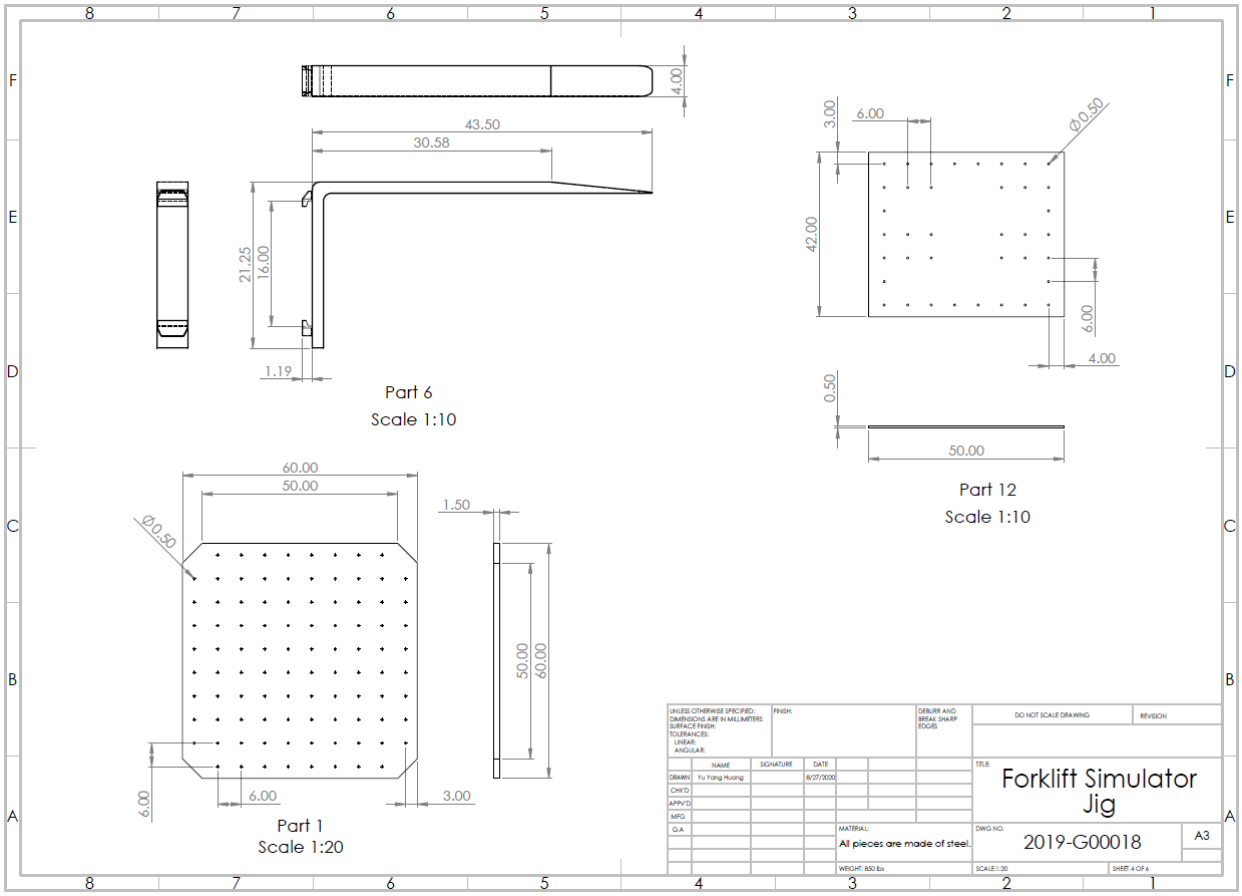
4.00
43.50
30.58
21.25
16.00
1.19
Part 6
Scale 1:10
3.00
6.00
Ø0.50
42.00
6.00
4.00
0.50
50.00
Part 12
Scale 1:10
60.00
50.00
Ø0.50
1.50
50.00
60.00
6.00
6.00
3.00
Part 1
Scale 1:20
Forklift Simulator Jig
2019-G00018
A3
All pieces are made of steel.

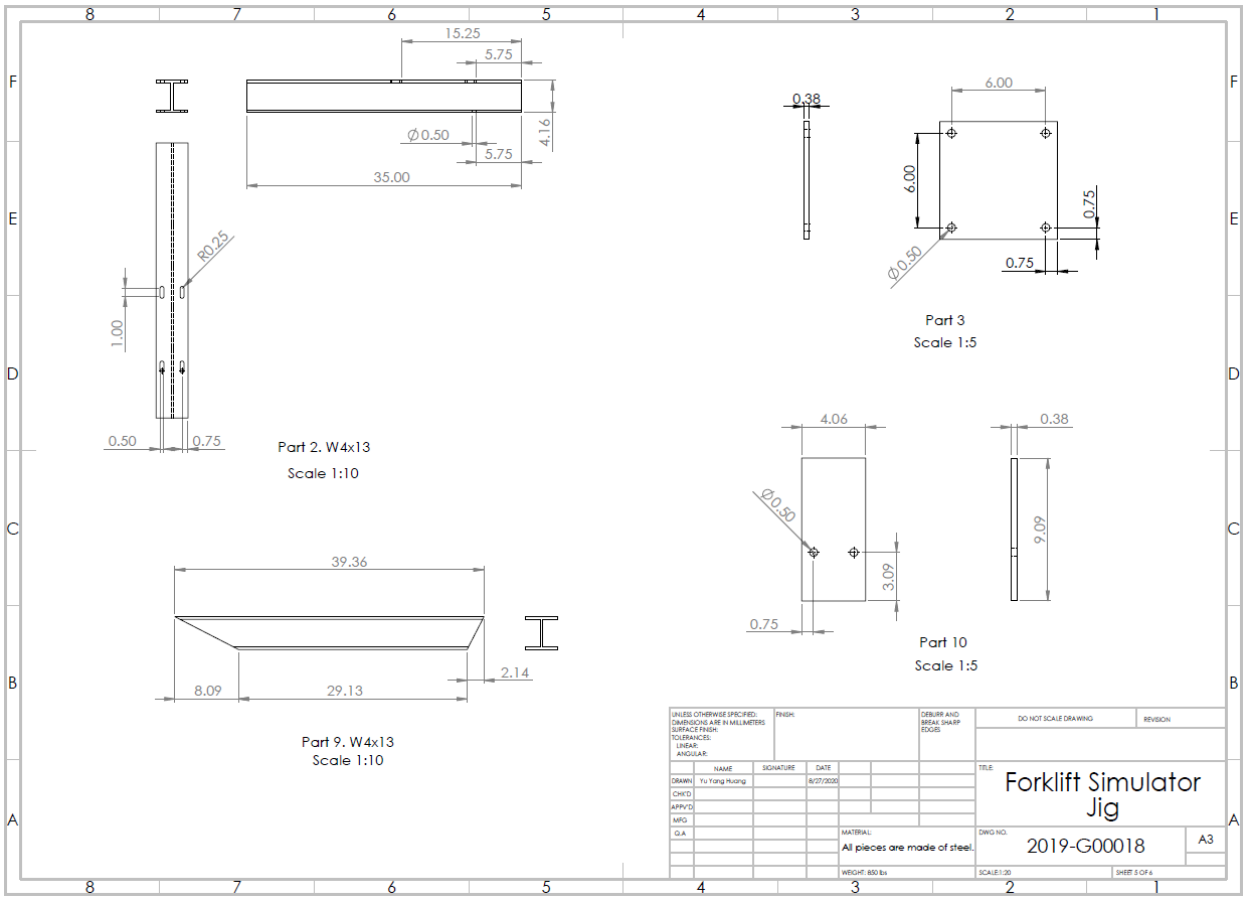
15.25
5.75
Ø0.50
5.75
4.16
35.00
R0.25
1.00
0.50
0.75
Part 2. W4x13
Scale 1:10
39.36
2.14
8.09
29.13
Part 9. W4x13
Scale 1:10
0.38
6.00
6.00
0.75
Ø0.50
0.75
Part 3
Scale 1:5
4.06
0.38
Ø0.50
3.09
9.09
0.75
Part 10
Scale 1:5
UNLESS OTHERWISE SPECIFIED:
DIMENSIONS ARE IN MILLIMETERS
SURFACE FINISH:
TOLERANCES:
LINEAR:
ANGULAR:
FINISH:
DEBURR AND BREAK SHARP EDGES
DO NOT SCALE DRAWING
REVISION
NAME
SIGNATURE
DATE
DRAWN
Yu Yang Huang
8/27/2020
CHK'D
APPV'D
MFG
Q.A
TITLE:
Forklift Simulator Jig
MATERIAL:
All pieces are made of steel.
WEIGHT: 850 lbs
DWG NO.
2019-G00018
A3
SCALE:1:20
SHEET 5 OF 6

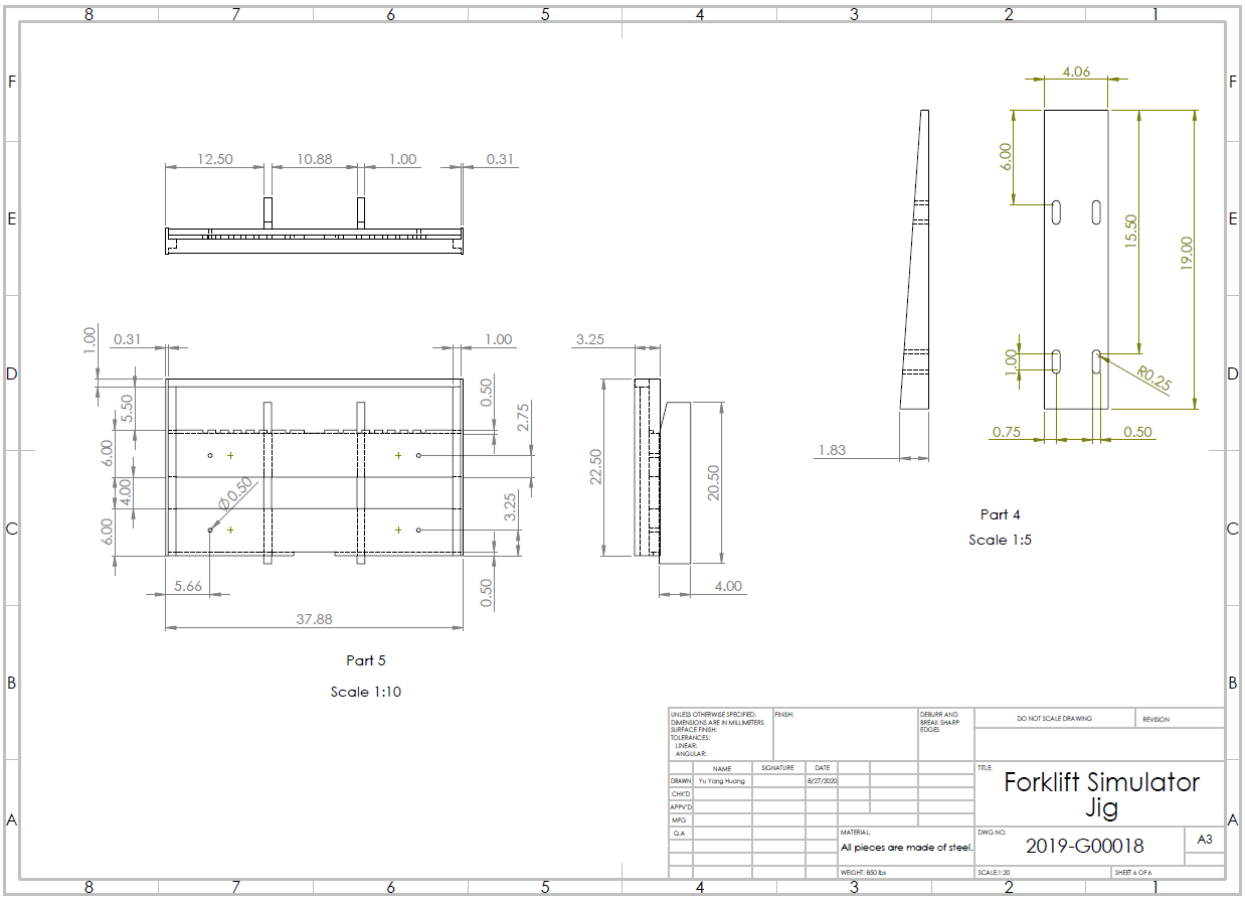

APPENDIX B

Study # 2 Data Collection

1. *Effect of bound unit load under static condition in the across the length orientation with level fork tines*

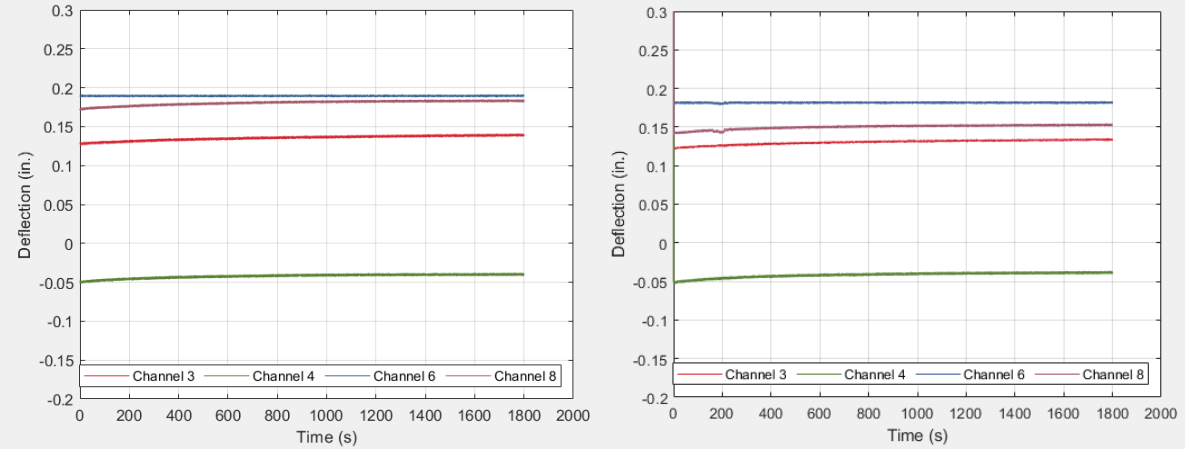

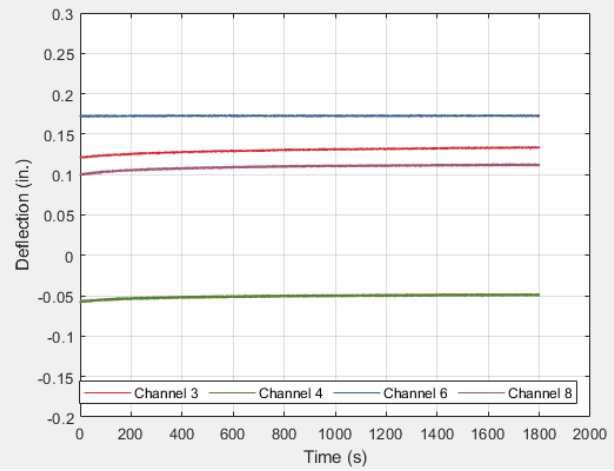

Table 21. Summary of the deflections (in.) measured for the bound unit load during the static condition in across the length orientation R1

		Pallet Deflection (in.) for Each Location									
Testing Condition		1	2	3	4	5	6	7	8	9	10
Initial Deflection		0.1091	0.1267	0.1280	-0.0498	0.1785	0.1894	-0.0729	0.1725	0.108	0.100
At 3 min	**Upper**	0.1142	0.1305	0.1311	-0.0456	0.1793	0.1898	-0.0693	0.1763	0.1225	0.1136
	Middle	0.1140	0.1303	0.1309	-0.0458	0.1791	0.1895	-0.0695	0.1761	0.0559	0.0486
	Lower	0.1138	0.1301	0.1307	-0.0460	0.1789	0.1893	-0.0698	0.1759	0.0009	-0.0026
At 30 min	**Upper**	0.1246	0.1410	0.1394	-0.0396	0.1806	0.1898	-0.0623	0.1834	0.1224	0.1131
	Middle	0.1244	0.1408	0.1392	-0.0398	0.1804	0.1897	-0.0626	0.1832	0.0566	0.0488
	Lower	0.1242	0.1406	0.1390	-0.0400	0.1802	0.1894	-0.0628	0.1830	0.0016	-0.0022

Table 22. Summary of the deflections (in.) measured for the bound unit load during the static condition in across the length orientation R2

		Pallet Deflection (in.) for Each Location									
Testing Condition		1	2	3	4	5	6	7	8	9	10
Initial Deflection		0.0577	0.1175	0.1207	-0.0524	0.1790	0.1818	-0.1126	0.1414	0.0900	0.0856
At 3 min	**Upper**	0.0649	0.1241	0.1263	-0.0460	0.1801	0.1811	-0.1063	0.1447	0.1030	0.0978

	Middle	0.0646	0.1238	0.1261	-0.0462	0.1798	0.1806	-0.1066	0.1440	0.0461	0.0418
	Lower	0.0641	0.1236	0.1257	-0.0464	0.1796	0.1801	-0.1068	0.1433	-0.0083	-0.0086
At 30 min	**Upper**	0.0725	0.1333	0.1340	-0.0381	0.1813	0.1819	-0.0982	0.1531	0.1039	0.0982
	Middle	0.0723	0.1331	0.1338	-0.0384	0.1811	0.1817	-0.0984	0.1529	0.0469	0.0421
	Lower	0.0721	0.1329	0.1335	-0.0385	0.1809	0.1815	-0.0987	0.1527	-0.0076	-0.0085

Table 23. Summary of the deflections (in.) measured for the bound unit load during the static condition in across the length orientation R3

		Pallet Deflection (in.) for Each Location									
Testing Condition		1	2	3	4	5	6	7	8	9	10
Initial Deflection		0.0953	0.1454	0.1193	-0.0577	0.1771	0.1723	-0.0933	0.0986	0.1034	0.0916
At 3 min	**Upper**	0.1017	0.1526	0.1256	-0.0533	0.1782	0.1727	-0.0873	0.1055	0.1210	0.1092
	Middle	0.1015	0.1524	0.1253	-0.0535	0.1780	0.1725	-0.0875	0.1053	0.0636	0.0527
	Lower	0.1013	0.1522	0.1250	-0.0537	0.1778	0.1723	-0.0877	0.1051	0.0091	0.0022
At 30 min	**Upper**	0.1090	0.1630	0.1339	-0.0486	0.1792	0.1731	-0.0803	0.1122	0.1212	0.1093
	Middle	0.1088	0.1628	0.1336	-0.0488	0.1790	0.1728	-0.0805	0.1120	0.0641	0.0532
	Lower	0.1086	0.1626	0.1333	-0.0490	0.1788	0.1726	-0.0807	0.1118	0.0095	0.0026

2. *Effect of bound unit load under dynamic condition in the across the length orientation with level fork tines*

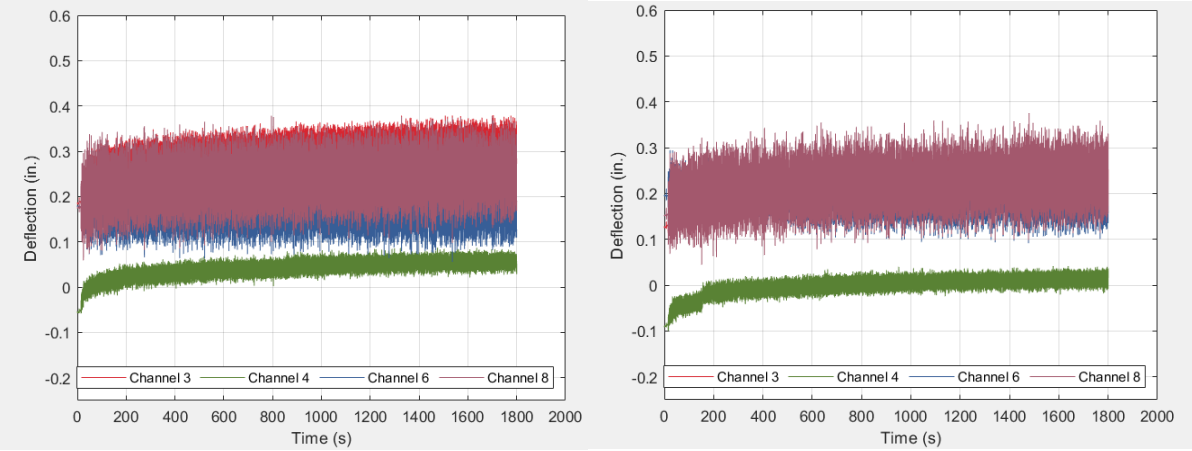

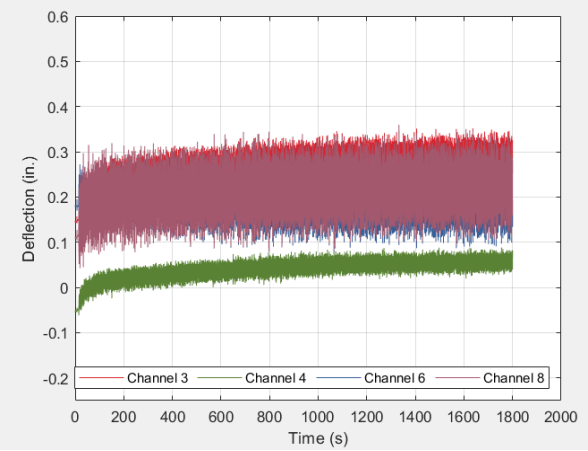

Table 24. Summary of the deflections (in.) measured for the bound unit load during the dynamic condition in across the length orientation R1

		Pallet Deflection (in.) for Each Location									
Testing Condition		1	2	3	4	5	6	7	8	9	10
Initial Deflection		0.0130	0.0830	0.1850	-0.0550	0.1650	0.1780	-0.1340	0.1750	0.0370	0.0600
At 3 min	**Upper**	0.1962	0.2316	0.3186	0.0420	0.2545	0.2528	-0.0354	0.3136	0.1986	0.2091
	Middle	0.1134	0.1883	0.2714	0.0203	0.1830	0.1775	-0.0635	0.2207	0.0998	0.1118
	Lower	0.0328	0.1423	0.2253	-0.0045	0.1179	0.1060	-0.0945	0.1299	0.0099	0.0257
At 30 min	**Upper**	0.2347	0.2813	0.3564	0.0747	0.2526	0.2447	-0.0012	0.3284	0.2011	0.2075
	Middle	0.1586	0.2437	0.3159	0.0559	0.1885	0.1789	-0.0245	0.2508	0.1040	0.1127
	Lower	0.0856	0.2065	0.2770	0.0353	0.1306	0.1170	-0.0557	0.1750	0.0211	0.0334

Table 25. Summary of the deflections (in.) measured for the bound unit load during the dynamic condition in across the length orientation R2

		Pallet Deflection (in.) for Each Location									
Testing Condition		1	2	3	4	5	6	7	8	9	10
Initial Deflection		0.0429	0.0950	0.1230	-0.0929	0.1929	0.1951	-0.1090	0.1485	0.1137	0.1059
At 3 min	**Upper**	0.2079	0.2309	0.2501	0.0042	0.2721	0.2700	-0.0207	0.2812	0.2289	0.2177
	Middle	0.1271	0.1892	0.2047	-0.0175	0.2008	0.1992	-0.0467	0.1996	0.1292	0.1213
	Lower	0.0420	0.1458	0.1607	-0.0396	0.1344	0.1264	-0.0738	0.1190	0.0391	0.0356
At 30 min	**Upper**	0.2500	0.2876	0.2994	0.0353	0.2735	0.2755	0.0126	0.3155	0.2287	0.2179
	Middle	0.1683	0.2454	0.2534	0.0135	0.2033	0.2005	-0.0118	0.2330	0.1302	0.1221
	Lower	0.0888	0.2041	0.2090	-0.0089	0.1371	0.1331	-0.0378	0.1500	0.0422	0.0390

Table 26. Summary of the deflections (in.) measured for the bound unit load during the dynamic condition in across the length orientation R3

	Pallet Deflection (in.) for Each Location									
Testing Condition	1	2	3	4	5	6	7	8	9	10

Initial Deflection		0.0421	0.1175	0.1440	-0.0533	0.1891	0.1793	-0.1235	0.1094	0.0943	0.0898
At 3 min	Upper	0.1829	0.2279	0.2798	0.0385	0.2565	0.2506	-0.0419	0.2719	0.2327	0.2274
	Middle	0.1099	0.1892	0.2399	0.0186	0.1957	0.1889	-0.0675	0.1961	0.1365	0.1337
	Lower	0.0386	0.1522	0.2030	-0.0055	0.1371	0.1301	-0.0966	0.1244	0.0521	0.0541
At 30 min	Upper	0.2106	0.2710	0.3265	0.0774	0.2585	0.2578	-0.0047	0.2988	0.2306	0.2257
	Middle	0.1410	0.2330	0.2884	0.0575	0.1973	0.1901	-0.0294	0.2243	0.1372	0.1345
	Lower	0.0727	0.1977	0.2511	0.0365	0.1415	0.1273	-0.0553	0.1542	0.0507	0.0517

3. *Effect of unbound unit load under static condition in the across the length orientation with level fork tines*

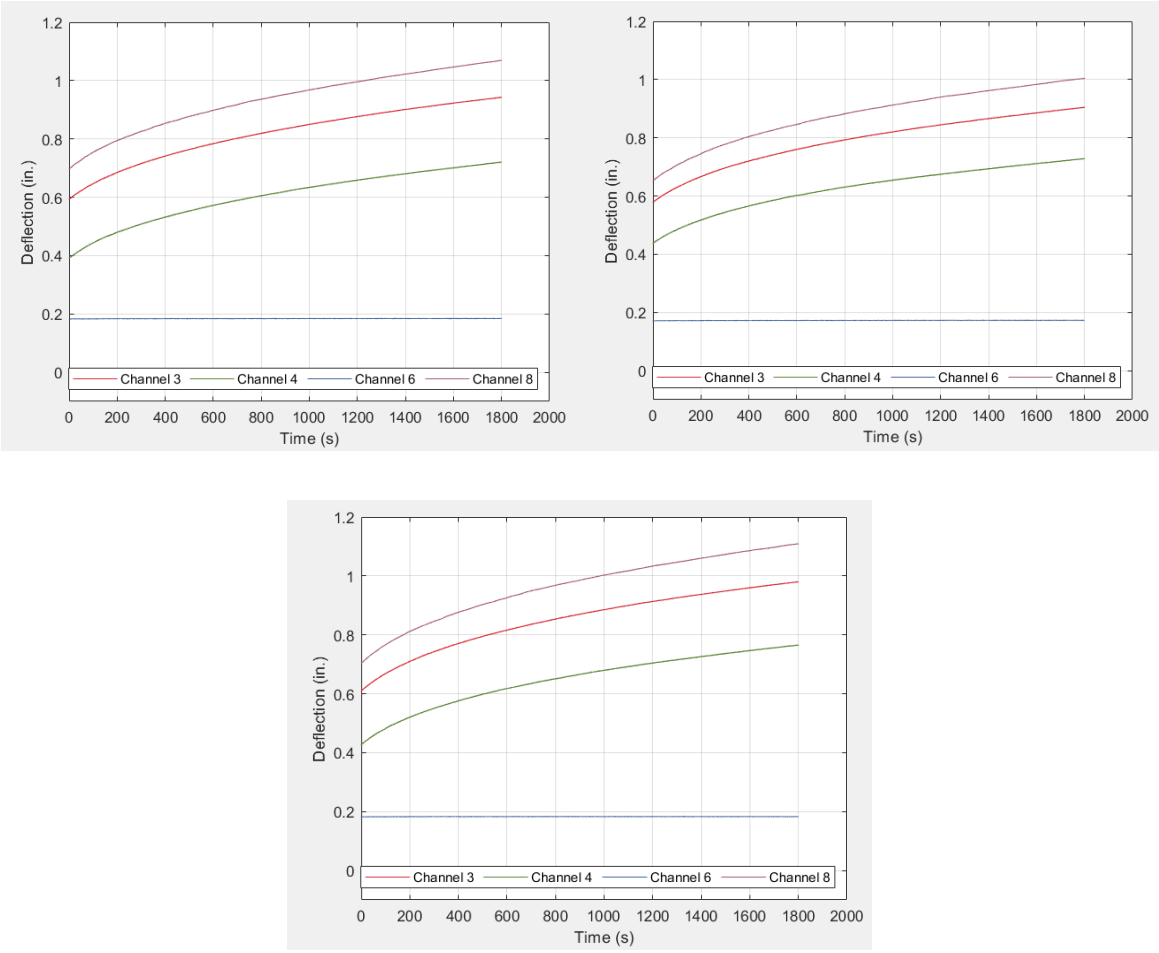

Table 27. Summary of the deflections (in.) measured for the unbound unit load during the static condition in across the length orientation R1

Pallet Deflection (in.) for Each Location

Testing Condition		1	2	3	4	5	6	7	8	9	10
Initial Deflection		0.577	0.505	0.571	0.370	0.183	0.182	0.374	0.674	0.109	0.103
At 3 min	Upper	0.692	0.610	0.681	0.476	0.185	0.184	0.471	0.790	0.199	0.193
	Middle	0.691	0.609	0.680	0.475	0.184	0.183	0.470	0.789	0.142	0.137
	Lower	0.690	0.608	0.679	0.474	0.184	0.183	0.470	0.788	0.088	0.087
At 30 min	Upper	0.962	0.857	0.943	0.720	0.186	0.184	0.696	1.069	0.199	0.194
	Middle	0.962	0.856	0.942	0.720	0.185	0.184	0.696	1.069	0.143	0.139
	Lower	0.962	0.856	0.942	0.719	0.185	0.184	0.696	1.068	0.088	0.088

Table 28. Summary of the deflections (in.) measured for the unbound unit load during the static condition in across the length orientation R2

		Pallet Deflection (in.) for Each Location									
Testing Condition		1	2	3	4	5	6	7	8	9	10
Initial Deflection		0.5751	0.5284	0.5543	0.4149	0.1867	0.1706	0.3672	0.6271	0.0810	0.0764
At 3 min	Upper	0.6946	0.6405	0.6624	0.5138	0.1876	0.1718	0.4750	0.7403	0.2014	0.1907
	Middle	0.6939	0.6397	0.6614	0.5129	0.1874	0.1716	0.4742	0.7392	0.1444	0.1346
	Lower	0.6930	0.6388	0.6605	0.5120	0.1872	0.1714	0.4732	0.7381	0.0897	0.0840
At 30 min	Upper	0.9643	0.8922	0.9046	0.7281	0.1888	0.1728	0.7050	1.0043	0.2019	0.1914
	Middle	0.9640	0.8918	0.9043	0.7278	0.1886	0.1726	0.7046	1.0039	0.1448	0.1353
	Lower	0.9637	0.8915	0.9039	0.7274	0.1884	0.1724	0.7042	1.0036	0.0903	0.0847

Table 29. Summary of the deflections (in.) measured for the unbound unit load during the static condition in across the length orientation R3

		Pallet Deflection (in.) for Each Location									
Testing Condition		1	2	3	4	5	6	7	8	9	10
Initial Deflection		0.5808	0.5294	0.5856	0.4043	0.1876	0.1818	0.3727	0.6792	0.1295	0.1303
At 3 min	Upper	0.7087	0.6454	0.7053	0.5162	0.1885	0.1828	0.4844	0.8065	0.1929	0.1939
	Middle	0.7075	0.6444	0.7042	0.5152	0.1883	0.1826	0.4836	0.8052	0.1369	0.1388
	Lower	0.7062	0.6433	0.7032	0.5142	0.1881	0.1824	0.4826	0.8038	0.0825	0.0884
At 30 min	Upper	0.9955	0.9111	0.9799	0.7651	0.1891	0.1829	0.7380	1.1089	0.1948	0.1962
	Middle	0.9951	0.9107	0.9795	0.7647	0.1889	0.1827	0.7376	1.1085	0.1368	0.1393
	Lower	0.9947	0.9103	0.9791	0.7643	0.1886	0.1825	0.7372	1.1081	0.0821	0.0886

4. *Effect of unbound unit load under dynamic condition in the across the length orientation with level fork tines*

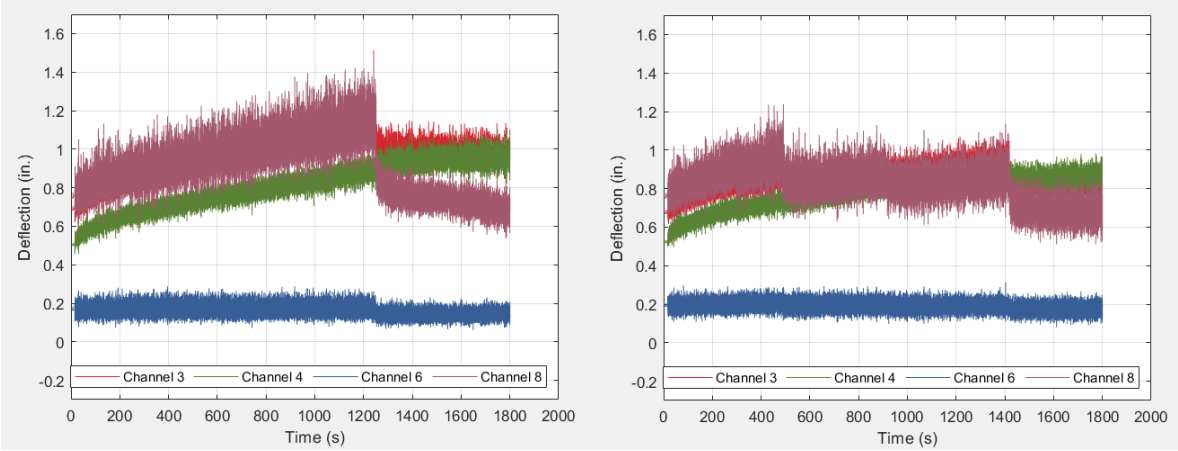

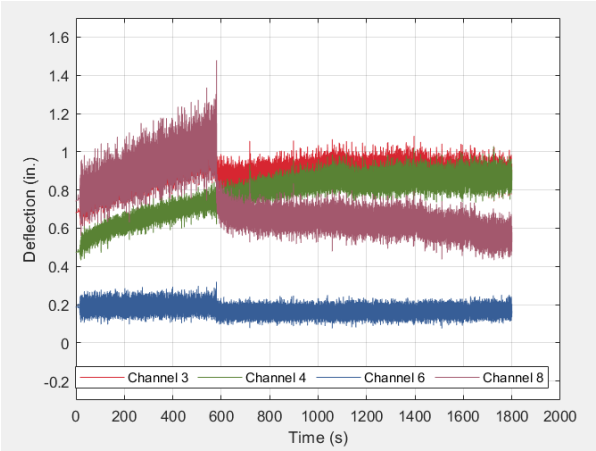

Table 30. Summary of the deflections (in.) measured for the unbound unit load during the dynamic condition in across the length orientation R1

		Pallet Deflection (in.) for Each Location									
Testing Condition		1	2	3	4	5	6	7	8	9	10
Initial Deflection		0.594	0.538	0.668	0.485	0.192	0.166	0.422	0.730	0.087	0.086
At 135s	**Upper**	0.8841	0.7561	0.9031	0.6717	0.2576	0.2342	0.6083	1.0024	0.2291	0.2261
	Middle	0.7448	0.6741	0.7971	0.6154	0.1960	0.1676	0.5661	0.8393	0.1396	0.1348
	Lower	0.6189	0.5964	0.7092	0.5648	0.1398	0.1062	0.5084	0.7111	0.0527	0.0524
At 140s	**Upper**	0.8794	0.7554	0.8992	0.6716	0.2510	0.2280	0.6096	0.9945	0.2265	0.2226
	Middle	0.7522	0.6787	0.8010	0.6186	0.1965	0.1678	0.5696	0.8434	0.1397	0.1349
	Lower	0.6250	0.5988	0.7174	0.5723	0.1435	0.1104	0.5174	0.7193	0.0544	0.0542

Table 31. Summary of the deflections (in.) measured for the unbound unit load during the dynamic condition in across the length orientation R2

		Pallet Deflection (in.) for Each Location

Testing Condition		1	2	3	4	5	6	7	8	9	10
Initial Deflection		0.6326	0.5150	0.5973	0.4515	0.1858	0.1887	0.3856	0.6716	0.0868	0.0657
At 135s	Upper	0.9643	0.7563	0.8470	0.6870	0.2538	0.2541	0.6077	0.9671	0.2340	0.2069
	Middle	0.8220	0.6737	0.7674	0.6313	0.1892	0.1944	0.5638	0.8352	0.1401	0.1175
	Lower	0.6999	0.5984	0.6934	0.5792	0.1374	0.1307	0.5178	0.7206	0.0528	0.0347

Table 32. Summary of the deflections (in.) measured for the unbound unit load during the dynamic condition in across the length orientation R3

		Pallet Deflection (in.) for Each Location									
Testing Condition		1	2	3	4	5	6	7	8	9	10
Initial Deflection		0.6195	0.5440	0.6106	0.4059	0.1864	0.1853	0.4090	0.6999	0.1101	0.0952
At 135s	Upper	0.9267	0.8296	0.8707	0.6470	0.2540	0.2559	0.6591	0.9682	0.1415	0.1272
	Middle	0.7948	0.7349	0.7853	0.5941	0.1887	0.1882	0.6091	0.8291	0.0508	0.0396
	Lower	0.6678	0.6488	0.6990	0.5388	0.1264	0.1255	0.5528	0.6934	-0.0379	-0.0445
At 620s	Upper	1.1085	1.0120	0.9424	0.8213	0.2563	0.2107	0.8501	0.7877	0.1424	0.1140
	Middle	0.9433	0.8986	0.8646	0.7595	0.1937	0.1621	0.7848	0.6999	0.0499	0.0293
	Lower	0.7993	0.8001	0.7893	0.6974	0.1353	0.1092	0.7201	0.6190	-0.0355	-0.0474

5. *Effect of unbound unit load under dynamic condition in across the width orientation with level fork tines*

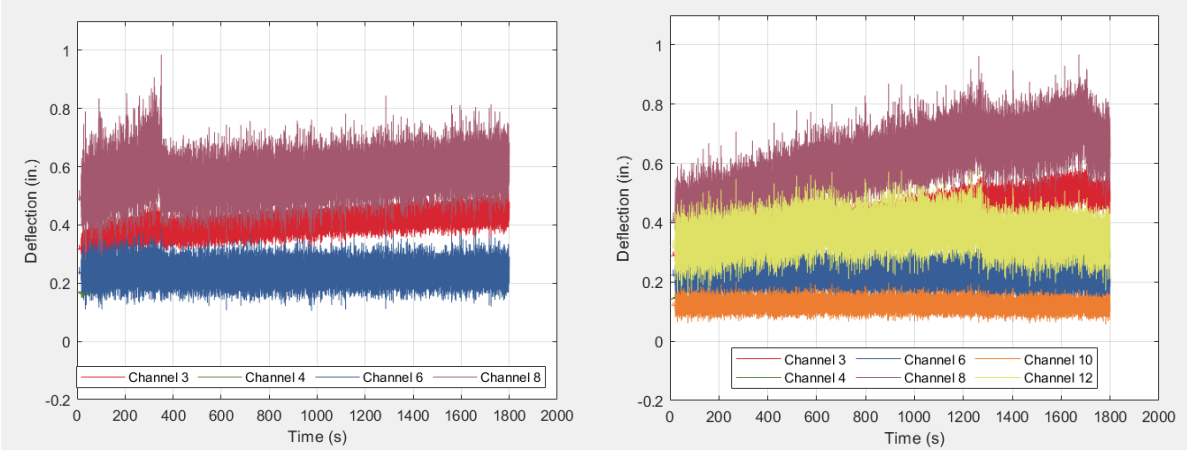

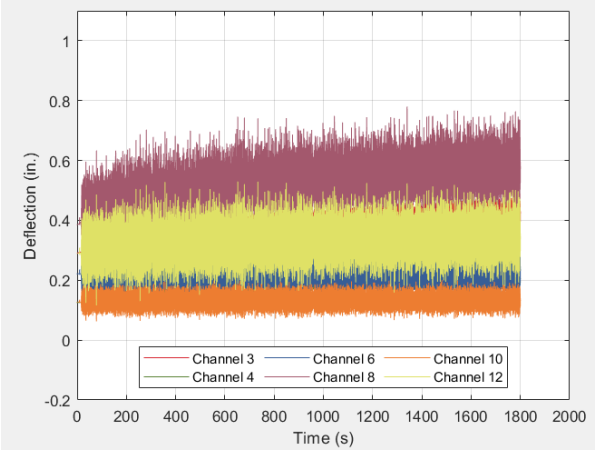

Table 33. Summary of the deflections (in.) measured for the unbound unit load during the dynamic condition in across the width orientation R1

		Pallet Deflection (in.) for Each Location									
Testing Condition		1	2	3	4	5	6	7	8	9	10
Initial Deflection		0.5002	0.2989	0.3159	0.1671	0.2294	0.2364	0.0827	0.4869	0.0434	0.0634
At 3 min	**Upper**	0.7006	0.4134	0.4287	0.2118	0.3239	0.3261	0.1529	0.7084	0.2034	0.2165
	Middle	0.5704	0.3515	0.3652	0.1965	0.2381	0.2414	0.1314	0.5567	0.1004	0.1135
	Lower	0.4529	0.2942	0.3071	0.1800	0.1659	0.1681	0.1111	0.4215	0.0014	0.0182
At 5:20 min	**Upper**	0.7221	0.4303	0.4527	0.2210	0.3207	0.3272	0.1686	0.7855	0.2067	0.2196
	Middle	0.5901	0.3678	0.3893	0.2066	0.2379	0.2434	0.1453	0.6163	0.1018	0.1145
	Lower	0.4763	0.3105	0.3270	0.1912	0.1639	0.1655	0.1234	0.4616	0.0038	0.0196

Table 34. Summary of the deflections (in.) measured for the unbound unit load during the dynamic condition in across the width orientation R2

		Pallet Deflection (in.) for Each Location											
Testing Condition		1	2	3	4	5	6	7	8	9	10	11	12
Initial Deflection		0.5591	0.2889	0.2875	0.1419	0.2463	0.2234	0.0299	0.4044	0.1230	0.1217	0.3277	0.3169
At 3 min	**Upper**	0.7306	0.4012	0.3771	0.2108	0.3253	0.2899	0.1066	0.5566	0.1666	0.1590	0.4535	0.4212
	Middle	0.6188	0.3432	0.3283	0.1949	0.2532	0.2256	0.0857	0.4645	0.1261	0.1232	0.3562	0.3400
	Lower	0.4956	0.2799	0.2770	0.1747	0.1736	0.1539	0.0625	0.3540	0.0823	0.0837	0.2501	0.2371
At 5:20 min	**Upper**	0.7655	0.4206	0.4017	0.2251	0.3376	0.2965	0.1185	0.6033	0.1730	0.1630	0.4748	0.4482
	Middle	0.6364	0.3586	0.3466	0.2078	0.2541	0.2262	0.0999	0.4993	0.1266	0.1236	0.3632	0.3583
	Lower	0.5195	0.3010	0.2966	0.1894	0.1777	0.1530	0.0746	0.3862	0.0845	0.0846	0.2585	0.2554
At 11:02 min	**Upper**	0.8211	0.4542	0.4544	0.2516	0.3356	0.3120	0.1477	0.7045	0.1738	0.1697	0.5011	0.4971
	Middle	0.7014	0.3929	0.3972	0.2338	0.2549	0.2323	0.1264	0.5895	0.1267	0.1261	0.3924	0.3984
	Lower	0.5796	0.3361	0.3444	0.2179	0.1773	0.1597	0.1041	0.4687	0.0860	0.0875	0.2832	0.2935

Table 35. Summary of the deflections (in.) measured for the unbound unit load during the dynamic condition in across the width orientation R3

		Pallet Deflection (in.) for Each Location											
Testing Condition		1	2	3	4	5	6	7	8	9	10	11	12
Initial Deflection		0.5166	0.2862	0.2901	0.1255	0.2420	0.2217	0.0842	0.3855	0.1199	0.1275	0.3868	0.2892
At 3 min	**Upper**	0.7351	0.4041	0.3905	0.1634	0.3365	0.3053	0.1503	0.5734	0.1707	0.1724	0.5340	0.4225
	Middle	0.5987	0.3385	0.3315	0.1478	0.2487	0.2268	0.1242	0.4564	0.1240	0.1300	0.4176	0.3144
	Lower	0.4754	0.2798	0.2801	0.1257	0.1727	0.1556	0.1003	0.3483	0.0805	0.0929	0.3113	0.2169
At 5:20 min	**Upper**	0.7936	0.4373	0.4140	0.1737	0.3543	0.3201	0.1658	0.6111	0.1800	0.1818	0.5569	0.4399
	Middle	0.6226	0.3570	0.3459	0.1568	0.2495	0.2278	0.1381	0.4771	0.1245	0.1304	0.4242	0.3205
	Lower	0.4689	0.2866	0.2878	0.1350	0.1587	0.1431	0.1144	0.3462	0.0720	0.0837	0.2916	0.2034
At 30 min	**Upper**	0.9658	0.5425	0.4786	0.2181	0.3424	0.3089	0.2447	0.7009	0.1779	0.1752	0.5880	0.4536
	Middle	0.7880	0.4640	0.4192	0.2015	0.2527	0.2312	0.2140	0.5766	0.1261	0.1313	0.4659	0.3442
	Lower	0.6155	0.3895	0.3601	0.1793	0.1632	0.1516	0.1831	0.4540	0.0774	0.0861	0.3346	0.2352

6. *Effect of unbound unit load under static condition in across the length orientation with 4° angle fork tines*

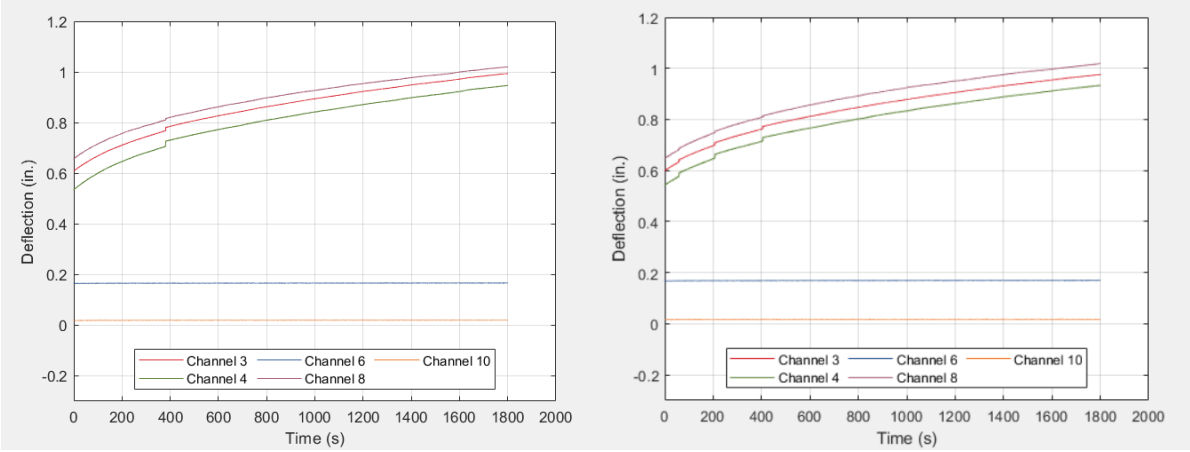

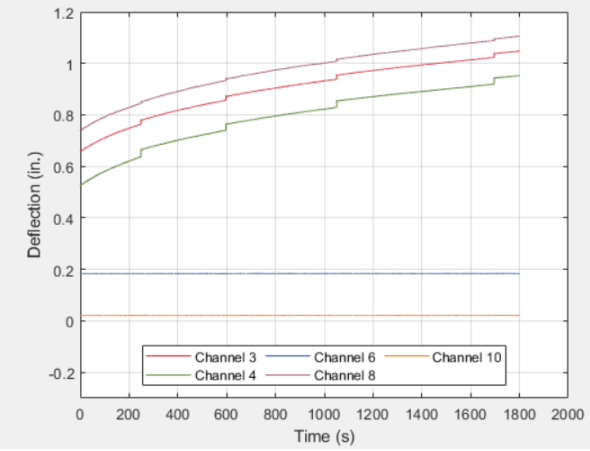

Table 36. Summary of the deflections (in.) measured for the unbound unit load during the static condition in across the length orientation R1

		Pallet Deflection (in.) for Each Location									
Testing Condition		1	2	3	4	5	6	7	8	9	10
Initial Deflection		0.3482	0.5176	0.6079	0.5355	0.1349	0.1650	0.5633	0.6571	0.0542	0.0186
At 3 min	**Upper**	0.5704	0.6099	0.7065	0.6417	0.1359	0.1659	0.6625	0.7524	0.0545	0.0195
	Middle	0.5696	0.6089	0.7054	0.6405	0.1357	0.1657	0.6614	0.7515	0.0543	0.0193
	Lower	0.5686	0.6079	0.7043	0.6393	0.1355	0.1655	0.6602	0.7505	0.0540	0.0190
At 30 min	**Upper**	0.8155	0.8799	0.9939	0.9464	0.1351	0.1666	0.9580	1.0197	0.0534	0.0201
	Middle	0.8153	0.8796	0.9936	0.9460	0.1349	0.1665	0.9577	1.0194	0.0532	0.0199
	Lower	0.8149	0.8792	0.9932	0.9456	0.1347	0.1662	0.9572	1.0191	0.0529	0.0196

Table 37. Summary of the deflections (in.) measured for the unbound unit load during the static condition in across the length orientation R2

		Pallet Deflection (in.) for Each Location									
Testing Condition		1	2	3	4	5	6	7	8	9	10
Initial Deflection		0.4516	0.5001	0.5992	0.5428	0.1316	0.1679	0.5391	0.6466	0.0438	0.0162
At 3 min	**Upper**	0.5320	0.5906	0.6929	0.6413	0.1317	0.1685	0.6386	0.7416	0.0437	0.0174
	Middle	0.5312	0.5897	0.6920	0.6401	0.1315	0.1683	0.6375	0.7405	0.0435	0.0172
	Lower	0.5303	0.5888	0.6910	0.6390	0.1313	0.1681	0.6364	0.7392	0.0433	0.0169
At 30 min	**Upper**	0.7708	0.8642	0.9760	0.9330	0.1298	0.1696	0.9520	1.0182	0.0415	0.0179
	Middle	0.7704	0.8639	0.9756	0.9327	0.1295	0.1694	0.9517	1.0178	0.0412	0.0177
	Lower	0.7701	0.8636	0.9751	0.9323	0.1293	0.1692	0.9513	1.0174	0.0410	0.0175

Table 38. Summary of the deflections (in.) measured for the unbound unit load during the static condition in across the length orientation R3

		Pallet Deflection (in.) for Each Location									
Testing Condition		1	2	3	4	5	6	7	8	9	10
Initial Deflection		0.4947	0.4292	0.6569	0.5255	0.1377	0.1829	0.5810	0.7384	0.0522	0.0209
At 3 min	**Upper**	0.5646	0.5116	0.7442	0.6164	0.1385	0.1835	0.6799	0.8246	0.0528	0.0215
	Middle	0.5637	0.5107	0.7432	0.6155	0.1383	0.1834	0.6787	0.8237	0.0526	0.0212
	Lower	0.5628	0.5097	0.7422	0.6146	0.1381	0.1832	0.6776	0.8228	0.0523	0.0210
At 30 min	**Upper**	0.8037	0.8133	1.0477	0.9525	0.1353	0.1841	1.0234	1.1056	0.0494	0.0218
	Middle	0.8034	0.8130	1.0474	0.9522	0.1351	0.1839	1.0231	1.1053	0.0491	0.0216
	Lower	0.8030	0.8127	1.0470	0.9518	0.1349	0.1837	1.0227	1.1049	0.0489	0.0213

7. *Effect of unbound unit load under dynamic condition in across the length orientation with 4° angle fork tines*

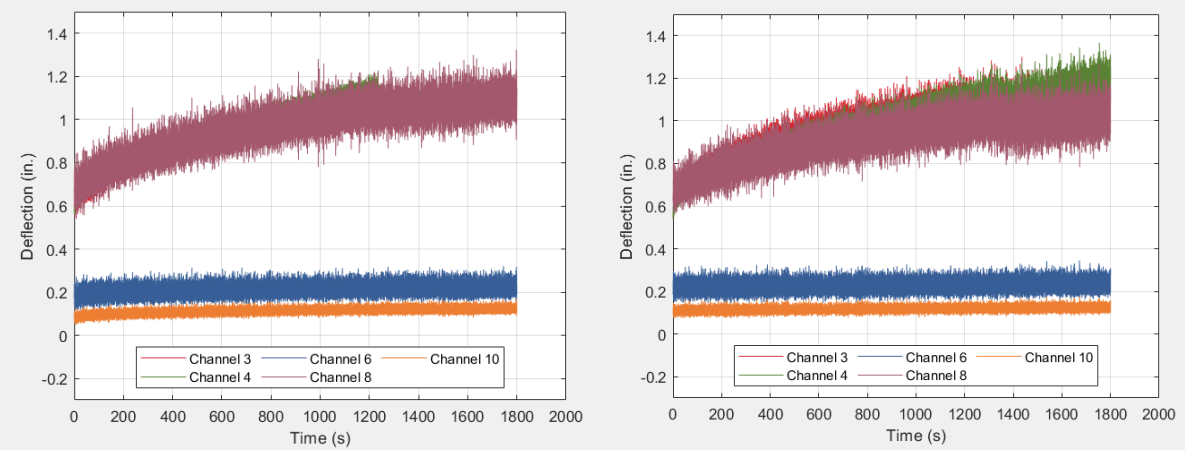

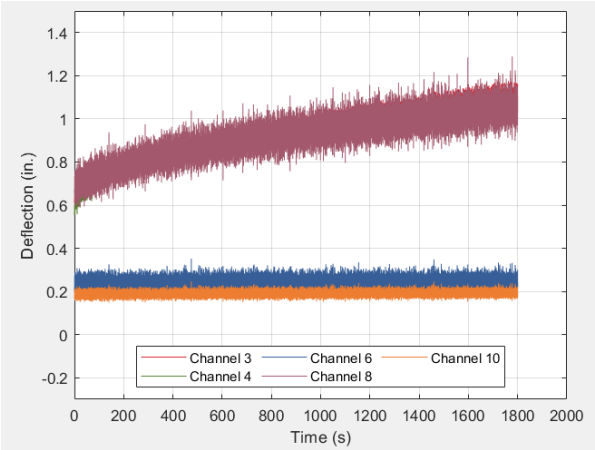

Table 39. Summary of the deflections (in.) measured for the unbound unit load during the dynamic condition in across the length orientation R1

		Pallet Deflection (in.) for Each Location									
Testing Condition		1	2	3	4	5	6	7	8	9	10
Initial Deflection		0.6138	0.5972	0.6099	0.5850	0.1566	0.1733	0.6616	0.6627	0.0810	0.0779
At 3 min	**Upper**	0.8750	0.8774	0.8550	0.8423	0.2470	0.2575	0.9494	0.9026	0.1360	0.1306
	Middle	0.7453	0.7829	0.7749	0.7914	0.1839	0.1985	0.8868	0.7980	0.1016	0.0986
	Lower	0.6360	0.6999	0.7079	0.7437	0.1287	0.1484	0.8277	0.7049	0.0735	0.0724
At 11:10 min	**Upper**	1.0409	1.0864	1.0348	1.0405	0.2610	0.2683	1.1671	1.0548	0.1447	0.1402
	Middle	0.8950	0.9723	0.9462	0.9782	0.1938	0.2104	1.0878	0.9432	0.1110	0.1105
	Lower	0.7622	0.8716	0.8586	0.9161	0.1320	0.1532	1.0142	0.8365	0.0800	0.0830
At 25:35 min	**Upper**	1.1930	1.2687	1.1742	1.1895	0.2663	0.2678	1.3729	1.1654	0.1485	0.1421
	Middle	1.0179	1.1275	1.0813	1.1287	0.1994	0.2170	1.2661	1.0532	0.1160	0.1175
	Lower	0.8585	1.0000	0.9877	1.0529	0.1390	0.1599	1.1551	0.9391	0.0867	0.0904

Table 40. Summary of the deflections (in.) measured for the unbound unit load during the dynamic condition in across the length orientation R2

Testing Condition		Pallet Deflection (in.) for Each Location									
		1	2	3	4	5	6	7	8	9	10
Initial Deflection		0.5728	0.5956	0.6237	0.5428	0.1736	0.1915	0.5912	0.6431	0.1127	0.0950
At 3 min	**Upper**	0.8710	0.8676	0.8845	0.8226	0.2748	0.2906	0.8508	0.8876	0.1616	0.1443
	Middle	0.7285	0.7822	0.8053	0.7683	0.2041	0.2217	0.8082	0.7663	0.1268	0.1116
	Lower	0.6064	0.6979	0.7333	0.7149	0.1420	0.1626	0.7586	0.6599	0.0949	0.0816
At 11:10 min	**Upper**	1.0134	1.0696	1.0521	1.0245	0.2680	0.2807	1.0548	1.0016	0.1574	0.1446
	Middle	0.8980	0.9871	0.9822	0.9709	0.2056	0.2244	1.0129	0.9045	0.1271	0.1151
	Lower	0.7938	0.9102	0.9166	0.9176	0.1538	0.1766	0.9589	0.8145	0.1025	0.0922

Table 41. Summary of the deflections (in.) measured for the unbound unit load during the dynamic condition in across the length orientation R3

Testing Condition		Pallet Deflection (in.) for Each Location									
		1	2	3	4	5	6	7	8	9	10
Initial Deflection		0.6159	0.6535	0.6224	0.5581	0.2021	0.2144	0.7252	0.6729	0.1312	0.1779
At 3 min	**Upper**	0.8382	0.8978	0.8303	0.7781	0.2817	0.2875	0.9973	0.8537	0.1688	0.2153
	Middle	0.7356	0.8185	0.7722	0.7474	0.2183	0.2316	0.9450	0.7750	0.1372	0.1867
	Lower	0.6433	0.7489	0.7107	0.7116	0.1669	0.1821	0.8897	0.6976	0.1109	0.1629
At 11:10 min	**Upper**	0.9742	1.0594	0.9698	0.9304	0.2732	0.2830	1.1829	0.9748	0.1642	0.2141
	Middle	0.8661	0.9765	0.9062	0.8938	0.2199	0.2343	1.1226	0.8921	0.1374	0.1888
	Lower	0.7636	0.8946	0.8364	0.8538	0.1654	0.1792	1.0524	0.8062	0.1072	0.1631
At 30 min	**Upper**	1.2167	1.3437	1.1668	1.1321	0.2877	0.2930	1.5089	1.1530	0.1678	0.2190
	Middle	1.0653	1.2164	1.0934	1.0875	0.2253	0.2379	1.4052	1.0520	0.1378	0.1922
	Lower	0.9349	1.1055	1.0189	1.0421	0.1684	0.1880	1.3061	0.9554	0.1105	0.1689

8. *Effect of unbound unit load under dynamic condition in across the width orientation with 4° angle fork tines*

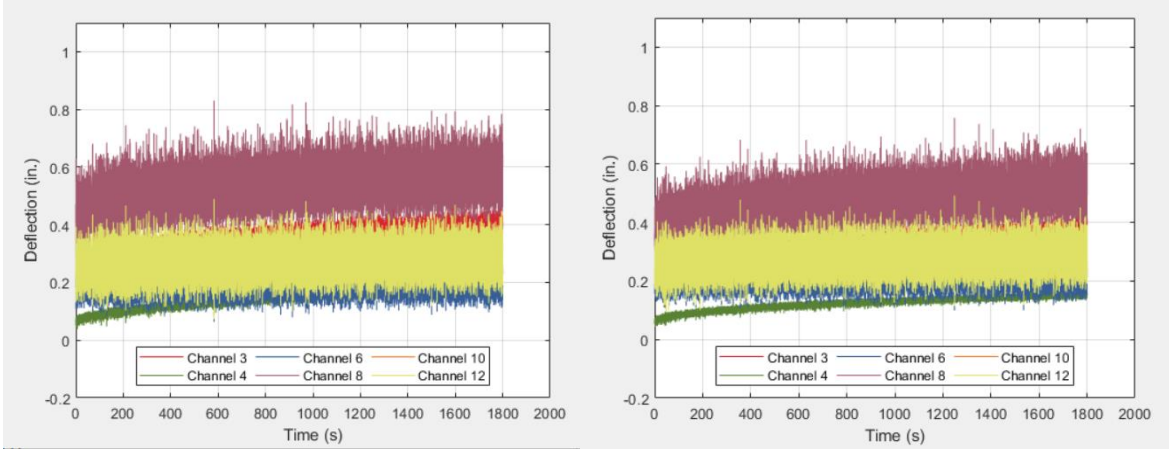

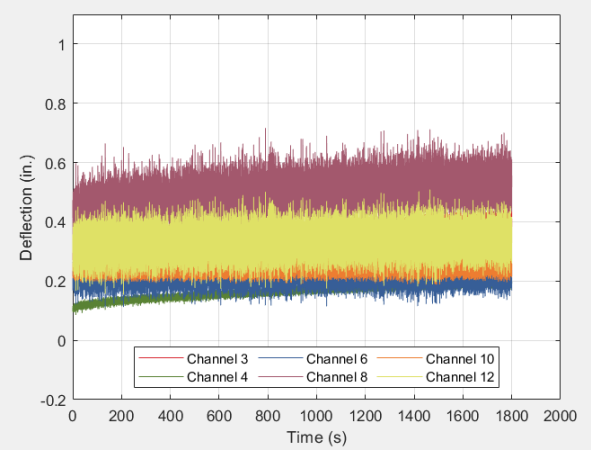

Table 42. Summary of the deflections (in.) measured for the unbound unit load during the dynamic condition in across the width orientation R1

		Pallet Deflection (in.) for Each Location											
Testing Condition		1	2	3	4	5	6	7	8	9	10	11	12
Initial Deflection		0.4156	0.2561	0.2618	0.0705	0.2341	0.2227	0.0881	0.4698	0.1108	0.2365	0.2579	0.2825
At 3 min	**Upper**	0.5106	0.3474	0.3531	0.1158	0.2897	0.2873	0.1484	0.6191	0.1441	0.2735	0.3356	0.3684
	Middle	0.4109	0.2918	0.2851	0.0993	0.2145	0.2029	0.1296	0.4795	0.1029	0.2274	0.2377	0.2598
	Lower	0.3082	0.2373	0.2235	0.0815	0.1398	0.1272	0.1062	0.3569	0.0623	0.1846	0.1466	0.1618
At 30 min	**Upper**	0.6115	0.4445	0.4562	0.1994	0.3162	0.3055	0.2049	0.7191	0.1637	0.2877	0.3698	0.4040
	Middle	0.4912	0.3805	0.3787	0.1832	0.2242	0.2129	0.1879	0.5782	0.1124	0.2375	0.2610	0.2881
	Lower	0.3826	0.3207	0.3130	0.1633	0.1415	0.1299	0.1660	0.4526	0.0664	0.1915	0.1578	0.1825

Table 43. Summary of the deflections (in.) measured for the unbound unit load during the dynamic condition in across the width orientation R2

		Pallet Deflection (in.) for Each Location											
Testing Condition		1	2	3	4	5	6	7	8	9	10	11	12
Initial Deflection		0.4284	0.2518	0.2220	0.0549	0.2017	0.1909	0.1336	0.3598	0.0946	0.2213	0.2052	0.2274
At 3 min	**Upper**	0.6062	0.3829	0.3376	0.1068	0.3158	0.2999	0.2034	0.5487	0.1586	0.2822	0.3507	0.3718
	Middle	0.4736	0.3129	0.2726	0.0920	0.2281	0.2175	0.1785	0.4264	0.1099	0.2376	0.2402	0.2664
	Lower	0.3390	0.2413	0.2115	0.0762	0.1378	0.1356	0.1460	0.3009	0.0577	0.1936	0.1303	0.1634
At 30 min	**Upper**	0.7130	0.4783	0.4157	0.1651	0.3214	0.3119	0.2690	0.6452	0.1662	0.2889	0.3734	0.3911
	Middle	0.5904	0.4081	0.3527	0.1528	0.2366	0.2256	0.2457	0.5231	0.1174	0.2443	0.2666	0.2912
	Lower	0.4758	0.3522	0.2956	0.1378	0.1615	0.1512	0.2249	0.4107	0.0748	0.2012	0.1694	0.1958

Table 44. Summary of the deflections (in.) measured for the unbound unit load during the dynamic condition in across the width orientation R3

	Pallet Deflection (in.) for Each Location											
Testing Condition	1	2	3	4	5	6	7	8	9	10	11	12

Initial Deflection		0.4427	0.2951	0.2890	0.1117	0.2411	0.2384	0.1849	0.4250	0.1240	0.2499	0.2731	0.3205
At 3 min	Upper	0.5371	0.3673	0.3627	0.1481	0.2990	0.3041	0.2245	0.5534	0.1567	0.2853	0.3655	0.4163
	Middle	0.4446	0.3178	0.3126	0.1331	0.2289	0.2299	0.2024	0.4505	0.1176	0.2449	0.2725	0.3232
	Lower	0.3501	0.2692	0.2654	0.1185	0.1620	0.1613	0.1780	0.3563	0.0782	0.2059	0.1870	0.2340
At 30 min	Upper	0.6070	0.4323	0.4377	0.2040	0.2931	0.3023	0.2929	0.6222	0.1549	0.2826	0.3736	0.4292
	Middle	0.5214	0.3906	0.3920	0.1906	0.2310	0.2338	0.2771	0.5305	0.1197	0.2482	0.2931	0.3449
	Lower	0.4418	0.3463	0.3471	0.1773	0.1689	0.1717	0.2587	0.4449	0.0874	0.2153	0.2192	0.2691

APPENDIX C

Matlab Data Analysis Code

```
clc

may1=xlsread('dynamicbound3processed.xlsb','Sheet1','A1:AD900000');
%time
S1=may1(:,1);
%Channel 1
C1=may1(:,3);
%Channel 2
C2=may1(:,6);
%Channel 3
C3=may1(:,9);
%Channel 4
C4=may1(:,12);
%Channel 5
C5=may1(:,15);
%Channel 6
C6=may1(:,18);
%Channel 7
C7=may1(:,21);
%Channel 8
C8=may1(:,24);
%Channel 9
C9=may1(:,27);
%Channel 10
C10=may1(:,30);

s=0:0.002:1799.998;

figure(1)
plot(s,C3,'Color','#d72631')

hold on
plot(s,C4,'Color','#00743f')
plot(s,C6,'Color','#1e3d59')
plot(s,C8,'Color','#a3586d')
%plot(s,C10,'color','#d47b22')
```

```
hold off

grid on;
%title('Displacement vs Time');
xlabel('Time (s)');
ylabel('Deflection (in.)');
%legend('Channel 3','Channel 4','Channel 6','Channel 8','Channel
10','Location','south','NumColumns',5);
legend('Channel 3','Channel 4','Channel 6','Channel
8','Location','south','NumColumns',4);
xlim([0 2000])
ylim([-0.5 1])

%Graph channel 1
figure(2)
plot (s,C1)
%Graph channel 2
figure(3)
plot (s,C2)
%Graph channel 3
figure(4)
plot (s,C3)
%Graph channel 4
figure(5)
plot (s,C4)
%Graph channel 5
figure(6)
plot (s,C5)
%Graph channel 6
figure(7)
plot (s,C6)
%Graph channel 7
figure(8)
plot (s,C7)
%Graph channel 8
figure(9)
plot (s,C8)
%Graph channel 9
figure(10)
plot (s,C9)
%Graph channel 10
figure(2)
plot (s,C10)

%-------------------------------------------------------------------------
---
%Analysis of 3 min with an interval of 10s
may310=xlsread('dynamicbound3processed.xlsb','Sheet1','A90001:AD95000'
);

%Time for interval
```

```
SA=may310(:,1);

%Channel 1
C1A=may310(:,3);
average1A=mean(C1A);
%findpeaks(C1A,SA,'MinPeakHeight',0.002);
maximaC1A=findpeaks(C1A,SA,'MinPeakHeight',average1A);
minimaC1A=findpeaks(-C1A,SA,'MinPeakHeight',-average1A);
averagemax1A=mean(maximaC1A);
averagemin1A=mean(-minimaC1A);

%Channel 2
C2A=may310(:,6);
%findpeaks(C2A,SA,'MinPeakHeight',0.002);
average2A=mean(C2A);
maximaC2A=findpeaks(C2A,SA,'MinPeakHeight',average2A);
minimaC2A=findpeaks(-C2A,SA,'MinPeakHeight',-average2A);
averagemax2A=mean(maximaC2A);
averagemin2A=mean(-minimaC2A);

%Channel 3
C3A=may310(:,9);
%findpeaks(C3A,SA,'MinPeakHeight',0.002);
average3A=mean(C3A);
maximaC3A=findpeaks(C3A,SA,'MinPeakHeight',average3A);
minimaC3A=findpeaks(-C3A,SA,'MinPeakHeight',-average3A);
averagemax3A=mean(maximaC3A);
averagemin3A=mean(-minimaC3A);

%Channel 4
C4A=may310(:,12);
%findpeaks(C4A,SA,'MinPeakHeight',0.002);
average4A=mean(C4A);
maximaC4A=findpeaks(C4A,SA,'MinPeakHeight',average4A);
minimaC4A=findpeaks(-C4A,SA,'MinPeakHeight',-average4A);
averagemax4A=mean(maximaC4A);
averagemin4A=mean(-minimaC4A);

%Channel 5
C5A=may310(:,15);
%findpeaks(C5A,SA,'MinPeakHeight',0.002);
average5A=mean(C5A);
maximaC5A=findpeaks(C5A,SA,'MinPeakHeight',average5A);
minimaC5A=findpeaks(-C5A,SA,'MinPeakHeight',-average5A);
averagemax5A=mean(maximaC5A);
averagemin5A=mean(-minimaC5A);

%Channel 6
C6A=may310(:,18);
%findpeaks(C6A,SA,'MinPeakHeight',0.002);
average6A=mean(C6A);
maximaC6A=findpeaks(C6A,SA,'MinPeakHeight',average6A);
```

```
minimaC6A=findpeaks(-C6A,SA,'MinPeakHeight',-average6A);
averagemax6A=mean(maximaC6A);
averagemin6A=mean(-minimaC6A);

%Channel 7
C7A=may310(:,21);
%findpeaks(C7A,SA,'MinPeakHeight',-0.06);
average7A=mean(C7A);
maximaC7A=findpeaks(C7A,SA,'MinPeakHeight',average7A);
minimaC7A=findpeaks(-C7A,SA,'MinPeakHeight',-average7A);
averagemax7A=mean(maximaC7A);
averagemin7A=mean(-minimaC7A);

%Channel 8
C8A=may310(:,24);
%findpeaks(C8A,SA,'MinPeakHeight',0.002);
average8A=mean(C8A);
maximaC8A=findpeaks(C8A,SA,'MinPeakHeight',average8A);
minimaC8A=findpeaks(-C8A,SA,'MinPeakHeight',-average8A);
averagemax8A=mean(maximaC8A);
averagemin8A=mean(-minimaC8A);

%Channel 9
C9A=may310(:,27);
%findpeaks(C9A,SA,'MinPeakHeight',0.002);
average9A=mean(C9A);
maximaC9A=findpeaks(C9A,SA,'MinPeakHeight',average9A);
minimaC9A=findpeaks(-C9A,SA,'MinPeakHeight',-average9A);
averagemax9A=mean(maximaC9A);
averagemin9A=mean(-minimaC9A);

%Channel 10
C10A=may310(:,30);
%findpeaks(C10A,SA,'MinPeakHeight',0.002);
average10A=mean(C10A);
maximaC10A=findpeaks(C10A,SA,'MinPeakHeight',average10A);
minimaC10A=findpeaks(-C10A,SA,'MinPeakHeight',-average10A);
averagemax10A=mean(maximaC10A);
averagemin10A=mean(-minimaC10A);

Title={'Max','Average','Min'};
Ch1A=[averagemax1A ; average1A ; averagemin1A];
Ch2A=[averagemax2A ; average2A ; averagemin2A];
Ch3A=[averagemax3A ; average3A ; averagemin3A];
Ch4A=[averagemax4A ; average4A ; averagemin4A];
Ch5A=[averagemax5A ; average5A ; averagemin5A];
Ch6A=[averagemax6A ; average6A ; averagemin6A];
Ch7A=[averagemax7A ; average7A ; averagemin7A];
Ch8A=[averagemax8A ; average8A ; averagemin8A];
Ch9A=[averagemax9A ; average9A ; averagemin9A];
Ch10A=[averagemax10A ; average10A ; averagemin10A];
```

```
T1=table(Ch1A,Ch2A,Ch3A,Ch4A,Ch5A,Ch6A,Ch7A,Ch8A,Ch9A,Ch10A,'Rownames'
,Title);

%-------------------------------------------------------------------
---------------

%Analysis of 30 min with an interval of 10s
may3010=xlsread('dynamicbound3processed.xlsb','Sheet1','A895001:AD9000
00');

%Time for interval
SA=may3010(:,1);

%Channel 1
C1C=may3010(:,3);
%findpeaks(C1C,SA,'MinPeakHeight',0.002);
average1C=mean(C1C);
maximaC1C=findpeaks(C1C,SA,'MinPeakHeight',average1C);
minimaC1C=findpeaks(-C1C,SA,'MinPeakHeight',-average1C);
averagemax1C=mean(maximaC1C);
averagemin1C=mean(-minimaC1C);

%Channel 2
C2C=may3010(:,6);
%findpeaks(C2C,SA,'MinPeakHeight',0.002);
average2C=mean(C2C);
maximaC2C=findpeaks(C2C,SA,'MinPeakHeight',average2C);
minimaC2C=findpeaks(-C2C,SA,'MinPeakHeight',-average2C);
averagemax2C=mean(maximaC2C);
averagemin2C=mean(-minimaC2C);

%Channel 3
C3C=may3010(:,9);
average3C=mean(C3C);
%findpeaks(C3C,SA,'MinPeakHeight',0.002);
maximaC3C=findpeaks(C3C,SA,'MinPeakHeight',average3C);
minimaC3C=findpeaks(-C3C,SA,'MinPeakHeight',-average3C);
averagemax3C=mean(maximaC3C);
averagemin3C=mean(-minimaC3C);

%Channel 4
C4C=may3010(:,12);
%findpeaks(C4C,SA,'MinPeakHeight',0.002);
average4C=mean(C4C);
maximaC4C=findpeaks(C4C,SA,'MinPeakHeight',average4C);
minimaC4C=findpeaks(-C4C,SA,'MinPeakHeight',-average4C);
averagemax4C=mean(maximaC4C);
average4C=mean(C4C);
averagemin4C=mean(-minimaC4C);

%Channel 5
C5C=may3010(:,15);
```

```
%findpeaks(C5C,SA,'MinPeakHeight',0.002);
average5C=mean(C5C);
maximaC5C=findpeaks(C5C,SA,'MinPeakHeight',average5C);
minimaC5C=findpeaks(-C5C,SA,'MinPeakHeight',-average5C);
averagemax5C=mean(maximaC5C);
averagemin5C=mean(-minimaC5C);

%Channel 6
C6C=may3010(:,18);
%findpeaks(C6C,SA,'MinPeakHeight',0.002);
average6C=mean(C6C);
maximaC6C=findpeaks(C6C,SA,'MinPeakHeight',average6C);
minimaC6C=findpeaks(-C6C,SA,'MinPeakHeight',-average6C);
averagemax6C=mean(maximaC6C);
averagemin6C=mean(-minimaC6C);

%Channel 7
C7C=may3010(:,21);
%findpeaks(C7C,SA,'MinPeakHeight',-0.06);
average7C=mean(C7C);
maximaC7C=findpeaks(C7C,SA,'MinPeakHeight',average7C);
minimaC7C=findpeaks(-C7C,SA,'MinPeakHeight',-average7C);
averagemax7C=mean(maximaC7C);
averagemin7C=mean(-minimaC7C);

%Channel 8
C8C=may3010(:,24);
%findpeaks(C8C,SA,'MinPeakHeight',0.002);
average8C=mean(C8C);
maximaC8C=findpeaks(C8C,SA,'MinPeakHeight',average8C);
minimaC8C=findpeaks(-C8C,SA,'MinPeakHeight',-average8C);
averagemax8C=mean(maximaC8C);
averagemin8C=mean(-minimaC8C);

%Channel 9
C9C=may3010(:,27);
%findpeaks(C9C,SA,'MinPeakHeight',0.002);
average9C=mean(C9C);
maximaC9C=findpeaks(C9C,SA,'MinPeakHeight',average9C);
minimaC9C=findpeaks(-C9C,SA,'MinPeakHeight',-average9C);
averagemax9C=mean(maximaC9C);
averagemin9C=mean(-minimaC9C);

%Channel 10
C10C=may3010(:,30);
%findpeaks(C10C,SA,'MinPeakHeight',0.002);
average10C=mean(C10C);
maximaC10C=findpeaks(C10C,SA,'MinPeakHeight',average10C);
minimaC10C=findpeaks(-C10C,SA,'MinPeakHeight',-average10C);
averagemax10C=mean(maximaC10C);
averagemin10C=mean(-minimaC10C);
```

```
Title={'Max','Average','Min'};
Ch1C=[averagemax1C ; average1C ; averagemin1C];
Ch2C=[averagemax2C ; average2C ; averagemin2C];
Ch3C=[averagemax3C ; average3C ; averagemin3C];
Ch4C=[averagemax4C ; average4C ; averagemin4C];
Ch5C=[averagemax5C ; average5C ; averagemin5C];
Ch6C=[averagemax6C ; average6C ; averagemin6C];
Ch7C=[averagemax7C ; average7C ; averagemin7C];
Ch8C=[averagemax8C ; average8C ; averagemin8C];
Ch9C=[averagemax9C ; average9C ; averagemin9C];
Ch10C=[averagemax10C ; average10C ; averagemin10C];

T3=table(Ch1C,Ch2C,Ch3C,Ch4C,Ch5C,Ch6C,Ch7C,Ch8C,Ch9C,Ch10C,'Rownames'
,Title);
```